9066

NACA TN 2699

TECH LIBRARY KAFB, NM
0065752

NATIONAL ADVISORY COMMITTEE FOR AERONAUTICS

TECHNICAL NOTE 2699

CALCULATION OF LIFT AND PITCHING MOMENTS DUE TO ANGLE OF ATTACK AND STEADY PITCHING VELOCITY AT SUPERSONIC SPEEDS FOR THIN SWEPTBACK TAPERED WINGS WITH STREAMWISE TIPS AND SUPERSONIC LEADING AND TRAILING EDGES

By John C. Martin, Kenneth Margolis, and Isabella Jeffreys

Langley Aeronautical Laboratory
Langley Field, Va.

Washington
June 1952

AFMDC
TECHNICAL LIBRARY
AFL 2811

TECH LIBRARY KAFB, NM
0065752

1D

NATIONAL ADVISORY COMMITTEE FOR AERONAUTICS

TECHNICAL NOTE 2699

CALCULATION OF LIFT AND PITCHING MOMENTS DUE TO ANGLE OF ATTACK AND STEADY PITCHING VELOCITY AT SUPERSONIC SPEEDS FOR THIN SWEPTBACK TAPERED WINGS WITH STREAMWISE TIPS AND SUPERSONIC LEADING AND TRAILING EDGES

By John C. Martin, Kenneth Margolis, and Isabella Jeffreys

SUMMARY

On the basis of linearized supersonic-flow theory the stability derivatives C_{m_α} and C_{m_q} (moment coefficients due to angle of attack and steady pitching velocity, respectively) and C_{L_q} (lift coefficient due to steady pitching velocity) were derived for a series of thin sweptback tapered wings with streamwise tips and supersonic leading and trailing edges. The results are valid for a range of Mach number for which the Mach lines from the leading edge of the center section cut the trailing edges. An additional limitation is that the foremost Mach line from either tip may not intersect the remote half of the wing.

The results of the analysis are presented as a series of design charts. Some illustrative variations of the derivatives and of the chordwise center-of-pressure location with the various wing design parameters are also included.

To facilitate the transformation of the calculated results to arbitrary moment-reference locations, the required data for C_{L_α} have been selected or computed from the charts and equations in NACA TN 2114 and are also presented in the form of design charts.

INTRODUCTION

The development of the linearized supersonic-flow theory has enabled the evaluation of stability derivatives for a variety of wing configurations at supersonic speeds. Fairly complete information is now available for the theoretical stability derivatives of rectangular, triangular, and arrowhead plan forms (references 1 to 6). For the sweptback tapered wing with streamwise tips, some of the available stability derivatives are the

lift-curve slope C_{L_α} (references 7 to 10) and the damping-in-roll derivative C_{l_p} (references 9 to 12). For this same wing, reference 13 treats the longitudinal-stability derivatives C_{m_α} and C_{m_q} (moment coefficients due to angle of attack and steady pitching velocity, respectively) and C_{L_q} (lift coefficient due to steady pitching velocity) for a range of Mach number for which the leading edge is subsonic and the trailing edge is supersonic. Reference 14 treats the derivative C_{m_q} for cases where all edges are subsonic.

In the present paper, the range of speeds considered in reference 13 is extended to the Mach number range for which the wing has supersonic leading and trailing edges. The wing plan forms considered herein are the same as those considered in reference 13. These wings have an arbitrary taper ratio, uniformly swept leading and trailing edges (leading edge swept back, trailing edge either swept back or swept forward), and wing tips that are not yawed with respect to the stream direction. The limiting case of zero leading-edge sweepback is also included. The analysis is limited to the range of Mach number for which the Mach lines from the leading edge of the center section cut the trailing edge. An additional restriction is that the foremost Mach line from either tip may not intersect the remote half-wing.

The results of the analysis are given in the form of generalized equations for the stability derivatives C_{m_α}, C_{L_q}, and C_{m_q}. Generalized design curves are also presented from which rapid estimations of the derivatives C_{m_α}, C_{L_q}, and C_{m_q} can be made for given values of aspect ratio, taper ratio, Mach number, and leading-edge sweep angle. Some illustrative variations of the derivatives with these parameters are also presented. Although the analysis is limited to the range of Mach number for which the Mach lines from the center section cut the trailing edges, the generalized curves for the derivatives are judiciously extended to include the Mach number range for which the Mach lines from the center section cut the tips. It is believed that for most combinations of planform parameters and Mach numbers the approximate values taken from these extended portions of the curves are quite close to the true values which would be found by the use of the linearized theory.

The applicability of the calculated results may be broadened considerably by use of the reversibility theorem as indicated in references 15 and 16.

SYMBOLS

A aspect ratio

$A' = AB$

B cotangent of Mach angle $\left(\sqrt{M^2 - 1}\right)$

c local chord in stream direction

ΔC_p pressure-difference coefficient $\left(\Delta P \Big/ \frac{1}{2}\rho V^2\right)$

c_l section lift coefficient $\left(\text{Lift per unit span} \Big/ \frac{1}{2}\rho V^2 c\right)$

c_r root chord

$\bar{c}$ mean aerodynamic chord $\left(\frac{2c_r(\lambda^2 + \lambda + 1)}{3(1 + \lambda)}\right)$

b wing span $\left(\frac{c_r A(1 + \lambda)}{2}\right)$

$J = A'(1 + \lambda)$

$$k = \frac{\cot \Lambda_{TE}}{\cot \Lambda} = \frac{A'(1 + \lambda)}{A'(1 + \lambda) - 4m'(1 - \lambda)}$$

Γ circulation along span $\left(\frac{V}{2}\int_{L.E.}^{T.E.} \Delta C_p \, dx = \frac{V}{2} c_l c\right)$

M free-stream Mach number

m slope of leading edge $(\cot \Lambda)$

$m' = Bm = B \cot \Lambda$

ΔP local pressure difference between upper and lower surfaces of airfoil; positive in sense of lift

q steady pitching velocity

S	wing area
S_3, S_4	areas of integration
u	incremental flight velocity along x stability axis
X, Y, Z	forces parallel to x, y, and z stability axes, respectively
x, y, z	Cartesian coordinates (see fig. 2(a))
x_1, y_1	coordinates of a source point in xy-plane
x_a, y_a	Cartesian coordinates measured from leading edge of tip section $\left(x_a = x - \frac{b/2}{m};\ y_a = y - \frac{b}{2}\right.$ on right half-wing$\left.\right)$
$\bar{x}$	distance from wing apex to center of pressure due to angle of attack $\left(-\bar{c}\,\frac{C_{m_\alpha}}{C_{L_\alpha}}\right)$
$\bar{x}_q$	distance from wing apex to center of pressure due to steady pitching
d	distance from wing apex to assumed center-of-gravity position
$a = d - \bar{x}$	(note that $\bar{x} - d$ when expressed as a function of $\bar{c}$ is defined as static margin)
α	angle of attack
Λ	leading-edge angle of sweepback
Λ_{TE}	trailing-edge angle of sweep, positive for sweepback (see fig. 1)
λ	taper ratio (ratio of tip chord to root chord)
μ	Mach angle $\left(\cot^{-1}B\right)$
ρ	density of air

ϕ disturbance-velocity potential on upper surface of airfoil

$\phi_x = \frac{\partial \phi}{\partial x}$

$\phi_z = \frac{\partial \phi}{\partial z}$

M' pitching moment

L normal force (approximately equal to lift)

V free-stream velocity

C_L lift coefficient $\left(\frac{L}{\frac{1}{2}\rho V^2 S}\right)$

C_m pitching-moment coefficient $\left(\frac{M'}{\frac{1}{2}\rho V^2 S\bar{c}}\right)$

C_X longitudinal-force coefficient $\left(\frac{X}{\frac{1}{2}\rho V^2 S\bar{c}}\right)$

$C_{L_\alpha} = \left(\frac{\partial C_L}{\partial \alpha}\right)_{\alpha \longrightarrow 0}$

$C_{m_\alpha} = \left(\frac{\partial C_m}{\partial \alpha}\right)_{\alpha \longrightarrow 0}$

$C_{L_q} = \left(\frac{\partial C_L}{\partial \frac{q\bar{c}}{2V}}\right)_{q \longrightarrow 0}$

$C_{m_q} = \left(\frac{\partial C_m}{\partial \frac{q\bar{c}}{2V}}\right)_{q \longrightarrow 0}$

$$C_{m_u} = \left(\frac{\partial C_m}{\partial \frac{u}{V}}\right)_{u \longrightarrow 0}$$

$$C_{X_q} = \left(\frac{\partial C_X}{\partial \frac{q\bar{c}}{2V}}\right)_{q \longrightarrow 0}$$

Subscripts:

R refers to reverse of a given wing, obtained by reversing flow direction

TE refers to trailing edge

Superscripts:

* refers to system of body axes with origin at $(\bar{x},0,0)$

' refers to system of body axes with origin at $(d,0,0)$

" refers to system of stability axes with origin at $(d,0,0)$

SCOPE

The types of wings analyzed in this paper are sketched in figure 1. The results of the analysis can, however, be extended to wings with swept-forward leading edges by the use of certain reversibility theorems. The orientation of the wing with respect to a body system of coordinate axes used in the analysis is indicated in figure 2(a). The surface velocity potentials, the pressure distribution, and the stability derivatives are derived with respect to this system. Figure 2(b) shows the wing oriented with respect to the system of stability axes with the origin at an arbitrary point rearward of the wing apex. Formulas for transforming the derivatives from body axes to stability axes are presented in table I.

The analysis is based on the linearized supersonic-flow theory, and the results, therefore, are subject to the usual limitations and restrictions. The derivatives are valid for the range of Mach number for which the leading and trailing edges are supersonic. A further restriction is that the Mach lines from either tip may not intersect the remote half-wing. The analysis is limited to the range of Mach number for which the Mach line from the wing apex cuts the trailing edge. The curves of the design charts, however, are extended (indicated by dashed lines) to the

points where the leading edge is sonic. Thus, estimates of the values of the derivatives in this range (where the Mach line from the apex cuts the tip) can be obtained from the dashed portions of the curves. The estimates so obtained are believed to be quite close to the true linearized-theory values for most combinations of plan-form parameter and Mach number.

ANALYSIS AND BASIC CONSIDERATIONS

The evaluation of the derivatives C_{m_α}, C_{L_q}, and C_{m_q} involves the integration over the wing of the disturbance pressures caused by an angle of attack α and by a steady pitching velocity q. In the treatment of motions involving small disturbances (such as those considered in this analysis), the disturbance pressures may be determined from the well-known relationship:

$$\Delta C_p = \frac{\Delta P}{\frac{1}{2}\rho V^2} = \frac{4}{V}\phi_x \tag{1}$$

The potential function ϕ must satisfy the linearized partial-differential equation of steady flow and the boundary conditions that are associated with the wing in its prescribed motion. The boundary condition on a wing which is at a constant angle of attack α is

$$\phi_z = -\alpha V \qquad (z = 0)$$

Similarly the boundary condition on a wing which has a constant rate of pitch is

$$\phi_z = -qx \qquad (z = 0)$$

(Note that the preceding boundary condition for pitching is independent of time. In stability calculations, a constant rate of pitch corresponds to the wing flying in a circle with a constant velocity.)

Development of Expressions for the Surface Velocity Potential and Lifting Pressure Distributions

The expressions for the potentials and pressures for the wings at a constant angle of attack were obtained from tables I and II of reference 10. This information is presented in tables II and III of the present paper.

The potentials and pressures for the wings performing a steady pitching motion were determined by an application of Evvard's method (see reference 17). The right half-wing is divided into four regions as indicated in figure 3. The expressions for the potentials and pressures are given by different mathematical formulas for each region. The potential or pressure at any point (x,y) in any region can, however, be obtained by taking the real part of the corresponding formula for the potential or pressure for region IV. This procedure is applicable for many steady motions, as can be seen from the following arguments. Only the potential will be considered; however, since the pressure is directly proportional to the x-derivative of the potential, the conclusions will also apply to the pressure. From reference 17, the potential at any point (x,y) in region IV can be expressed as

$$\phi(x,y) = -\frac{1}{\pi}\iint_{S_4} \frac{\phi_z}{\sqrt{(x - x_1)^2 - B^2(y - y_1)^2}}\, dx_1\, dy_1 \tag{2}$$

The area of integration S_4 is indicated in figure 4. Similarly, the potential in region III is given by

$$\phi(x,y) = -\frac{1}{\pi}\iint_{S_3} \frac{\phi_z}{\sqrt{(x - x_1)^2 - B^2(y - y_1)^2}}\, dx_1\, dy_1 \tag{3}$$

The area of integration S_3 is indicated in figure 5.

Figure 6 indicates the effect on the area of integration S_4 when the point (x,y) is moved from region IV to region III. Note that the wing area inside the effective forward Mach cone from the point (x,y) is the same as the area S_3. For a point (x,y) in region III, the right side of equation (2) can be written as

$$-\frac{1}{\pi}\iint_{S_4}\frac{\phi_z}{\sqrt{(x - x_1)^2 - B^2(y - y_1)^2}}\,dx_1\,dy_1 =$$

$$-\frac{1}{\pi}\iint_{S_3}\frac{\phi_z\,dx_1\,dy_1}{\sqrt{(x - x_1)^2 - B^2(y - y_1)^2}} -$$

$$\frac{1}{\pi}\iint_{S_4-S_3}\frac{\phi_z}{\sqrt{(x - x_1)^2 - B^2(y - y_1)^2}}\,dx_1\,dy_1 \tag{4}$$

The area $S_4 - S_3$ is the portion of S_4 which is outside the forward Mach cone from the point (x,y). The integral over the area $S_4 - S_3$ will be purely imaginary because the radical of the integrand is always imaginary. Only the integral over the area S_3 will contribute to the real part of equation (4), and the integral over S_3 is, by equation (3), the potential in region III. Thus, the real part of the expression for the potential of region IV will yield the expression for the potential in region III as the point (x,y) is moved from region IV to region III. Analogous reasoning can be presented for regions I and II. The integrations were performed for the various regions and the resulting potentials are presented in table IV. Application of equation (1) yielded the corresponding formulas for the pressures; these are presented in table V.

Some illustrative chordwise and spanwise pressure distributions are presented in figure 7 for the angle-of-attack case and in figure 8 for the steady-pitching case. Integration of the chordwise pressure distribution yields the spanwise loading (also obtainable by use of the previously derived potentials evaluated at the trailing edge - see, for example, reference 10, equation (4)). The circulation along the span Γ, which is directly related to the spanwise loading, is presented, for illustrative purposes, in figures 9 and 10.

Derivation of Formulas for C_{m_α}, C_{L_q}, and C_{m_q}

The derivatives C_{m_α}, C_{L_q}, and C_{m_q} are obtained by integrating the lifting pressure or the first moment of the lifting pressure over the wing area. These derivatives can be expressed as follows:

$$C_{m_\alpha} = -\frac{1}{\alpha S\bar{c}} \iint_S x\,\Delta C_p\,dx\,dy \tag{5}$$

$$C_{L_q} = \frac{1}{\frac{q\bar{c}}{2V}\,S} \iint_S \Delta C_p\,dx\,dy \tag{6}$$

$$C_{m_q} = -\frac{1}{\frac{q\bar{c}}{2V}\,S\bar{c}} \iint_S x\,\Delta C_p\,dx\,dy \tag{7}$$

where $\Delta C_p = \frac{4}{V}\phi_x$.

As indicated previously, the real part of the expression for the pressure-difference coefficient in region IV is also the expression for the pressure-difference coefficient for all other regions. Equations (5), (6), and (7) can, therefore, be written as

$$C_{m_\alpha} = \text{-R.P.}\ \frac{1}{\alpha S\bar{c}} \iint_S x\left(\Delta C_p\right)_{IV} dx\,dy \tag{8}$$

$$C_{L_q} = \text{R.P.}\ \frac{1}{\frac{q\bar{c}}{2V}\,S} \iint_S \left(\Delta C_p\right)_{IV} dx\,dy \tag{9}$$

$$C_{m_q} = \text{-R.P.}\ \frac{1}{\frac{q\bar{c}}{2V}\,S\bar{c}} \iint_S x\left(\Delta C_p\right)_{IV} dx\,dy \tag{10}$$

where the operator R.P. indicates that only the real part is to be retained, and $\left(\Delta C_p\right)_{IV}$ denotes the expression for ΔC_p in region IV.

The expression for the derivative C_{L_q} may be simplified by the following consideration: Since the potential function ϕ is continuous in the stream direction and is zero along the leading edge of the wing,

$$\int_{L.E.}^{T.E.} \Delta C_p \, dx = \frac{4}{V}\int_{L.E.}^{T.E.} \phi_x \, dx = \frac{4}{V}\phi_{TE} \tag{11}$$

It follows that equation (9) can be expressed as

$$C_{L_q} = R.P. \frac{4}{\frac{q\bar{c}}{2V} SV}\int_{-b/2}^{b/2} \phi_{TE_{IV}} \, dy \tag{12}$$

where the potential is evaluated along the wing trailing edge.

RESULTS AND DISCUSSION

Formulas and Computations for the Derivatives C_{m_α}, C_{L_q}, and C_{m_q}

The formulas for the derivatives C_{m_α}, C_{L_q}, and C_{m_q} obtained by evaluating the integral expressions of equations (8), (10), and (12) are presented in the appendix. The formulas for these derivatives are also given for the case where the leading edge is sonic.

The results of computations for C_{m_α} are presented in figures 11 to 15, for C_{L_q} in figures 16 to 20, and for C_{m_q} in figures 21 to 25. The data are shown for a range of taper ratios from 0 to 1.0 and for a range of the aspect-ratio parameter ($A' = AB$) from 3 to 20. (Curves for $A' = 2$ are included for the $\lambda = 1.0$ cases.) The range of leading-edge-sweepback angles is included in values of $\cot^{-1}m'$ from 0° to 45°. The dashed portions of the curves do not represent actual calculations, since these regions correspond to the condition where the Mach line from the wing apex intersects the tip. However, calculations were made for the sonic-leading-edge condition and the dashed extensions of the curves to these calculated end points are believed to yield results quite close to the true linearized-theory values for most cases.

The derivatives C_{L_q} and C_{m_q} given by these generalized curves (figs. 16 to 25) are for the wing pitching about the center of pressure due to angle of attack. The generalized curves for the derivative C_{m_α} (figs. 11 to 15) are for the wing pitching about the wing apex. In all cases, the moments are measured about the axis of pitch. The derivatives for wings pitching about an arbitrary origin (with moments measured about the origin) may be obtained by use of the transformation formulas presented in table I. The first three columns of table I present the derivatives in a system of body axes with rotation and moments measured about the points (0,0,0), $(\bar{x},0,0)$, and (d,0,0). The fourth column transfers the derivatives to the system of stability axes with rotation and moments measured about the point (d,0,0). Since the lift-curve slope C_{L_α} must be known in order to apply the transformation formulas, design-chart data for this derivative are presented in figures 26 to 30. These figures were prepared from the figures and formulas presented in reference 10.

For convenience in locating the desired design-chart data for the derivatives, an index to figures 11 to 30 is presented in tables VI to IX. Inasmuch as the parameter $\cot^{-1}m'$ is used rather than the usual m', it is felt worthwhile to present in figure 31 some data showing the correspondence between the parameters.

Some illustrative variations of the derivatives C_{m_α}, C_{L_q}, and C_{m_q} (in the system of stability axes) with each of the parameters - Mach number, aspect ratio, leading-edge sweepback, and taper ratio - are presented in figures 32 to 34.

Chordwise Center-of-Pressure Location

The center-of-pressure location for a wing at a constant angle of attack and for a wing with a constant rate of pitch can be determined from a knowledge of the derivatives C_{m_α}, C_{L_q}, C_{m_q}, and C_{L_α}. The expressions for the chordwise location of the center of pressure are as follows: For a constant angle of attack,

$$\frac{\bar{x}}{c_r} = -\frac{\bar{c}}{c_r}\frac{C_{m_\alpha}}{C_{L_\alpha}} \tag{13}$$

where $\bar{x}$ is measured from the wing apex. For a constant rate of pitch

with the axis of pitch located at distance d downstream of the wing apex,

$$\frac{\bar{x}_q}{c_r} = -\frac{\bar{c}}{c_r}\frac{C_{m_q} - \frac{2d}{\bar{c}}C_{m_\alpha}}{C_{L_q} - \frac{2d}{\bar{c}}C_{L_\alpha}} \tag{14}$$

where $\bar{x}_q$ is measured from the wing apex. The derivatives used in equations (13) and (14) are referred to the system of body axes with its origin at the wing apex. Some illustrative variations of the center-of-pressure location with each of the parameters - Mach number, aspect ratio, leading-edge sweep, and taper ratio - are presented in figures 35 and 36.

Extensions of the Results by the Use of Reversibility Theorems

The results for the derivatives can be extended by the use of certain reversibility theorems. (See references 15 and 16.) The derivatives C_{m_α}, C_{L_q}, and C_{m_q} for the reverse wing are given by (reference 15, table I)

$$\left(C_{m_\alpha}\right)_R = \frac{1}{2}C_{L_q}$$

$$\left(C_{L_q}\right)_R = 2C_{m_\alpha}$$

$$\left(C_{m_q}\right)_R = C_{m_q}$$

where the subscript R refers to the reversed wing. In these reversibility equations, the axis about which the moments are taken and about which the wing is pitching must be the same for the wing and its reverse. The axis is fixed in the wing configuration (that is, invariant with the direction of flow). For example, if the axis of pitch and the moment axis are taken at the leading edge of the root section of a wing in a forward flow, then the axis of pitch and the moment axis will be at the trailing edge of the root section of the wing in a reversed flow.

CONCLUDING REMARKS

On the basis of the linearized theory for steady supersonic flow, formulas for the stability derivatives C_{m_α}, C_{L_q}, and C_{m_q} were derived for a series of thin sweptback tapered wings with streamwise tips and with supersonic leading and trailing edges. The numerical results are presented in a series of design charts which permit estimation of the derivatives for various values of aspect ratio, taper ratio, leading-edge sweepback, and Mach number. Some illustrative variations of the derivatives and center-of-pressure location with these parameters are also included.

Langley Aeronautical Laboratory
National Advisory Committee for Aeronautics
Langley Field, Va., February 19, 1952

APPENDIX

SUMMARY OF FORMULAS FOR C_{m_α}, C_{L_q}, AND C_{m_q}

The following formulas for C_{m_α}, C_{L_q}, and C_{m_q} refer to wings which have an arbitrary taper ratio, leading and trailing edges that are each uniformly swept at a constant angle (including zero sweep angle), and wing tips that are not yawed with respect to the free-stream direction. Note that the trailing edge may be either swept-forward or sweptback, although the leading edge is restricted to sweep-back. An additional limitation is that the foremost Mach line from either tip may not intersect the remote half of the wing.

The proper use of the formulas requires that the positive root of the quantity under a radical sign be taken; thus, if a is a positive number,

$$\sqrt{(\pm a)^2} = a$$

Also, note that

$$\sqrt{-a}\ \sqrt{-a} = i\sqrt{a}\ i\sqrt{a} = -a$$

Formulas for C_{m_α}

<u>Sweptback leading edge, $m' = 1$ (sonic leading edge).</u>-

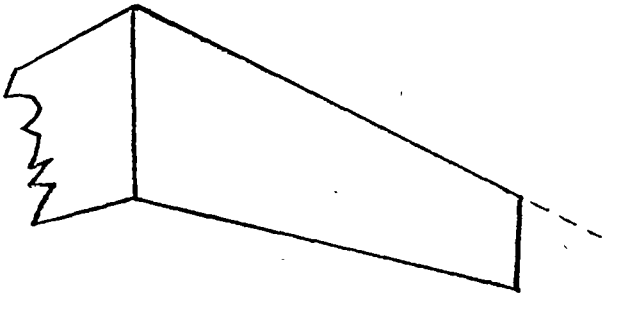

For arbitrary taper ratio,

$$C_{m_\alpha} = \frac{8J^2k^2}{\pi B\left[48k^2 - 12Jk(k - 1) + J^2(k - 1)^2\right]}\left(\frac{32(1 - 4k^2)}{J^3(1 - k^2)^2} + \right.$$

$$\frac{32k^3(1 + 2k^2)}{J^3(1 - k^2)^2\sqrt{k - 1}\sqrt{k + 1}}\left[\sin^{-1}\frac{J(1 - k) + 2k}{2k} - \sin^{-1}\frac{1}{k}\right] +$$

$$\frac{k^2\sqrt{4k + J - Jk}}{15(1 - k)^2(k + 1)^{5/2}\sqrt{J}}\left\{-\frac{60}{J}\left[-\frac{2(k - 1)}{k} - \frac{4(4k - 1)}{J}\right] - \right.$$

$$\left. 2(1 - k)^2\left[\frac{7(2J + 4k)^2}{k^2J^2} + \frac{4(2J - 4)}{kJ^2}(3J + 4k + kJ)\right]\right\} -$$

$$2\sqrt{2}\left\{\frac{(4kJ + J - 36)\left[2(4k - kJ + J)\right]^{3/2}}{30J^2\sqrt{J}(k + 1)^{5/2}} - \right.$$

$$\frac{2k^2(8 - J) - (kJ - J - 4k)}{2kJ(k + 1)}\left[-\frac{(J + 4k - 3kJ)\sqrt{2(4k - Jk + J)}}{8J\sqrt{J}(k + 1)^{3/2}} - \right.$$

$$\left.\left.\left.\frac{(kJ + J + 4k)^2\sqrt{k}}{16kJ^2(k + 1)^{3/2}}\left(\frac{\pi}{2} + \sin^{-1}\frac{4k + J - 3kJ}{kJ + J + 4k}\right)\right]\right\}\right) \qquad \text{(A1)}$$

For taper ratio of 1,

$$C_{m_\alpha} = -\frac{8}{BA'\pi}\left[-\frac{14}{45} + \frac{(303A'^2 + 350A' + 75)\sqrt{A'}}{1440} - \frac{(A' - 5)(A' + 1)^2}{192}\cos^{-1}\frac{A' - 1}{A' + 1}\right] \tag{A2}$$

Sweptback leading edge; $m' > 1$ and $A' > \dfrac{4m'\lambda}{(1 + \lambda)(m' - 1)}$.

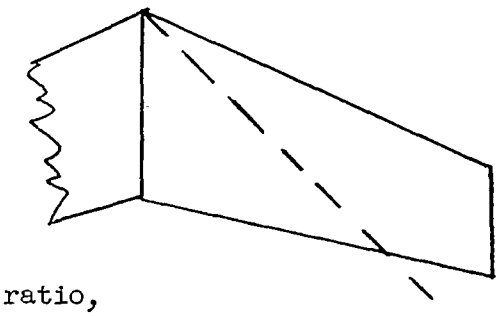

For arbitrary taper ratio,

$$C_{m_\alpha} = -\frac{768k^2m'^3}{\pi BJ\sqrt{m'^2 - 1}\left[J^2(k - 1)^2 - 12km'J(k - 1) + 48k^2m'^2\right]}\left\{\frac{km'(3k^2 - 1)}{3(k^2 - 1)^2}\cos^{-1}\frac{1}{m'} + \frac{k^3m'(2m'^2k^4 - k^2 - 1)\sqrt{m'^2 - 1}}{3(k^2 - 1)^2(m'^2k^2 - 1)\sqrt{m'k - 1}\sqrt{m'k + 1}}\cos^{-1}\frac{1}{km'} + \frac{k^3m'\sqrt{m'^2 - 1}}{3(k^2 - 1)(k^2m'^2 - 1)} + \frac{\left[4km' - J(k - 1)\right]^2\pi}{32}\left[\frac{(1 - 4m'k^2 + 2m'k - 3k)\sqrt{m' + 1}}{6m'\sqrt{k}(k - 1)^2(1 + m'k)\sqrt{m'k + 1}} - \frac{J(3k + 2m'k^2 + 2m'k + 1)\sqrt{m' + 1}}{24km'^2(k - 1)(1 + m'k)\sqrt{k}\sqrt{m'k + 1}}\right]\right\} \tag{A3}$$

For taper ratio of 1,

$$C_{m_\alpha} = -\frac{1}{A'B}\left[\frac{2m'^2(-3m'^4 + 10m'^2 - 4)}{3\pi(m'^2 - 1)^2\sqrt{m'^2 - 1}}\cos^{-1}\frac{1}{m'} - \frac{2m'^4}{\pi(m'^2 - 1)^2} + \frac{A'^2}{\sqrt{m'^2 - 1}} + \right.$$

$$\left.\frac{A'm'(2m' + 1)}{(m' + 1)\sqrt{m'^2 - 1}} + \frac{6m'^6 - 8m'^5 - 17m'^4 + 2m'^3 + 5m'^2}{6(m'^2 - 1)^2\sqrt{m'^2 - 1}}\right] \tag{A4}$$

Unswept leading edge ($m' = \infty$).-

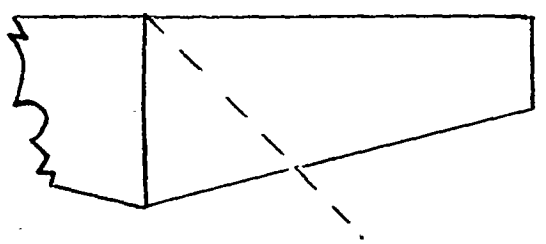

For arbitrary taper ratio,

$$C_{m_\alpha} = -\frac{24}{B(\lambda^2 + \lambda + 1)}\left(\frac{J^2}{192} + \frac{(J - 4)^2\left[-J^2 - 8J\lambda + 16(1 - \lambda)\right]}{192\left[J - 4(1 - \lambda)\right]^2} + \right.$$

$$\lambda^3\left\{\frac{1}{12(1 - \lambda)} + \frac{2\left[J - 2(1 - \lambda)\right]}{3\left[J - 4(1 - \lambda)\right]^2} + \frac{J}{12\sqrt{J\left[J - 4(1 - \lambda)\right]}}\left[-\frac{1}{1 - \lambda} - \right.\right.$$

$$\left.\left.\left.\frac{2}{J - 4(1 - \lambda)}\right]\right\}\right) \tag{A5}$$

For taper ratio of 1,

$$C_{m_\alpha} = \frac{4 - 6A'}{3A'B} \tag{A6}$$

Formulas for C_{L_q}

Sweptback leading edge, $m' = 1$ (sonic leading edge).-

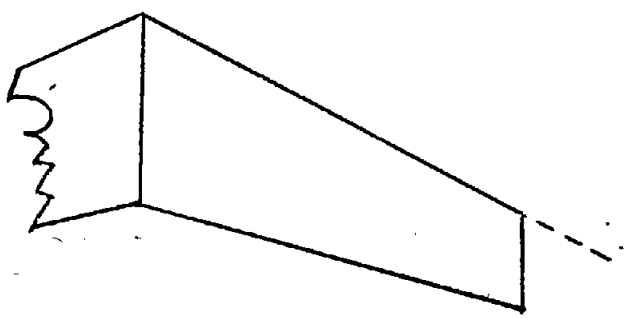

For arbitrary taper ratio,

$$C_{L_q} = \frac{32k^4J^2}{\pi B(k+1)^2\left[48k^2 - 12Jk(k-1) + J^2(k-1)^2\right]}\left[\frac{k^2}{3(1-k)^2}\left(\frac{k\sqrt{4k+J-Jk}}{5(1+k)^{3/2}\sqrt{J}}\left\{\frac{20}{k^2J^2}\left[\frac{(2-5k^2)(2J+4k)}{k^2} + (2+k^2)(2J-4)\right] - \frac{2(1-k)^2(1+k)}{k^3J^2}\left[(2J-4)^2 - \frac{2(2J-4)(2J+4k)}{k} - \frac{4(2J+4k)^2}{k^2}\right]\right\} - \right.$$

(Equation continued on next page)

$$\frac{96k}{J^3\sqrt{k+1}\sqrt{k-1}}\left[\sin^{-1}\frac{J(1-k)+2k}{2k}-\sin^{-1}\frac{1}{k}\right]-\frac{32(2-5k^2)}{k^3J^3}\Bigg)+$$

$$\frac{\sqrt{k}}{\sqrt{k+1}}\left\{-\frac{(3kJ+7J+48k)(4k+J-kJ)}{15k^2J^2}\sqrt{\frac{4k+J-kJ}{kJ}}-\right.$$

$$\frac{J(5-3k)(k+1)+4k(9k+5)}{16\sqrt{2}k^2J}\left[\frac{-J-4k+3kJ}{kJ\sqrt{kJ}}\sqrt{2(4k-kJ+J)}-\right.$$

$$\left.\left.\left.\frac{(kJ+J+4k)^2}{2k^2J^2}\left(\sin^{-1}\frac{4k+J-3kJ}{4k+J+kJ}+\frac{\pi}{2}\right)\right]\right\}\right] \tag{A7}$$

For taper ratio of 1,

$$C_{L_q}=\frac{16}{3\pi A'B}\left[\frac{(A'+7)(A'+1)^2}{32}\cos^{-1}\frac{A'-1}{A'+1}-\frac{16}{15}+\right.$$

$$\left.\frac{(81A'^2+190A'+105)\sqrt{A'}}{240}\right] \tag{A8}$$

Sweptback leading edge, $m' > 1$ and $A' > \dfrac{4m'\lambda}{(1 + \lambda)(m' - 1)}$.-

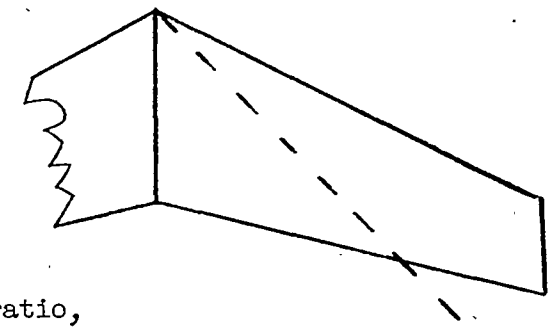

For arbitrary taper ratio,

$$C_{L_q} = \frac{48}{B\pi J(\lambda^2 + \lambda + 1)k^2m'(m'^2 - 1)^{3/2}}\left[\frac{k^2m'\sqrt{m'^2 - 1}}{\sqrt{m'k + 1}\sqrt{m'k - 1}}\left\{\frac{k^5m'^6}{(m'^2k^2 - 1)^2} - \right.\right.$$

$$\frac{2k^3m'^2(-k^4m'^4 + m'^2k^4 - 2 - m'^4k^2)}{(m'^2k^2 - 1)(1 - k^2)^2} -$$

$$\left.\left.\frac{\left\{\begin{array}{l} k^2m'^2\left[6(m'^2k^2 - 1)(2km'^2 + m'^2k^3) + \right. \\ \quad 2k^5m'^6(k^2 + 3) + m'^4k^3(k^4 - 10k^2 - 15) + \\ \quad \left. 2m'^2k(-k^4 + 7k^2 + 6) - 4k(3 - k^2)\right] \end{array}\right\}}{3(m'^2k^2 - 1)^2(1 - k^2)^2}\right\}\cos^{-1} - \frac{1}{km'} +$$

$$\frac{2k^3m'^3(-4k^2 + 3m'^2k^2 - m'^2 + 2)}{3(1 - k^2)^2}\cos^{-1}\frac{1}{m'} +$$

(Equation continued on next page)

$$\frac{m'^3k^3\sqrt{m'^2 - 1}}{3(m'^2k^2 - 1)^2(1 - k^2)}\left\{(5m'^2k^2 - 2)(1 - k^2) - k\left[2k^3m'^4 + m'^2k(1 - 5k^2) + 2k\right]\right\} + \frac{k\pi\left[4m'k + J(1 - k)\right]\sqrt{m' + 1}}{4(1 - k)\sqrt{m'k + 1}\sqrt{k}}\left(k^2m'^2(m'^2 - 2) - \frac{km'(k + m'^2 - 2)\left[4km'(3 + 2m'k - k) - J(1 - k)(1 + k + 2m'k)\right]}{8(1 - k)(1 + m'k)} + \frac{2 - m'^2(k + 1)}{3}\left\{-\frac{m'^2k^2}{1 - k} + \frac{\left\{\left[-4m'k + J(1 + k + 2m'k)\right]\left[4m'k(3 + 2m'k - k) - J(1 - k)(1 + k + 2m'k)\right]\right\}}{64(m'k + 1)^2} + \frac{(k - 1)\left[4m'k + J(1 - k)\right]^2}{64(m'k + 1)^2}\right\} + \frac{\left\{\left[J(1 - k) + 4m'k\right](1 - k)\left[4m'k(-6 - 4m' + 5m'^2 - 12m'k - 7m'^2k + 8m'^3k) + J(-6 - 4m' + 8m'^3k + 5m'^2 - 8m'k - 6k + 7m'^2k^2 + 4m'^3k^2)\right]\right\}}{384(1 + m'k)^2}\right)\Bigg] \tag{A9}$$

For taper ratio of 1,

$$C_{L_q} = \left\{ \frac{2m'^2}{\pi A' B(m'^2 - 1)^{3/2}} \left[-\frac{2(m'^2 - 2)}{\sqrt{m'^2 - 1}} + \frac{2(-3m'^6 + 11m'^4 - 16m'^2 + 8)}{3(m'^2 - 1)^2} \cos^{-1}\frac{1}{m'} + \frac{\pi(6m'^6 - 4m'^5 - 19m'^4 + 14m'^3 + 26m'^2 - 10m' - 13)}{6(m'^2 - 1)^2} \right] + \frac{2A'}{B\sqrt{m'^2 - 1}} + \frac{2m'(2m'^2 - m' - 3)}{B(m'^2 - 1)^{3/2}} \right\} \tag{A10}$$

Unswept leading edge, $m' = \infty$.-

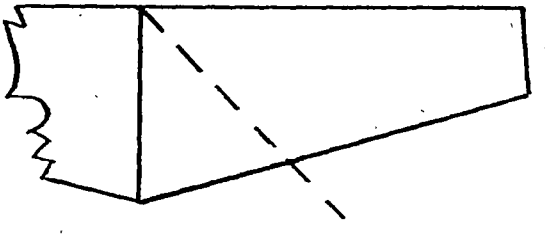

For arbitrary taper ratio,

$$C_{L_q} = \frac{48}{B(\lambda^2 + \lambda + 1)} \left(\frac{J^2}{192} + \frac{(J - 4)^2 \left[J^2 - 8J\lambda + 16(1 - \lambda) \right]}{192 \left[J - 4(1 - \lambda) \right]^2} + \lambda^3 \left\{ \frac{1}{12(1 - \lambda)} + \frac{2\left[J - 2(1 - \lambda) \right]}{3\left[J - 4(1 - \lambda) \right]^2} - \frac{J}{12(1 - \lambda)\sqrt{J\left[J - 4(1 - \lambda) \right]}} \right\} \right) \tag{A11}$$

For taper ratio of 1,

$$C_{L_q} = \frac{12A' - 4}{3A'B} \tag{A12}$$

Formulas for C_{m_q}

<u>Sweptback leading edge, $m' = 1$ (sonic leading edge).</u>-

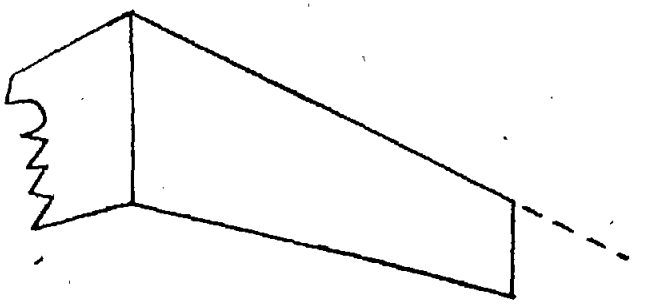

For arbitrary taper ratio,

$$C_{m_q} = -\frac{8k^7J^4}{BA'\pi(k+1)^3\left[48k^2 - 12Jk(k-1) + J^2(k-1)^2\right]^2}\left[\frac{6k^3}{(1-k)^3}\left\{\frac{128(2+3k^2)}{J^4k\sqrt{k+1}\sqrt{k-1}}\left[\sin^{-1}\frac{2(1-k)J+4k}{4k} - \sin^{-1}\frac{1}{k}\right] - \frac{128}{3k^5J^4}(4 - 12k^2 + 23k^4)\right\} + \frac{\sqrt{k}}{\sqrt{k+1}}\frac{(kJ + J + 4k)^2}{32k^2J^2\sqrt{2}}\left\{\frac{8(k+1)}{k}\left[\frac{(4k-2)(k+1)}{k^2} - \frac{12(3k^2 - 5k - 6)}{Jk^2} + \frac{304}{J^2}\right] + \frac{2k^2 - k + 9}{k^2}\left[\frac{5(Jk + J - 4k)^2}{k^2J^2} + \frac{16(k+1)}{Jk}\right]\right\}\left(\frac{\pi}{2} + \sin^{-1}\frac{4k + J - 3kJ}{4k + J + kJ}\right) +$$

(Equation continued on next page)

$$\frac{\sqrt{4k + J - Jk}}{\sqrt{J(k + 1)}}\left(\frac{2k^5}{(1 - k)^3(1 + k)^2}\left\{\frac{4}{Jk^7}(16 - 40k^2 + 32k^4 - 8k^6) + \right.\right.$$

$$\frac{16}{J^2k^6}(16 - 8k - 48k^2 + 6k^3 + 38k^4 + 2k^5 - 6k^6) + \frac{64}{J^3k^5}(6 + 27k^3 +$$

$$24k^4 + 3k^5) + \frac{2(1 - k)^3(1 + k)^2}{35k^5}\left[(-512 - 368k + 32k^2 + 8k^3)\frac{1}{k^3} + \right.$$

$$\left.\left.\frac{4}{Jk^2}(-584 - 400k + 4k^2) + \frac{16}{J^2k}(-192 - 102k) - \frac{960}{J^3}\right]\right\} + \left[\frac{4}{J^3k^2}(45 + \right.$$

$$147k + 162k^2) + \frac{1}{J^2k^3}(-570k^3 - 237k^2 + 228k + 135) + \frac{1}{4Jk^4}(294k^4 -$$

$$147k^3 - 561k^2 + 15k + 135) + \frac{1}{16k^5}(-126k^5 - 147k^4 - 72k^3 -$$

$$\left.\left.162k^2 - 66k + 45)\right]\right)\right] \tag{A13}$$

For taper ratio of 1,

$$C_{m_q} = -\frac{16}{3\pi BA'}\left[-\frac{64}{105} + \frac{(33A'^2 + 66A' + 177)(A' + 1)^2}{1536}\cos^{-1}\frac{A' - 1}{A' + 1} + \right.$$

$$\left.\frac{(2685A'^3 + 8309A'^2 + 12635A' + 6195)\sqrt{A'}}{26880}\right] \tag{A14}$$

Sweptback leading edge, $m' > 1$ and $A' > \dfrac{4m'\lambda}{(1 + \lambda)(m' - 1)}$.-

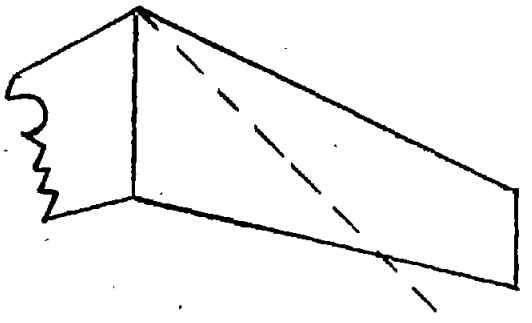

For arbitrary taper ratio,

$$C_{m_q} = -\frac{8km' + J(1 - k)}{BJ\left[J^2(1 - k)^2 + 12Jkm'(1 - k) + 48m'^2k^2\right]^2(m'^2 - 1)^{3/2}}\Bigg(-1.5m'k^3J^4(2m'^2 - 1) +$$

$$3m'J(4km' + J)^2\left[1.5kJ + (m'^2 - 2)(4km' + J)\right] - \frac{384m'^5k^7(1 + k - 2m'^2)}{(1 - k)^3} -$$

$$\frac{1536k^4m'^5\left[m'^2(1 - 3k^2 + 6k^4) - 2 + 6k^2 - 8k^4\right]}{\pi(1 - k^2)^3}\cos^{-1}\frac{1}{m'} -$$

(Equation continued on next page)

$$\frac{1536k^7m'^5\left[m'^4k^3(1 + 3k^2) - m'^2k(2 + 3k^2 + 3k^4) + 2k(k^2 + 1)\right]\sqrt{m'^2 - 1}}{\pi(1 - k^2)^3(m'^2k^2 - 1)\sqrt{m'k + 1}\sqrt{m'k - 1}}\cos^{-1} - \frac{1}{km'} +$$

$$\frac{1536k^4m'^5(3k^4m'^2 - 2k^2 - k^4 + 1 - k^2m'^2)\sqrt{m'^2 - 1}}{\pi(1 - k^2)^2(m'^2k^2 - 1)} + 12m'^2k(J + 4m'k)^2\left[kJ - 2k^2m' +\right.$$

$$\left.(m'^2 - 2)(J + 4m'k)\right] - \frac{6m'^2k^2\left[4km' + J(1 - k)\right]^3}{(1 - k)^2}\left\{\frac{11k - 4 - 9k^2 - 2m'^2(3k - 1 - 3k^2)}{k(1 - k)} +\right.$$

$$\frac{J(7k - 4 - k^2 - 2km'^2 + 2m'^2 - 2k^2m'^2)}{4k^2m'} +$$

$$\frac{(-6m' + 9 - 8m'^2k + 30m'k - 26k + 24m'^2k^2 - 54m'k^2 + 25k^2 + 30m'k^3 - 24m'^2k^3)(m' + 1)\sqrt{m' + 1}}{4(1 - k)(m'k + 1)\sqrt{m'k + 1}\sqrt{k}} +$$

$$\left.\frac{J(-18k - 2m'k^3 - 14m'k^2 + k^2 + 22m'k + 8m'^2k^3 + 8m'^2k^2 - 6m' + 9 - 8m'^2k)(m' + 1)\sqrt{m' + 1}}{16km'(m'k + 1)\sqrt{k}\sqrt{m'k + 1}}\right\} +$$

$$\frac{18m'k^3J^2\left[4km' + J(1 - k)\right]^2}{1 - k}\left[\frac{(m'^2 - 1)\sqrt{m' + 1}}{\sqrt{k}\sqrt{m'k + 1}} - \frac{(m'^2 - 1)}{k}\right] -$$

(Equation continued on next page)

$$\frac{18m'k^2J\left[4km' + J(1 - k)\right]^3}{(1 - k)^2}\left[\frac{(m'^2 - 2 - 2km'^2 + 3k)}{k} + \frac{(4km' - 5k - 2m' + 3)(m' + 1)\sqrt{m' + 1}}{2\sqrt{k}\sqrt{m'k + 1}}\right]\Bigg) \tag{A15}$$

For taper ratio of 1,

$$C_{m_q} = \frac{1}{B}\Bigg(-\frac{m'^2}{A'\pi(m'^2 - 1)^3}\Bigg[\frac{-21m'^6 + 85m'^4 - 92m'^2 + 28}{9(m'^2 - 1)} + \frac{-7m'^6 + 26m'^4 - 40m'^2 + 16}{3\sqrt{m'^2 - 1}}\cos^{-1}\frac{1}{m'} +$$

$$\frac{\pi(7m'^6 + 24m'^5 + 15m'^4 - 40m'^3 - 33m'^2 + 16m' + 11)m'^2}{6(m'^2 - 1)\sqrt{m'^2 - 1}}\Bigg] - \frac{2}{(m'^2 - 1)^{3/2}}\Bigg\{\frac{A'^2(m'^2 - 1)}{3m'} +$$

$$\frac{A'(82m'^2 - 45m' - 74)}{90} + \frac{\left[A'(m' + 1) - m'\right](-14m'^3 + 32m'^2 + 32m')}{90A'(m' + 1)^2} +$$

$$\frac{A'm'(136m'^3 + 54m'^2 - 257m' - 183)(m' + 1) + \left[A'(m' + 1) - m'\right]\left[A'(m' + 1)(8m'^2 - 16) - 16m'^4\right]}{90(m' + 1)^2A'} +$$

$$\frac{m'^2(-964m'^5 - 1196m'^4 + 1227m'^3 + 978m'^2 - 353m' - 172)}{360A'(m'^2 - 1)^2}\Bigg\}\Bigg) \tag{A16}$$

Unswept leading edge, $m' = \infty$.-

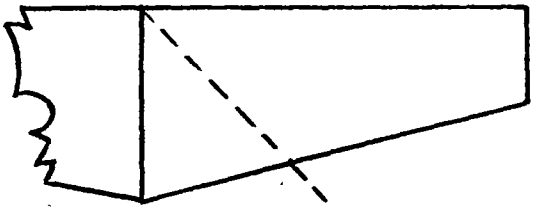

For arbitrary taper ratio,

$$C_{m_q} = -\frac{12}{A'B(\lambda^2 + \lambda + 1)^2}\left[\frac{J(J - 4)}{J - 4(1 - \lambda)}\left\{1 - \frac{3(1 - \lambda)(J - 4)}{2\left[J - 4(1 - \lambda)\right]} + \frac{(1 - \lambda)^2(J - 4)^2}{\left[J - 4(1 - \lambda)\right]^2} - \frac{(1 - \lambda)^3(J - 4)^3}{4\left[J - 4(1 - \lambda)\right]^3}\right\} + \frac{J^4}{64}\left\{-\frac{J - 4}{J - 4(1 - \lambda)} + \frac{3(J - 4)^2}{2\left[J - 4(1 - \lambda)\right]^2} - \frac{(J - 4)^3}{\left[J - 4(1 - \lambda)\right]^3} + \frac{(J - 4)^4}{4\left[J - 4(1 - \lambda)\right]^4} + \frac{1}{4}\right\} - \frac{J^4\lambda^4}{\left[J - 4(1 - \lambda)\right]^4} - \frac{J\lambda^4}{4}\left(-\frac{J^4}{(1 - \lambda)\left[J - 4(1 - \lambda)\right]^4} + \frac{J}{(1 - \lambda)\sqrt{J\left[J - 4(1 - \lambda)\right]}}\left\{\frac{J + 8(1 - \lambda)}{J - 4(1 - \lambda)} + \frac{8(1 - \lambda)\left[7(1 - \lambda) - J\right]}{\left[J - 4(1 - \lambda)\right]^2} + \frac{2(1 - \lambda)}{J - 4(1 - \lambda)} + \frac{2(1 - \lambda)^2\left[22(1 - \lambda) - 3J\right]}{\left[J - 4(1 - \lambda)\right]^3}\right\}\right) + \frac{\lambda^4 J^2\left[75J^2 - 330J(1 - \lambda) + 420(1 - \lambda)^2\right]}{60\left[J - 4(1 - \lambda)\right]^3\sqrt{J\left[J - 4(1 - \lambda)\right]}}\right] \tag{A17}$$

For taper ratio of 1,

$$C_{m_q} = \frac{3 - 8A'}{3A'B} \tag{A18}$$

REFERENCES

1. Harmon, Sidney M.: Stability Derivatives at Supersonic Speeds of Thin Rectangular Wings with Diagonals ahead of Tip Mach Lines. NACA Rep. 925, 1949. (Supersedes NACA TN 1706.)

2. Ribner, Herbert S., and Malvestuto, Frank S., Jr.: Stability Derivatives of Triangular Wings at Supersonic Speeds. NACA Rep. 908, 1948. (Supersedes NACA TN 1572.)

3. Malvestuto, Frank S., Jr., and Margolis, Kenneth: Theoretical Stability Derivatives of Thin Sweptback Wings Tapered to a Point with Sweptback or Sweptforward Trailing Edges for a Limited Range of Supersonic Speeds. NACA Rep. 971, 1950. (Supersedes NACA TN 1761.)

4. Brown, Clinton E.: Theoretical Lift and Drag of Thin Triangular Wings at Supersonic Speeds. NACA Rep. 839, 1946. (Supersedes NACA TN 1183.)

5. Brown, Clinton E., and Adams, Mac C.: Damping in Pitch and Roll of Triangular Wings at Supersonic Speeds. NACA Rep. 892, 1948. (Supersedes NACA TN 1566.)

6. Jones, Arthur L., and Alksne, Alberta: The Damping Due to Roll of Triangular, Trapezoidal, and Related Plan Forms in Supersonic Flow. NACA TN 1548, 1948.

7. Cohen, Doris: The Theoretical Lift of Flat Swept-Back Wings at Supersonic Speeds. NACA TN 1555, 1948.

8. Cohen, Doris: Theoretical Loading at Supersonic Speeds of Flat Swept-Back Wings with Interacting Trailing and Leading Edges. NACA TN 1991, 1949.

9. Malvestuto, Frank S., Jr., Margolis, Kenneth, and Ribner, Herbert S.: Theoretical Lift and Damping in Roll at Supersonic Speeds of Thin Sweptback Tapered Wings with Streamwise Tips, Subsonic Leading Edges, and Supersonic Trailing Edges. NACA Rep. 970, 1950. (Supersedes NACA TN 1860.)

10. Harmon, Sidney M., and Jeffreys, Isabella: Theoretical Lift and Damping in Roll of Thin Wings with Arbitrary Sweep and Taper at Supersonic Speeds. Supersonic Leading and Trailing Edges. NACA TN 2114, 1950.

11. Lagerstrom, P. A., and Graham, Martha E.: Some Aerodynamic Formulas in Linearized Supersonic Theory for Damping in Roll and Effect of Twist for Trapezoidal Wings. Rep. No. SM-13200, Douglas Aircraft Co., Inc., March 12, 1948.

12. Walker, Harold J., and Ballantyne, Mary B.: Pressure Distribution and Damping in Steady Roll at Supersonic Mach Numbers of Flat Swept-Back Wings with Subsonic Edges. NACA TN 2047, 1950.

13. Malvestuto, Frank S., Jr., and Hoover, Dorothy M.: Lift and Pitching Derivatives of Thin Sweptback Tapered Wings with Streamwise Tips and Subsonic Leading Edges at Supersonic Speeds. NACA TN 2294, 1951.

14. Walker, Harold J., and Ballantyne, Mary B.: Pressure Distribution and Damping in Steady Pitch at Supersonic Mach Numbers of Flat Swept-Back Wings Having All Edges Subsonic. NACA TN 2197, 1950.

15. Harmon, Sidney M.: Theoretical Relations between the Stability Derivatives of a Wing in Direct and in Reverse Supersonic Flow. NACA TN 1943, 1949.

16. Brown, Clinton E.: The Reversibility Theorem for Thin Airfoils in Subsonic and Supersonic Flow. NACA Rep. 986, 1950. (Supersedes NACA TN 1944.)

17. Evvard, John C.: Use of Source Distributions for Evaluating Theoretical Aerodynamics of Thin Finite Wings at Supersonic Speeds. NACA Rep. 951, 1950.

TABLE I.- FORMULAS FOR TRANSFORMATION OF THE STABILITY DERIVATIVES C_{m_α}, C_{L_q}, AND C_{m_q} FROM BODY AXES TO STABILITY AXES

Body axes Origin[1] at $x = 0$, $y = 0$, $z = 0$	Body axes Origin[1] at $x = \bar{x}$, $y = 0$, $z = 0$		Body axes Origin[1] at $x = d$, $y = 0$, $z = 0$ ($d = \bar{x} + a$)		Stability axes Origin[1] at $x = d$, $y = 0$, $z = 0$	
Stability derivative	Stability derivative	Shift in origin from (0,0,0) to ($\bar{x}$,0,0)	Stability derivative	Shift in origin from ($\bar{x}$,0,0) to (d,0,0)	Stability derivative	Origin at (d,0,0). Rotation through angle α (2)
C_{m_α}	$C_{m_\alpha}{}^*$	0	$C_{m_\alpha}{}'$	$\frac{a}{\bar{c}} C_{L_\alpha}$	$C_{m_\alpha}{}''$	$C_{m_\alpha}{}' - \alpha C_{m_u}{}' \approx C_{m_\alpha}{}'$
C_{L_q}	$C_{L_q}{}^*$	$C_{L_q} + 2C_{m_\alpha}$	$C_{L_q}{}'$	$C_{L_q}{}^* - 2\frac{a}{\bar{c}} C_{L_\alpha}$	$C_{L_q}{}''$	$C_{L_q}{}' - \alpha C_{X_q}{}' \approx C_{L_q}{}'$
C_{m_q}	$C_{m_q}{}^*$	$C_{m_q} - \frac{C_{m_\alpha} C_{L_q}}{C_{L_\alpha}}$	$C_{m_q}{}'$	$C_{m_q}{}^* + \frac{a}{\bar{c}} C_{L_q}{}^* - 2\frac{a^2}{\bar{c}^2} C_{L_\alpha}$	$C_{m_q}{}''$	$C_{m_q}{}'$

NACA

[1]The origin refers to the Cartesian system of coordinates as used in the analysis. (See fig. 2(a).)

[2]The value of $\alpha C_{m_u}{}'$ in the transformation for $C_{m_\alpha}{}''$ and the value of $\alpha C_{X_q}{}'$ in the transformation for $C_{L_q}{}''$ are generally small and can be neglected for estimates of $C_{m_\alpha}{}''$ and $C_{L_q}{}''$. These values have not been obtained in this paper.

TABLE II.- FORMULAS FOR POTENTIAL DISTRIBUTIONS DUE TO ANGLE OF ATTACK

Region (see sketch)	Formula for ϕ (reference 10)
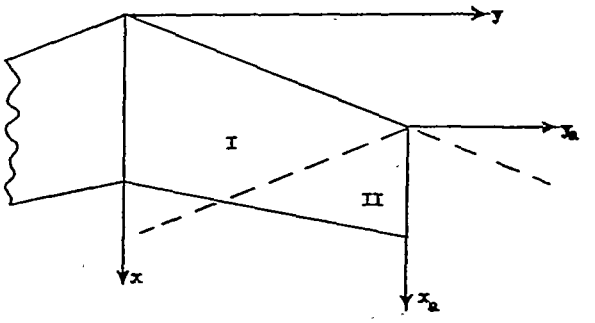 $\left[B \cot \Lambda = 1;\ \left\lvert B \cot \Lambda_{TE}\right\rvert \geqq 1\ ;\ BA \geqq \frac{4B \cot \Lambda}{(1 + \lambda)(1 + B \cot \Lambda)}\right]$	
I	$\frac{2\alpha V}{B\pi}\sqrt{x^2 - B^2y^2}$
II	$\frac{2\alpha V}{\pi}\sqrt{\frac{-2y_a}{B}\left(By_a + 2B\frac{b}{2} + x_a\right)}$
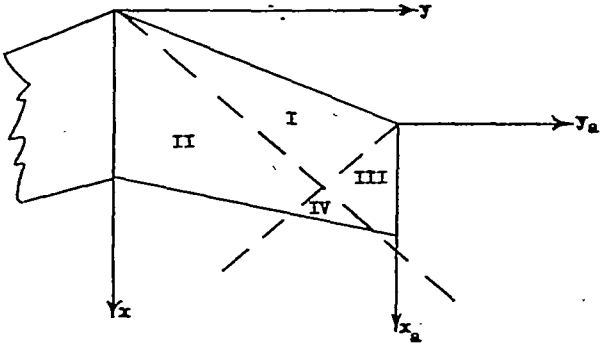 $\left[B \cot \Lambda \geqq 1;\ \left\lvert B \cot \Lambda_{TE}\right\rvert \geqq 1\ ;\ BA \geqq \frac{4B \cot \Lambda}{(1 + \lambda)(1 + B \cot \Lambda)};\ BA \geqq \frac{4B\lambda \cot \Lambda}{(1 + \lambda)(B \cot \Lambda - 1)}\right]$	
I	$\frac{V\alpha(mx - y)}{\sqrt{B^2m^2 - 1}}$
II	$\frac{V\alpha}{\pi\sqrt{B^2m^2 - 1}}\left[(mx - y)\cos^{-1}\frac{x - B^2my}{B(mx - y)} + (mx + y)\cos^{-1}\frac{x + B^2my}{B(mx + y)}\right]$
III	$\frac{V\alpha}{\pi\sqrt{B^2m^2 - 1}}\left[(mx_a - y_a)\cos^{-1}\frac{mx_a + y_a(2Bm + 1)}{mx_a - y_a} + 2\sqrt{-my_a(x_a + By_a)(Bm + 1)}\right]$
IV	$\frac{V\alpha}{\pi\sqrt{B^2m^2 - 1}}\left\{(mx_a - y_a)\left[\cos^{-1}\frac{mx_a + y_a(2Bm + 1)}{mx_a - y_a} - \cos^{-1}\frac{-mx_a + B^2m^2y_a + \frac{b}{2}(B^2m^2 - 1)}{Bm(mx_a - y_a)}\right] + \left(mx_a + 2\frac{b}{2} + y_a\right)\cos^{-1}\frac{mx_a + B^2m^2y_a + \frac{b}{2}(B^2m^2 + 1)}{Bm\left(mx_a + y_a + 2\frac{b}{2}\right)} + 2\sqrt{-my_a(x_a + By_a)(Bm + 1)}\right\}$

NACA

TABLE III.- FORMULAS FOR PRESSURE DISTRIBUTIONS DUE TO ANGLE OF ATTACK

Region (see sketch)	Formula for ΔC_p (reference 10)
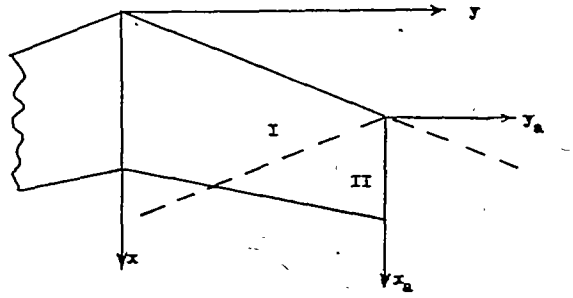 $\left[B \cot \Lambda = 1;\ \left\lvert B \cot \Lambda_{TE} \right\rvert \geqq 1\ ;\ BA \geqq \frac{4B \cot \Lambda}{(1 + \lambda)(1 + B \cot \Lambda)}\right]$	
I	$\frac{8\alpha x}{Bx\sqrt{x^2 - B^2y^2}}$
II	$\frac{4\alpha}{Bx} \frac{\sqrt{-2By_a}}{\sqrt{By_a + x_a + 2B\frac{b}{2}}}$
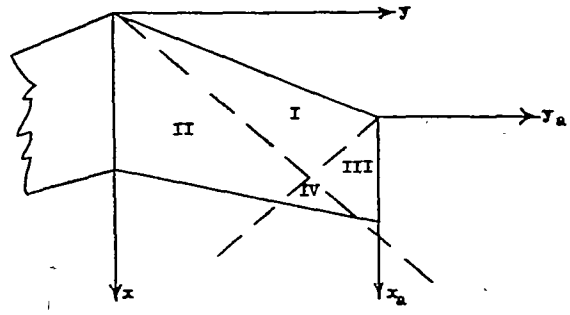 $\left[B \cot \Lambda \geqq 1;\ \left\lvert B \cot \Lambda_{TE} \right\rvert \geqq 1\ ;\ BA \geqq \frac{4B \cot \Lambda}{(1 + \lambda)(1 + B \cot \Lambda)};\ BA \geqq \frac{4BA \cot \Lambda}{(1 + \lambda)(B \cot \Lambda - 1)}\right]$	
I	$\frac{4\alpha m}{\sqrt{B^2m^2 - 1}}$
II	$\frac{4\alpha m}{\pi\sqrt{B^2m^2 - 1}}\left[\cos^{-1} \frac{x - B^2my}{B(mx - y)} + \cos^{-1} \frac{x + B^2my}{B(mx + y)}\right]$
III	$\frac{4\alpha m}{\pi\sqrt{B^2m^2 - 1}} \cos^{-1} \frac{mx_a + y_a(2Bm + 1)}{mx_a - y_a}$
IV	$\frac{4\alpha m}{\pi\sqrt{B^2m^2 - 1}}\left\{\cos^{-1} \frac{mx_a + \frac{b}{2} - B^2m^2\left(y_a + \frac{b}{2}\right)}{Bm(mx_a - y_a)} + \cos^{-1} \frac{mx_a + \frac{b}{2} + B^2m^2\left(y_a + \frac{b}{2}\right)}{Bm(mx_a + y_a + b)} - \cos^{-1} \frac{-\left[mx_a + y_a(2Bm + 1)\right]}{mx_a - y_a}\right\}$

TABLE IV.- FORMULAS FOR POTENTIAL DISTRIBUTIONS DUE TO STEADY PITCHING VELOCITY

Region (see sketch)	Formula for ϕ
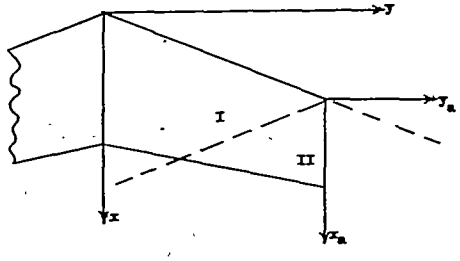 $\left[B \cot \Lambda = 1;\ \left\lvert B \cot \Lambda_{TE}\right\rvert \gtrless 1\ ;\ BA \gtrless \frac{4B \cot \Lambda}{(1 + \lambda)(1 + B \cot \Lambda)}\right]$	
I	$\frac{4qx\sqrt{x^2 - B^2y^2}}{3\pi B}$
II	$\frac{q\sqrt{2}}{3\pi B}\left[\left(5x_a + 4B\frac{b}{2} + By_a\right)\sqrt{-By_a\left(x_a + By_a + 2B\frac{b}{2}\right)}\right]$
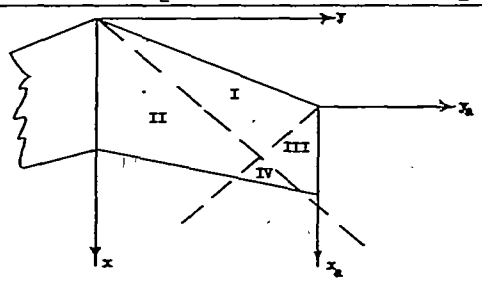 $\left[B \cot \Lambda = 1;\ \left\lvert B \cot \Lambda_{TE}\right\rvert \gtrless 1\ ;\ BA \gtrless \frac{4B \cot \Lambda}{(1 + \lambda)(1 + B \cot \Lambda)};\ BA \geq \frac{4BA \cot \Lambda}{(1 + \lambda)(B \cot \Lambda - 1)}\right]$	
I	$\frac{q}{2\left(B^2m^2 - 1\right)^{3/2}}\left[x^2\left(-2m + B^2m^3\right) + 2xy - B^2y^2m\right]$
II	$\frac{q}{\pi}\left[\frac{mx\sqrt{x^2 - B^2y^2}}{B^2m^2 - 1} + \frac{mx^2\left(B^2m^2 - 2\right) - 2yx - B^2y^2m}{2\left(B^2m^2 - 1\right)^{3/2}} \cos^{-1} \frac{x + B^2my}{Bmx + By} + \frac{mx^2\left(B^2m^2 - 2\right) + 2yx - B^2y^2m}{2\left(B^2m^2 - 1\right)^{3/2}} \cos^{-1} \frac{x - B^2my}{Bmx - By}\right]$
III	$\frac{q}{3\pi}\left\{\frac{-6mx_a - B^2m^2y_a - 4m^2Bx_a + 2B^3y_am^3 + 5x_aB^2m^3 + 6\frac{b}{2}\left(B^2m^2 - 1\right)}{m\left(B^2m^2 - 1\right)}\sqrt{\frac{-y_am\left(x_a + By_a\right)}{(Bm - 1)}} + \frac{3\left[2mx_ay_a - 2m^2x_a^2 - B^2y_a^2m^2 + B^2m^4x_a^2 + 2\frac{b}{2}\left(mx_a - y_a\right)\left(B^2m^2 - 1\right)\right]}{2m\left(B^2m^2 - 1\right)\sqrt{B^2m^2 - 1}} \cos^{-1} \frac{mx_a + y_a(2Bm + 1)}{mx_a - y_a}\right\}$
IV	$\frac{q}{\pi}\left\{\frac{2\frac{b}{2}\left(mx_a - y_a\right)\left(B^2m^2 - 1\right) + 2x_amy_a - 2m^2x_a^2 - B^2y_a^2m^2 + B^2m^4x_a^2}{2m\left(B^2m^2 - 1\right)^{3/2}}\left[\cos^{-1} \frac{mx_a + y_a(2Bm + 1)}{mx_a - y_a} - \cos^{-1} \frac{-mx_a + B^2m^2y_a + \frac{b}{2}\left(B^2m^2 - 1\right)}{Bm\left(mx_a - y_a\right)}\right] + \frac{\left(mx_a + \frac{b}{2}\right)\sqrt{\left(mx_a + \frac{b}{2}\right)^2 - B^2m^2\left(y_a + \frac{b}{2}\right)^2}}{m\left(B^2m^2 - 1\right)} + \frac{6\frac{b}{2}\left(B^2m^2 - 1\right) - 6mx_a - B^2m^2y_a - 4m^2Bx_a + 2B^3y_am^3 + 5x_aB^2m^3}{3m\left(B^2m^2 - 1\right)}\sqrt{\frac{-y_am\left(x_a + By_a\right)}{(Bm - 1)}} + \frac{\left(mx_a + \frac{b}{2}\right)^2\left(-2 + B^2m^2\right) - 2\left(mx_a + \frac{b}{2}\right)\left(y_a + \frac{b}{2}\right) - m^2B^2\left(y_a + \frac{b}{2}\right)^2}{2m\left(B^2m^2 - 1\right)^{3/2}} \cos^{-1} \frac{mx_a + B^2m^2y_a + \frac{b}{2}\left(B^2m^2 + 1\right)}{Bm\left(mx_a + y_a + 2b\right)}\right\}$

NACA

TABLE V.- FORMULAS FOR PRESSURE DISTRIBUTIONS DUE TO STEADY PITCHING VELOCITY

Region (see sketch)	Formula for ΔC_p
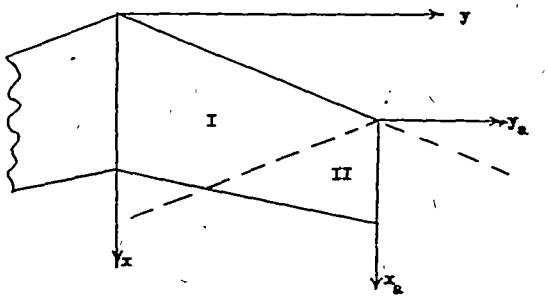 $\left[B \cot \Lambda = 1;\ \left\lvert B \cot \Lambda_{TE}\right\rvert \geqq 1\ ;\ BA \geqq \frac{4B \cot \Lambda}{(1+\lambda)(1+B \cot \Lambda)}\right]$	
I	$\frac{16q}{3\pi VB} \cdot \frac{\left(2x^2 - B^2y^2\right)}{\sqrt{x^2 - B^2y^2}}$
II	$\frac{-4q}{3\pi V} \frac{y_a\left(15x_a + 24\frac{b}{2}B + 11By_a\right)}{\sqrt{-2By_a\left(x_a + 2\frac{b}{2}B + By_a\right)}}$
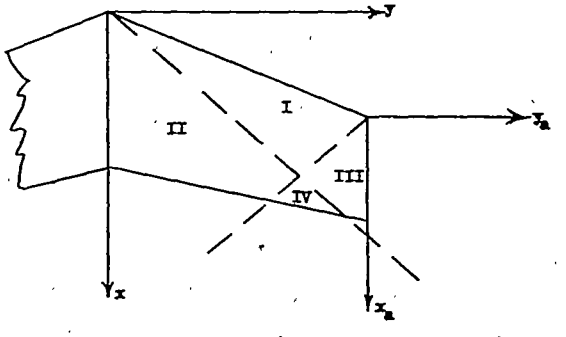 $\left[B \cot \Lambda = 1;\ \left\lvert B \cot \Lambda_{TE}\right\rvert \geqq 1\ ;\ BA \geqq \frac{4B \cot \Lambda}{(1+\lambda)(1+B \cot \Lambda)};\ BA \geqq \frac{4B\lambda \cot \Lambda}{(1+\lambda)(B \cot \Lambda - 1)}\right]$	
I	$\frac{2q}{V\left(B^2m^2 - 1\right)^{3/2}}\left[2mx\left(B^2m^2 - 2\right) + 2y\right]$
II	$\frac{4q}{\pi V}\left\{\frac{2m\sqrt{x^2 - B^2y^2}}{B^2m^2 - 1} + \frac{2mx\left(B^2m^2 - 2\right) - 2y}{2\left(B^2m^2 - 1\right)^{3/2}} \cos^{-1} \frac{x + B^2my}{Bmx + By} + \frac{2mx\left(B^2m^2 - 2\right) + 2y}{2\left(B^2m^2 - 1\right)^{3/2}} \cos^{-1} \frac{x - B^2my}{Bmx - By}\right\}$
III	$\frac{4q}{\pi V}\left[\frac{2mx_a\left(B^2m^2 - 2\right) + 2y_a + 2\frac{b}{2}\left(B^2m^2 - 1\right)}{2\left(B^2m^2 - 1\right)^{3/2}} \cos^{-1} \frac{mx_a + (2Bm + 1)y_a}{mx_a - y_a} - \frac{2\left(1 + Bm - B^2m^2\right)}{B^2m^2 - 1}\sqrt{\frac{-my_a\left(x_a + By_a\right)}{Bm - 1}}\right]$
IV	$\frac{4q}{\pi V}\left\{\frac{2mx_a\left(B^2m^2 - 2\right) + 2y_a + 2\frac{b}{2}\left(B^2m^2 - 1\right)}{2\left(B^2m^2 - 1\right)^{3/2}}\left[\cos^{-1} \frac{mx_a + (2Bm + 1)y_a}{mx_a - y_a} - \cos^{-1} \frac{-mx_a + B^2m^2y_a + \frac{b}{2}\left(B^2m^2 - 1\right)}{Bm\left(mx_a - y_a\right)}\right] - \frac{2\left(1 + Bm - B^2m^2\right)}{B^2m^2 - 1}\sqrt{\frac{-my_a\left(x_a + By_a\right)}{Bm - 1}} + \frac{2\sqrt{\left(mx_a + \frac{b}{2}\right)^2 - B^2m^2\left(y_a + \frac{b}{2}\right)^2}}{B^2m^2 - 1} + \frac{2mx_a\left(B^2m^2 - 2\right) - 2y_a + 2\frac{b}{2}\left(B^2m^2 - 3\right)}{2\left(B^2m^2 - 1\right)^{3/2}} \cos^{-1} \frac{mx_a + B^2m^2y_a + \frac{b}{2}\left(B^2m^2 + 1\right)}{Bm\left(mx_a + y_a + 2\frac{b}{2}\right)}\right\}$

NACA

TABLE VI.- INDEX TO DESIGN CHARTS FOR BC_{m_α}

[Pitching and moments measured about (0,0,0)]

λ	A'	$\cot^{-1}m'$ (deg)	m'	Figure	Page
0	3	18.4 to 45	3 to 1	11(a)	49
	4	0 to 45	∞ to 1		
	5				
	6				
	8				
	8			11(b)	50
	12				
	20				
	4	0 to 12	∞ to 4.7	11(c)	51
	5				
	6				
	8				
	12				
	20	0 to 10.8	∞ to 5.2		
0.25	3	3.81 to 45	15.06 to 1	12(a)	52
	4	0 to 45	∞ to 1		
	5				
	6				
	6			12(b)	53
	8				
	12				
	20				
	3	3.81 to 12	15.06 to 4.7	12(c)	54
	4	0 to 12	∞ to 4.7		
	5				
	6				
	8				
	12	0 to 9	∞ to 6.31		
	20	0 to 5.3	∞ to 10.78		
0.50	3	0 to 45	∞ to 1	13(a)	55
	4				
	5				
	6				
	8				
	8			13(b)	56
	12				
	20				

λ	A'	$\cot^{-1}m'$ (deg)	m'	Figure	Page
0.50	3	0 to 12	∞ to 4.7	13(c)	57
	4				
	5				
	6				
	8				
	12				
	20	0 to 11.6	∞ to 4.87		
0.75	3	0 to 45	∞ to 1	14(a)	58
	4				
	5				
	6				
	8	0 to 38.2	∞ to 1.27		
	8	0 to 45	∞ to 1	14(b)	59
	12				
	20				
	3	0 to 12	∞ to 4.7	14(c)	60
	4				
	5				
	6				
	8				
	12				
	20	0 to 10.4	∞ to 5.45		
1.0	2	0 to 45	∞ to 1	15(a)	61
	3				
	4				
	5				
	6				
	6			15(b)	62
	8				
	12				
	20				
	2	0 to 6	∞ to 9.4	15(c)	63
	3				
	4				
	5				
	6				
	8				
	12				
	20				

NACA

TABLE VII.- INDEX TO DESIGN CHARTS FOR BC_{L_q}*

[Pitching and moments measured about $(\bar{x},0,0)$]

λ	A'	$\cot^{-1}m'$ (deg)	m'	Figure	Page
0	3	18.4 to 45	3 to 1	16(a)	64
	4	0 to 45	∞ to 1		
	5				
	6				
	8			16(b)	65
	8				
	12				
	20				
	4	0 to 34	∞ to 1.48	16(c)	66
	5				
	6	0 to 33.7	∞ to 1.5		
	8	0 to 27	∞ to 1.96		
	12	0 to 18	∞ to 3.08		
	20	0 to 11.2	∞ to 5.14		
0.25	3	3.81 to 45	15.06 to 1	17(a)	67
	4	0 to 45	∞ to 1		
	5				
	6				
	8			17(b)	68
	8				
	12				
	20				
	3	3.81 to 12.6	15.06 to 4.47	17(c)	69
	4	0 to 24	∞ to 2.25		
	5				
	6				
	8				
	12				
	20	0 to 23.6	∞ to 2.29		

λ	A'	$\cot^{-1}m'$ (deg)	m'	Figure	Page
0.50	3	0 to 45	∞ to 1	18(a)	70
	4				
	5				
	5			18(b)	71
	6				
	8				
	8			18(c)	72
	12				
	20				
0.75	3	0 to 45		19(a)	73
	4				
	5				
	6	0 to 32.6	∞ to 1.56		
	8	0 to 29.2	∞ to 1.79		
	12	0 to 27.1	∞ to 1.95		
	20	0 to 25.3	∞ to 2.12		
	6	32.4 to 45	1.56 to 1	19(b)	74
	8	29.4 to 45	1.77 to 1		
	12	27 to 45	1.95 to 1		
	20	25 to 45	2.13 to 1		
1.0	2	0 to 45	∞ to 1	20(a)	75
	3				
	4				
	5				
	6	0 to 34.6	∞ to 1.45		
	8	0 to 31	∞ to 1.66		
	12	0 to 29	∞ to 1.8		
	20	0 to 27.4	∞ to 1.96		
	6	26 to 45	2.05 to 1	20(b)	76
	8				
	12				
	20				

NACA

TABLE VIII.- INDEX TO DESIGN CHARTS FOR $BC_{m_q}{}^*$

[Pitching and moments measured about $(\bar{x},0,0)$]

λ	A'	cot⁻¹m' (deg)	m'	Figure	Page
0	3	18.4 to 45	3 to 1	21(a)	77
	4	0 to 45	∞ to 1		
	5				
	6				
	8	0 to 37.2	∞ to 1.36		
	12	0 to 26	∞ to 2.05		
	20	0 to 15.4	∞ to 3.63		
	8	26 to 45	2.05 to 1	21(b)	78
	12	19.4 to 45	2.84 to 1		
	20	13 to 45	4.33 to 1		
0.25	3	3.81 to 45	15.06 to 1	22(a)	79
	4	0 to 45	∞ to 1		
	5	0 to 41.2	∞ to 1.14		
	6	0 to 36	∞ to 1.38		
	8	0 to 27.6	∞ to 1.91		
	12	0 to 18.6	∞ to 2.97		
	20	0 to 11.2	∞ to 5.05		
	5	32 to 45	1.6 to 1	22(b)	80
	6	26 to 45	2.05 to 1		
	8	20 to 45	2.75 to 1		
	12	14 to 45	4.01 to 1		
	20	8 to 45	7.12 to 1		
0.50	3	0 to 45	∞ to 1	23(a)	81
	4				
	5				
	6	0 to 41.2	∞ to 1.14		
	8	0 to 34.6	∞ to 1.45		
	12	0 to 22.2	∞ to 2.45		
	20	0 to 13.6	∞ to 4.13		
	6	35 to 45	1.43 to 1	23(b)	82
	8	26 to 45	2.05 to 1		
	12	17 to 45	3.27 to 1		
	20	10.4 to 45	5.45 to 1		
	3	0 to 14	∞ to 4	23(c)	83
	4				
	5				
	6				
	8				
	12	0 to 13.4	∞ to 4.2		
	20	0 to 7.8	∞ to 7.3		
0.75	3	0 to 45	∞ to 1	24(a)	84
	4				
	5				
	6				
	8				
	12				
	20	0 to 35.6	∞ to 1.4		
	3	0 to 14	∞ to 4	24(b)	85
	4				
	5				
	6				
	8				
	12				
	20	0 to 9.1	∞ to 6.24		
	8	29 to 45	1.8 to 1	24(c)	86
	12				
	20				
1.0	2	0 to 45	∞ to 1	25(a)	87
	3				
	4				
	5	0 to 38.4	∞ to 1.26		
	6	0 to 33.3	∞ to 1.52		
	8	0 to 24.5	∞ to 2.19		
	12	0 to 16.8	∞ to 3.31		
	20	0 to 9.2	∞ to 6.17		
	5	0 to 45	∞ to 1	25(b)	88
	6				
	8				
	12				
	20				

TABLE IX.- INDEX TO DESIGN CHARTS FOR BC_{L_α}

λ	A'	$\cot^{-1}m'$ (deg)	m'	Figure	Page	λ	A'	$\cot^{-1}m'$ (deg)	m'	Figure	Page
0	3	18.4 to 45	3 to 1	26(a)	89	0.50	3	0 to 45	∞ to 1	28	93
	4	0 to 45	∞ to 1				4				
	5						5				
	6						6				
	8						8				
	12						12				
	20						20				
	4	0 to 12	∞ to 4.7	26(b)	90	0.75	3	0 to 45		29	94
	5						4				
	6						5				
	8						6				
	12						8				
	20						12				
							20				
0.25	3	3.81 to 45	15.06 to 1	27(a)	91						
	4	0 to 45	∞ to 1			1.0	2	0 to 45		30	95
	5						3				
	6						4				
	8						5				
	12						6				
	20						8				
							12				
	3	3.81 to 12	15.06 to 4.7	27(b)	92		20				
	4	0 to 12	∞ to 4.7								
	5										
	6										
	8										
	12										
	20										

NACA

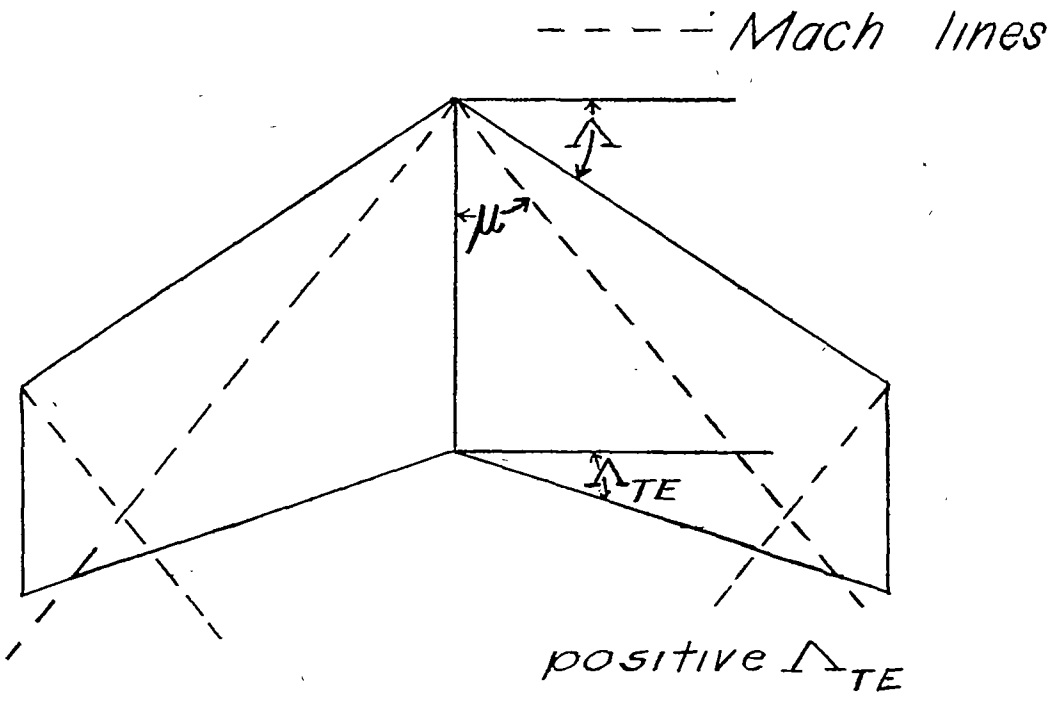

(a) Sweptback trailing edge.

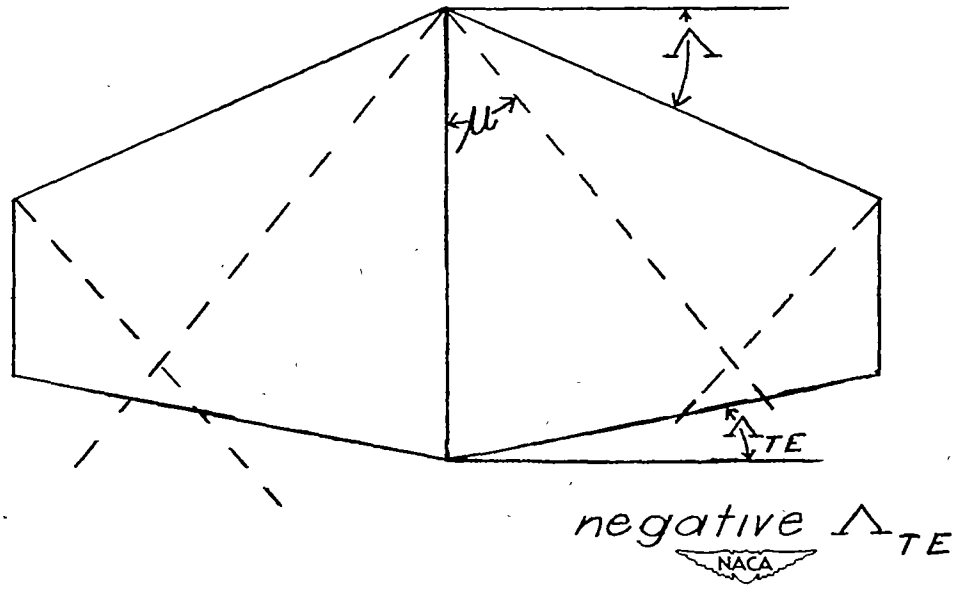

(b) Sweptforward trailing edge.

Figure 1.- Types of wings analyzed.

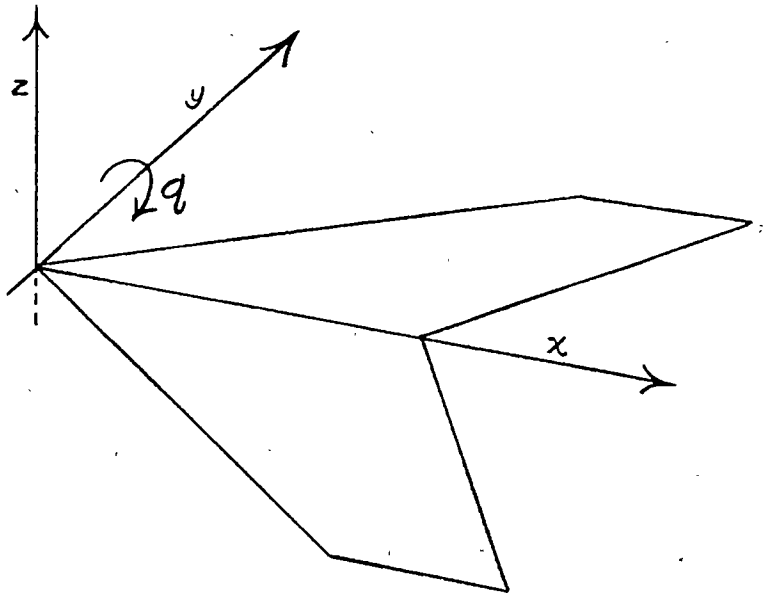

(a) Notation and body axes used in analysis.

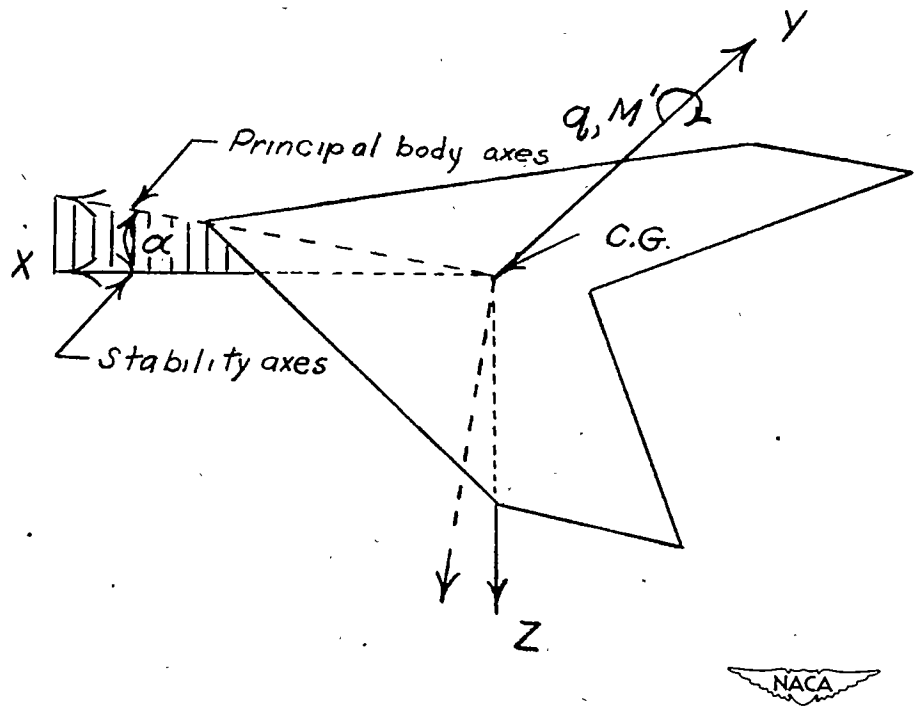

(b) Stability axes (principal body axes dashed for comparison).

Figure 2.- Systems of axes and associated data.

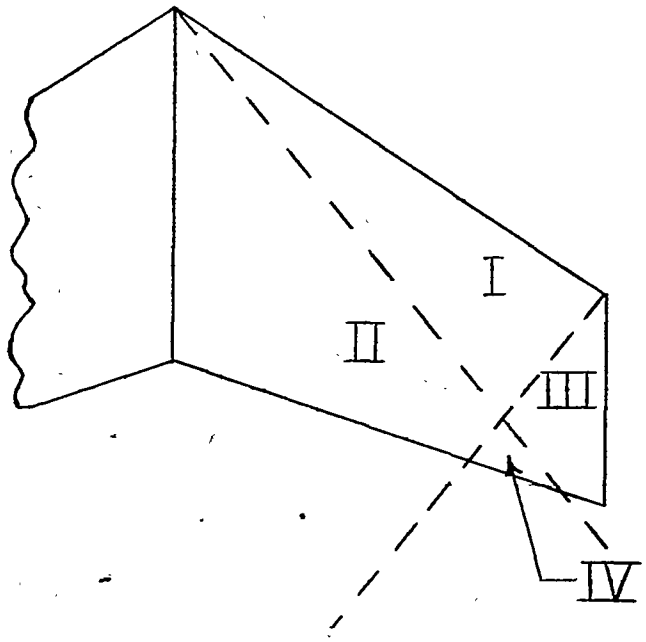

Figure 3.- Regions of wing.

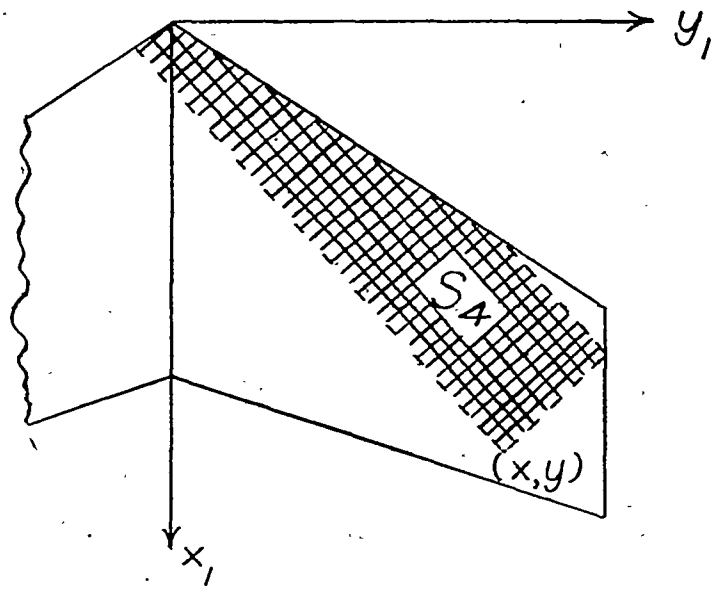

Figure 4.- Area of integration used to evaluate the potentials in region IV.

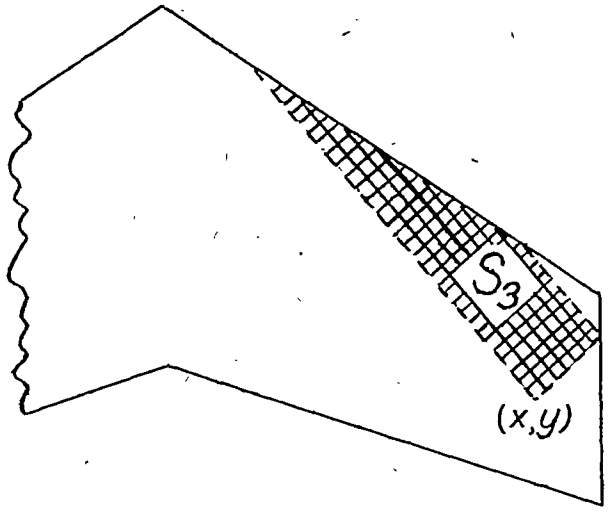

Figure 5.- Area of integration used to evaluate the potentials in region III.

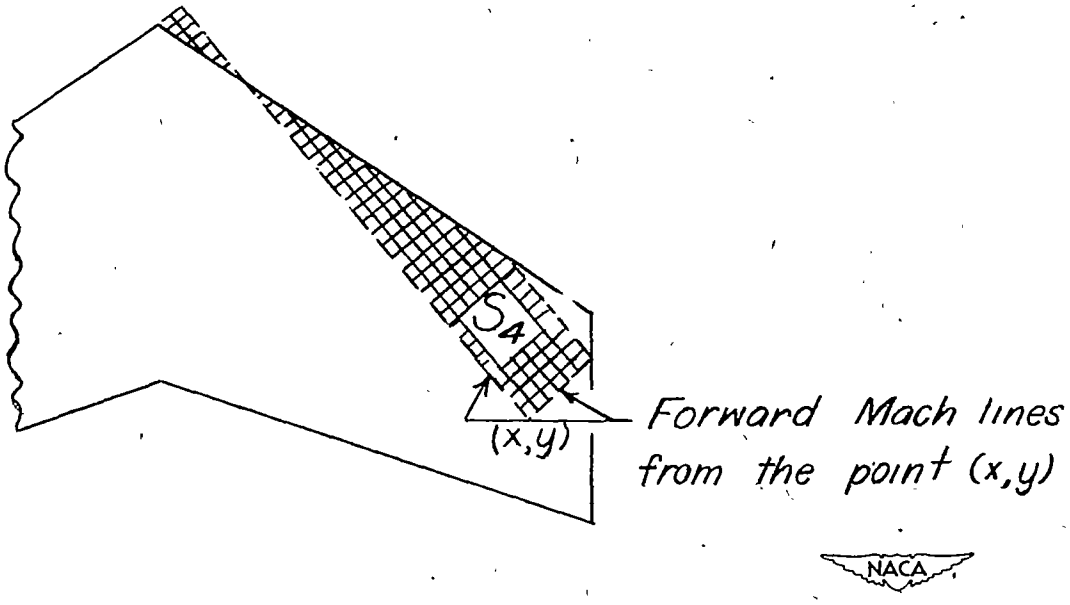

Figure 6.- The area S_4 for a point (x,y) in region III.

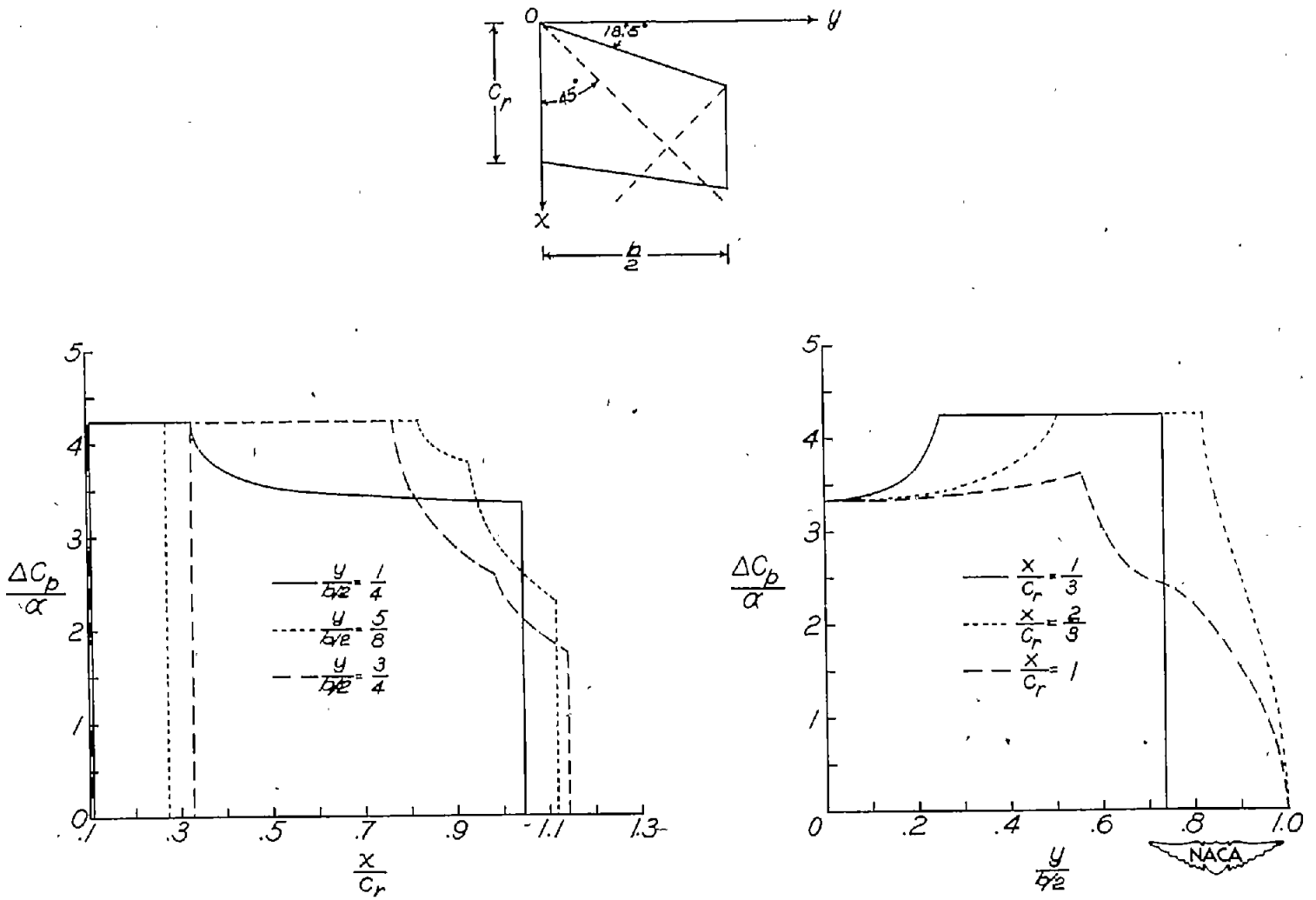

Figure 7.- Chordwise and spanwise pressure distributions for angle of attack. $A = 3$; $\Lambda = 18.5^{\circ}$; $\lambda = 0.75$; $M = \sqrt{2}$.

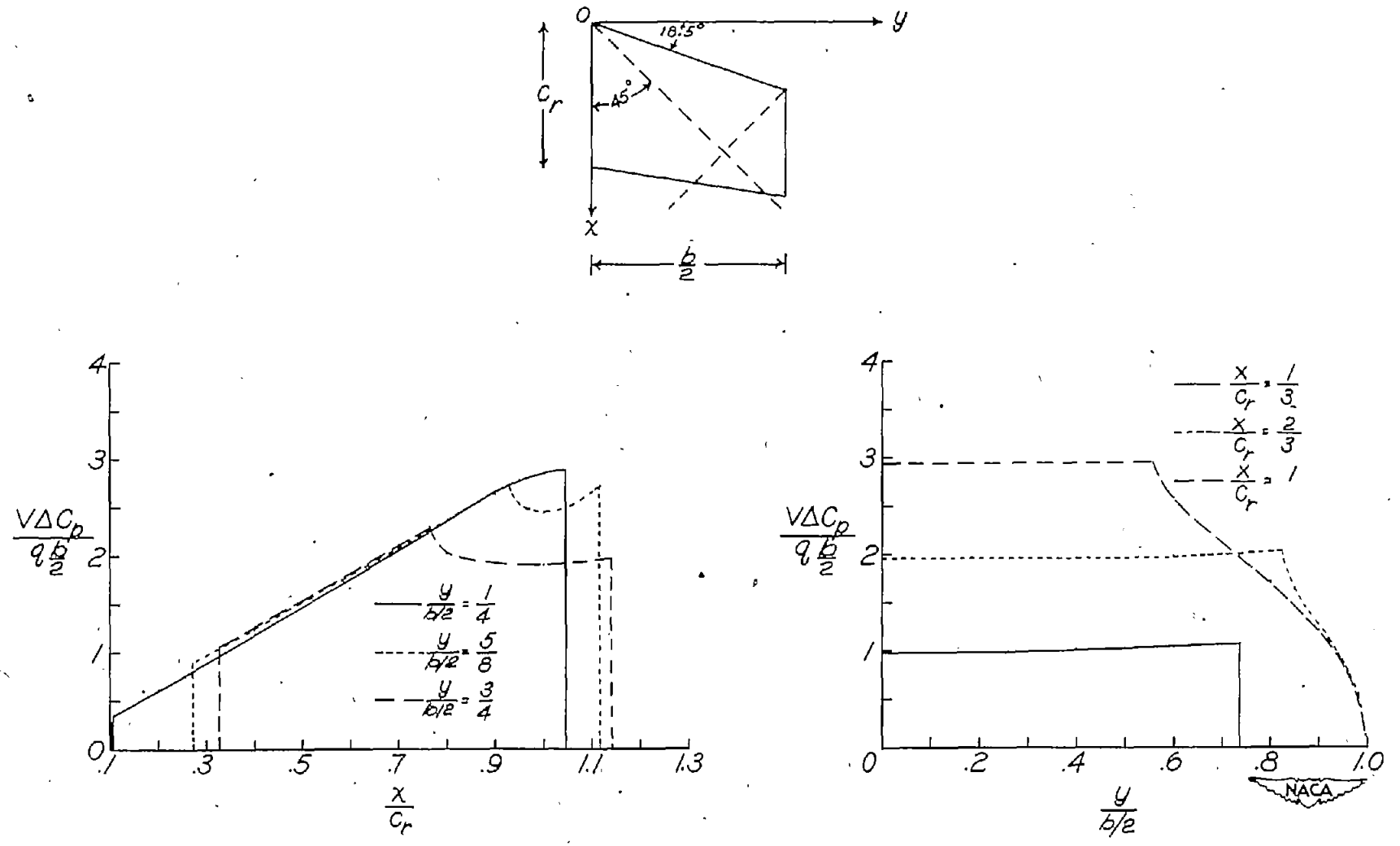

Figure 8.- Chordwise and spanwise pressure distributions for steady pitching velocity. $A = 3$; $\Lambda = 18.5^{\circ}$; $\lambda = 0.75$; $M = \sqrt{2}$.

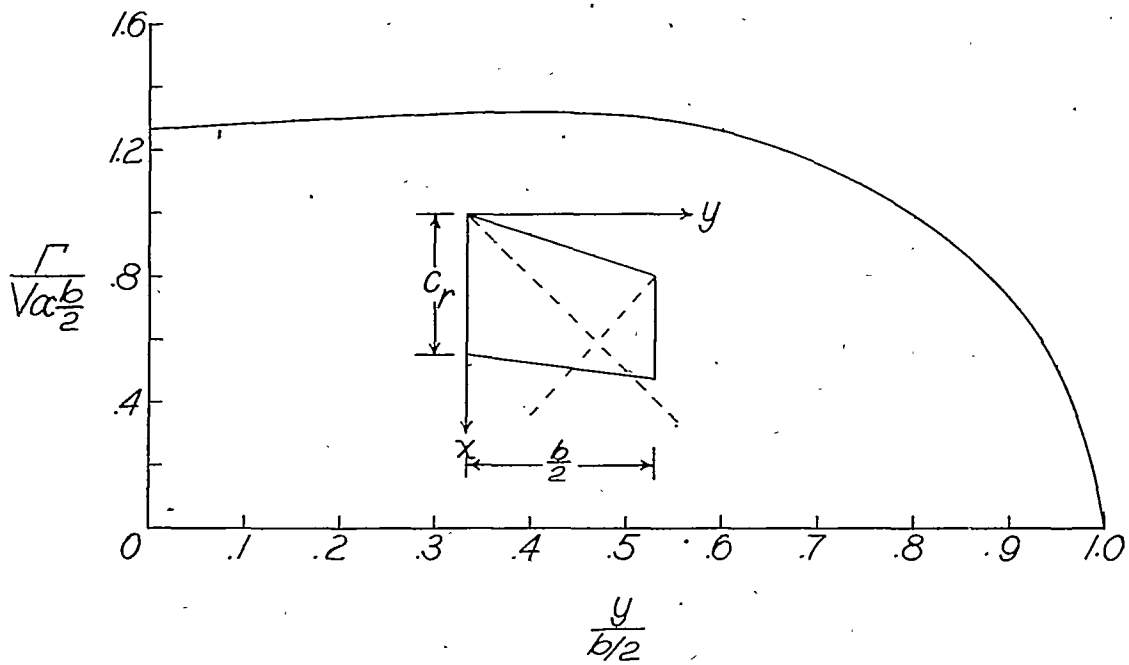

Figure 9.- Circulation along the span for angle of attack. A = 3; $\Lambda = 18.5^{\circ}$; $\lambda = 0.75$; $M = \sqrt{2}$.

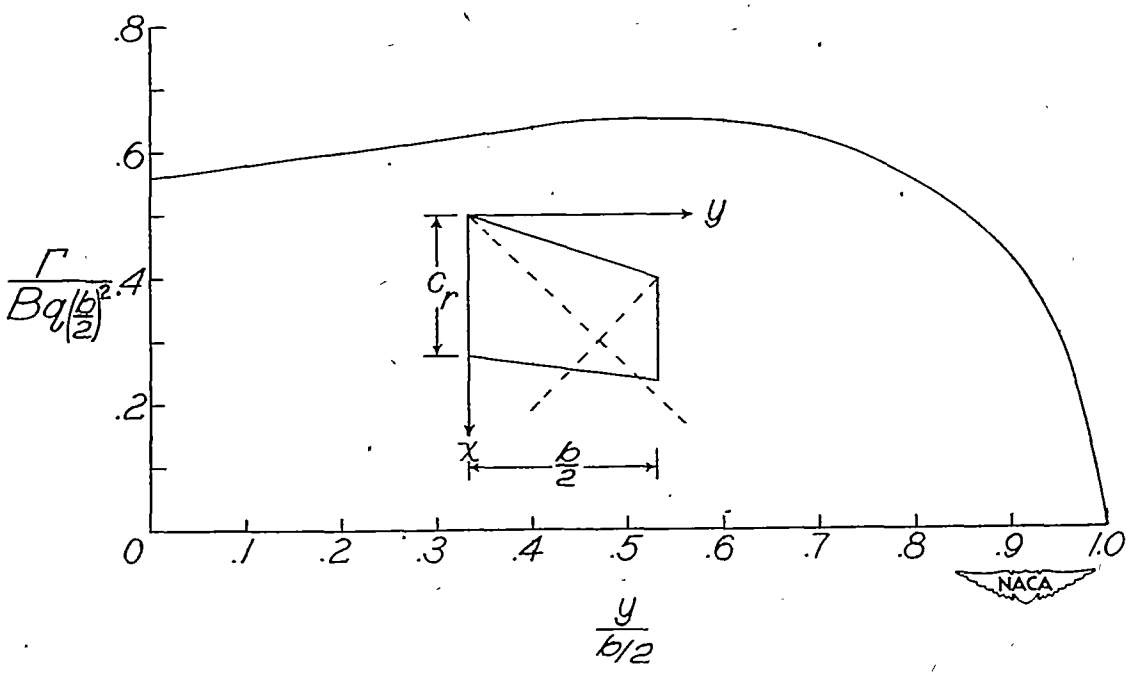

Figure 10.- Circulation along the span for steady pitching velocity. A = 3; $\Lambda = 18.5^{\circ}$; $\lambda = 0.75$; $M = \sqrt{2}$.

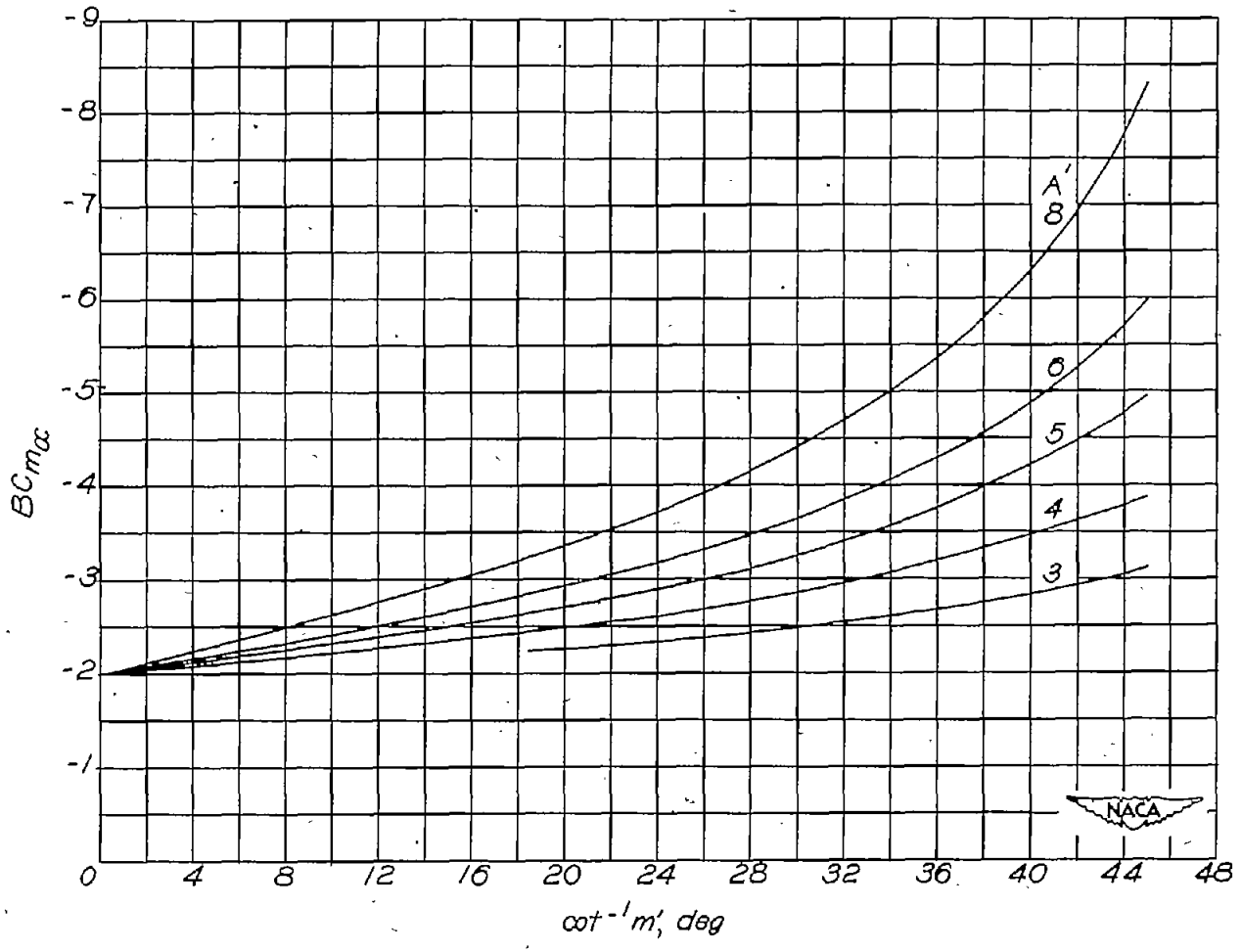

(a) $\lambda = 0$; $A' = 3$ to 8; $m' = \infty$ to 1.

Figure 11.- Variation of BC_{m_α} with $\cot^{-1}m'$ for various values of A'. System of body axes with origin at (0,0,0).

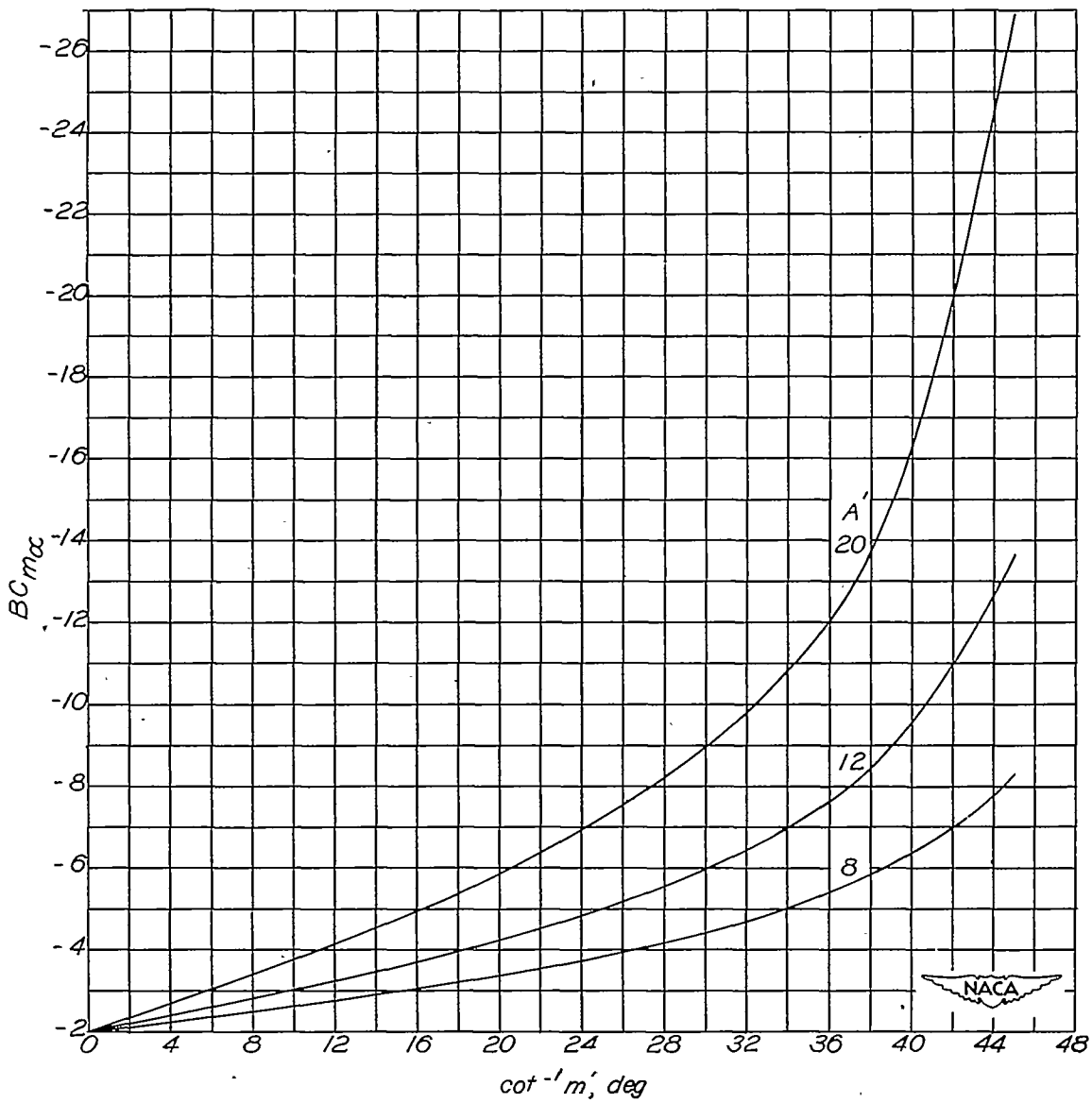

(b) $\lambda = 0$; $A' = 8$ to 20; $m' = \infty$ to 1.

Figure 11.- Continued.

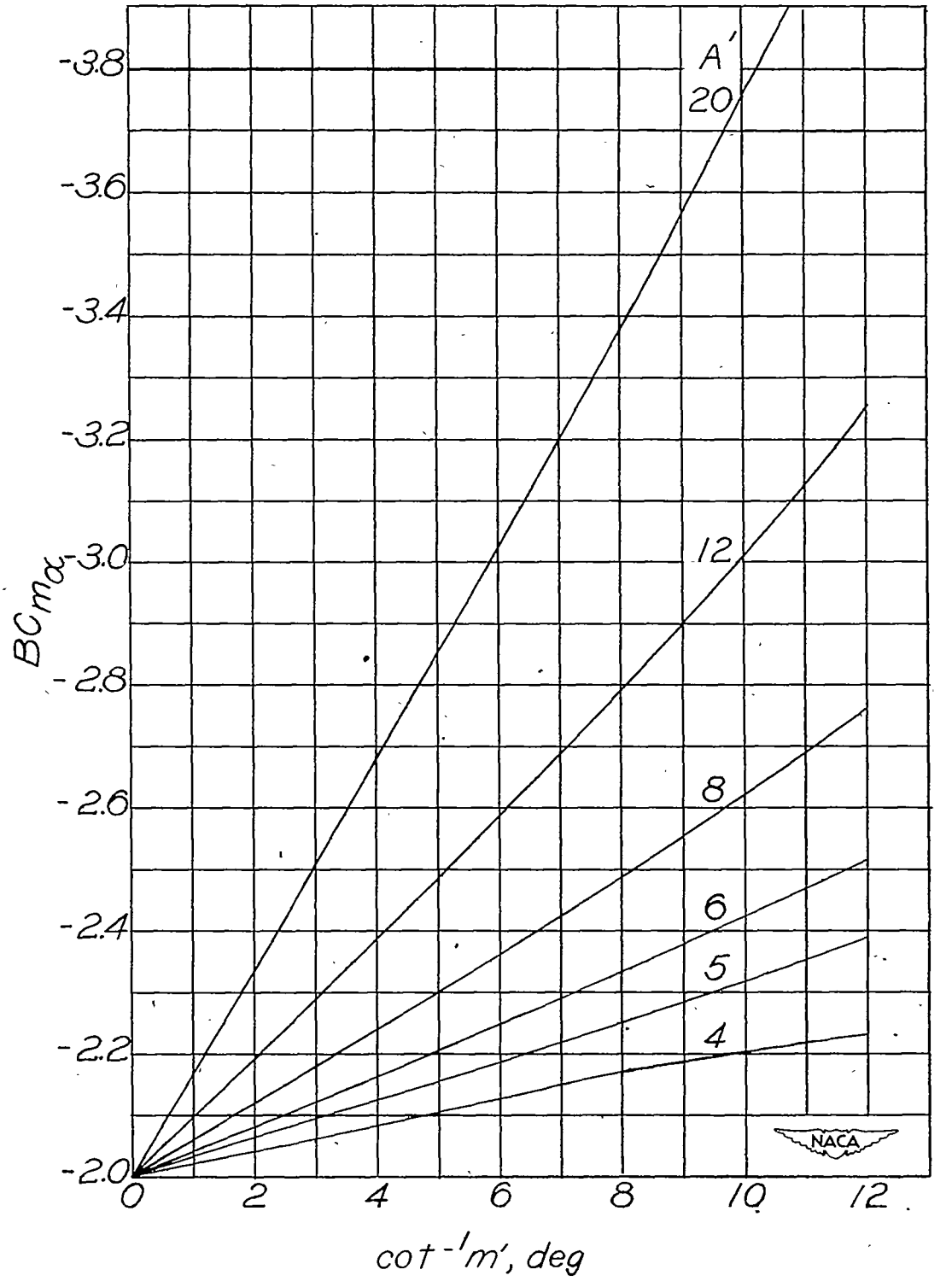

(c) $\lambda = 1$; $A' = 4$ to 20; $m' = \infty$ to 4.7.

Figure 11.- Concluded.

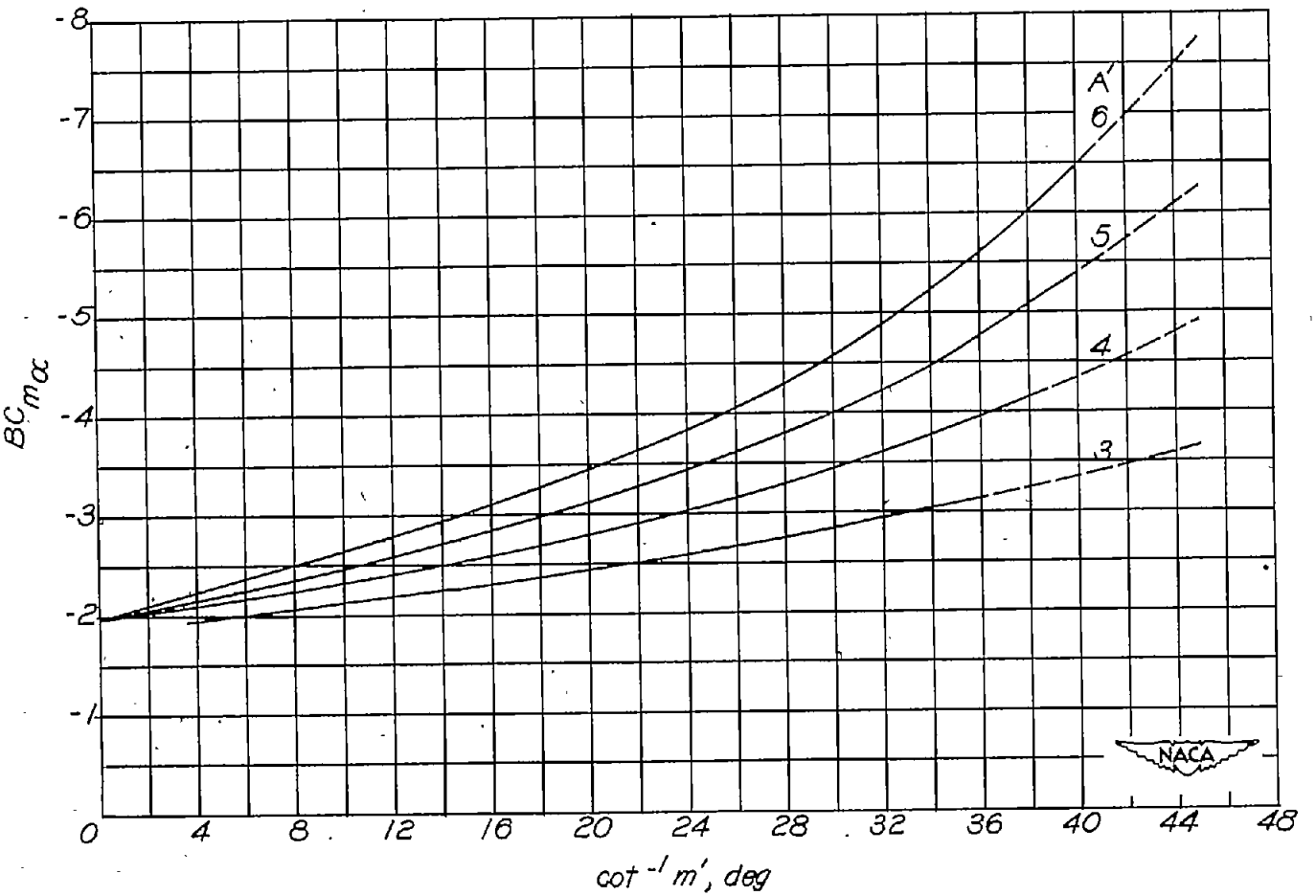

(a) $\lambda = 0.25$; $A' = 3$ to 6; $m' = \infty$ to 1.

Figure 12.- Variation of BC_{m_α} with $\cot^{-1}m'$ for various values of A'. System of body axes with origin at (0,0,0). (See text, p. 11, for significance of dashed portions of curves.)

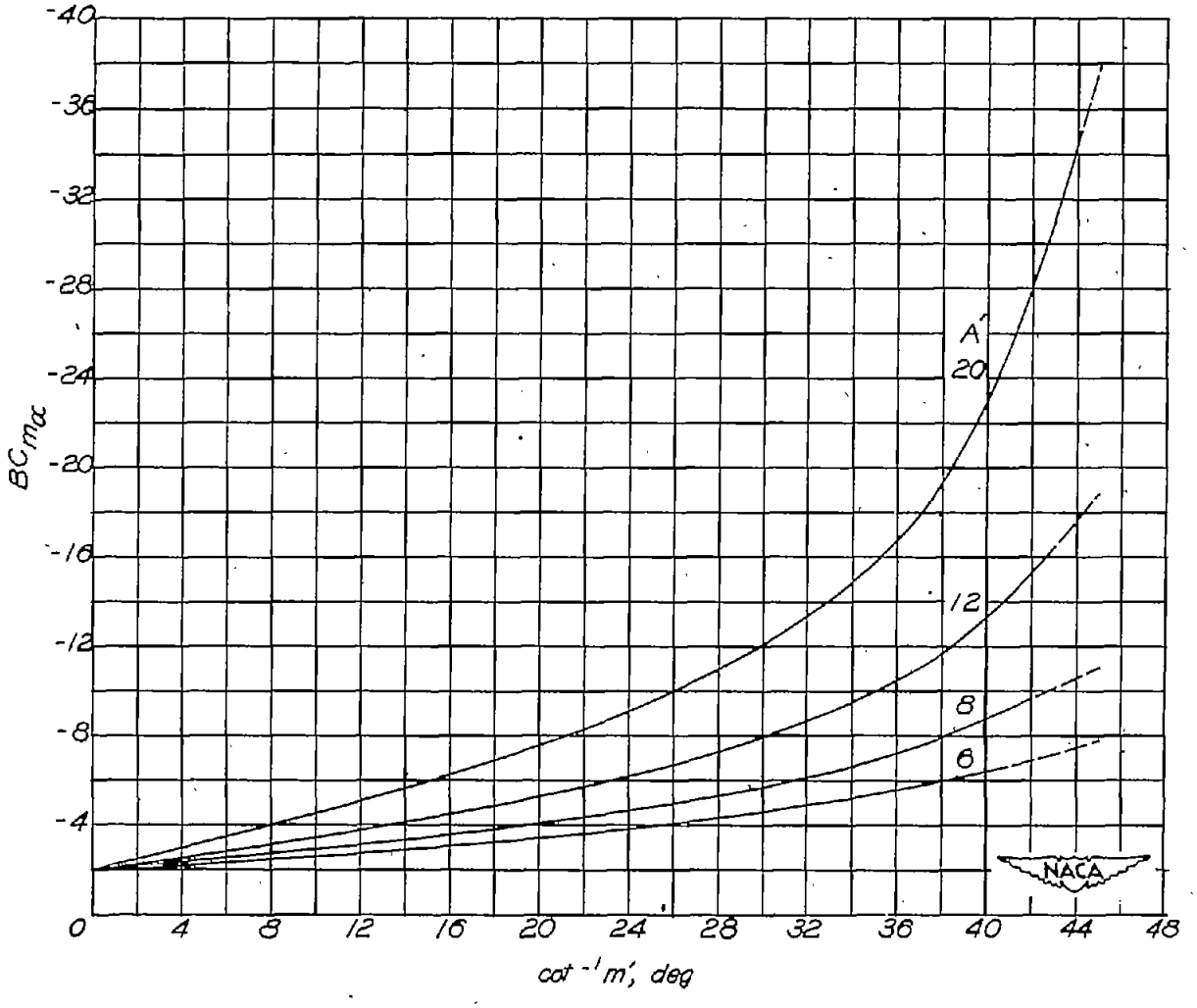

(b) $\lambda = 0.25$; $A' = 6$ to 20; $m' = \infty$ to 1.

Figure 12.- Continued.

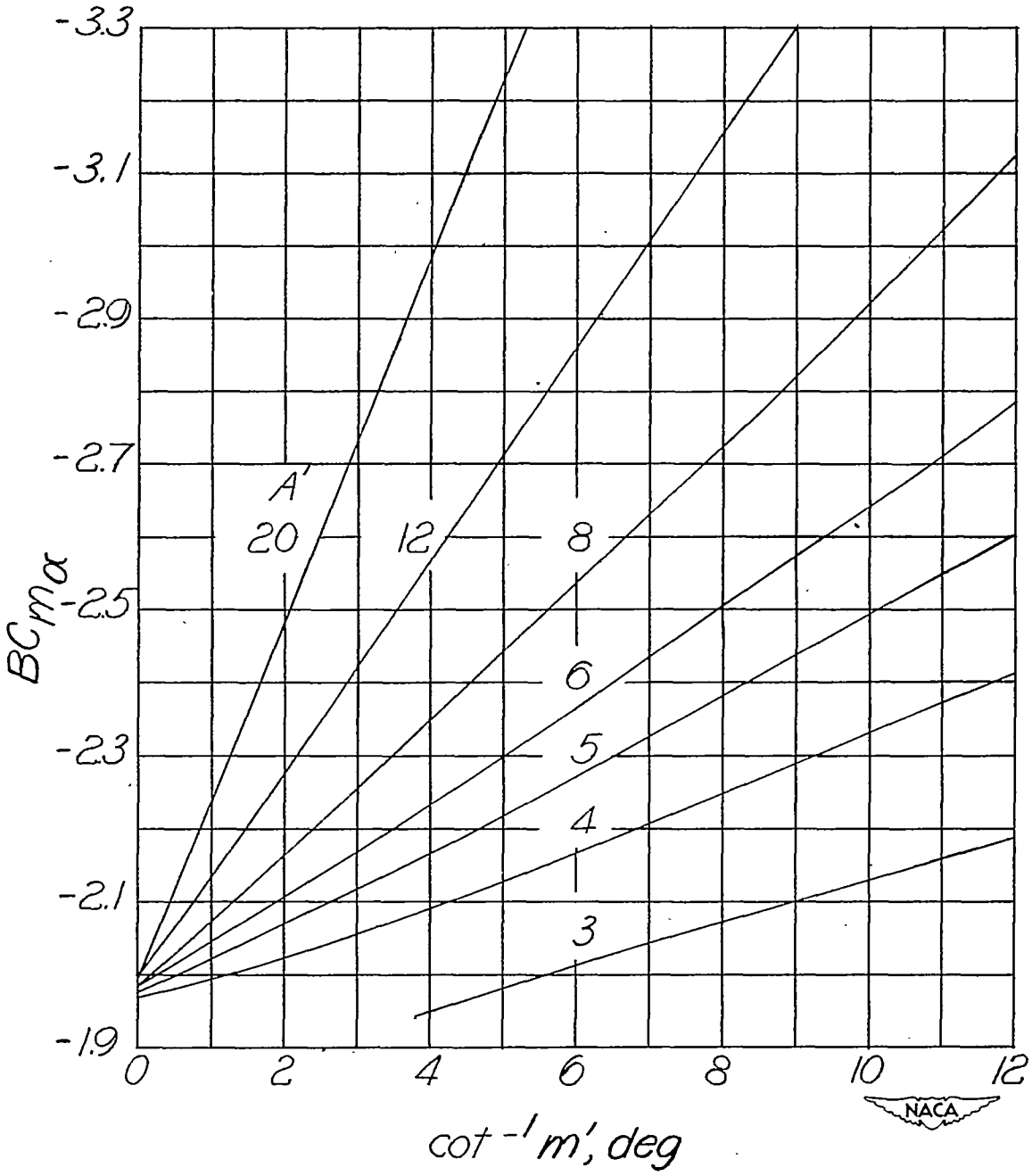

(c) $\lambda = 0.25$; $A' = 3$ to 20; $m' = \infty$ to 4.7.

Figure 12.- Concluded.

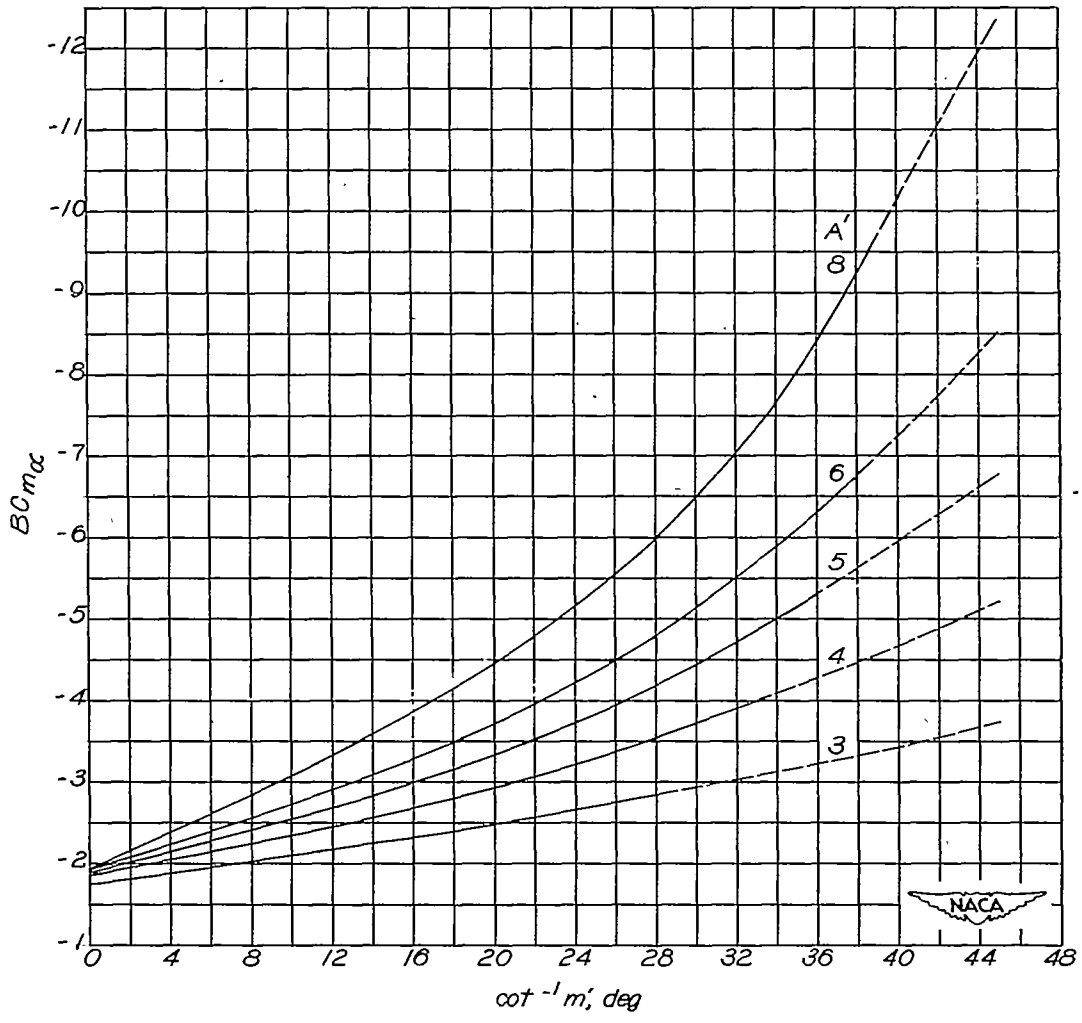

(a) $\lambda = 0.50$; $A' = 3$ to 8; $m' = \infty$ to 1.

Figure 13.- Variation of BC_{m_α} with $\cot^{-1}m'$ for various values of A'. System of body axes with origin at (0,0,0). (See text, p. 11, for significance of dashed portions of curves.)

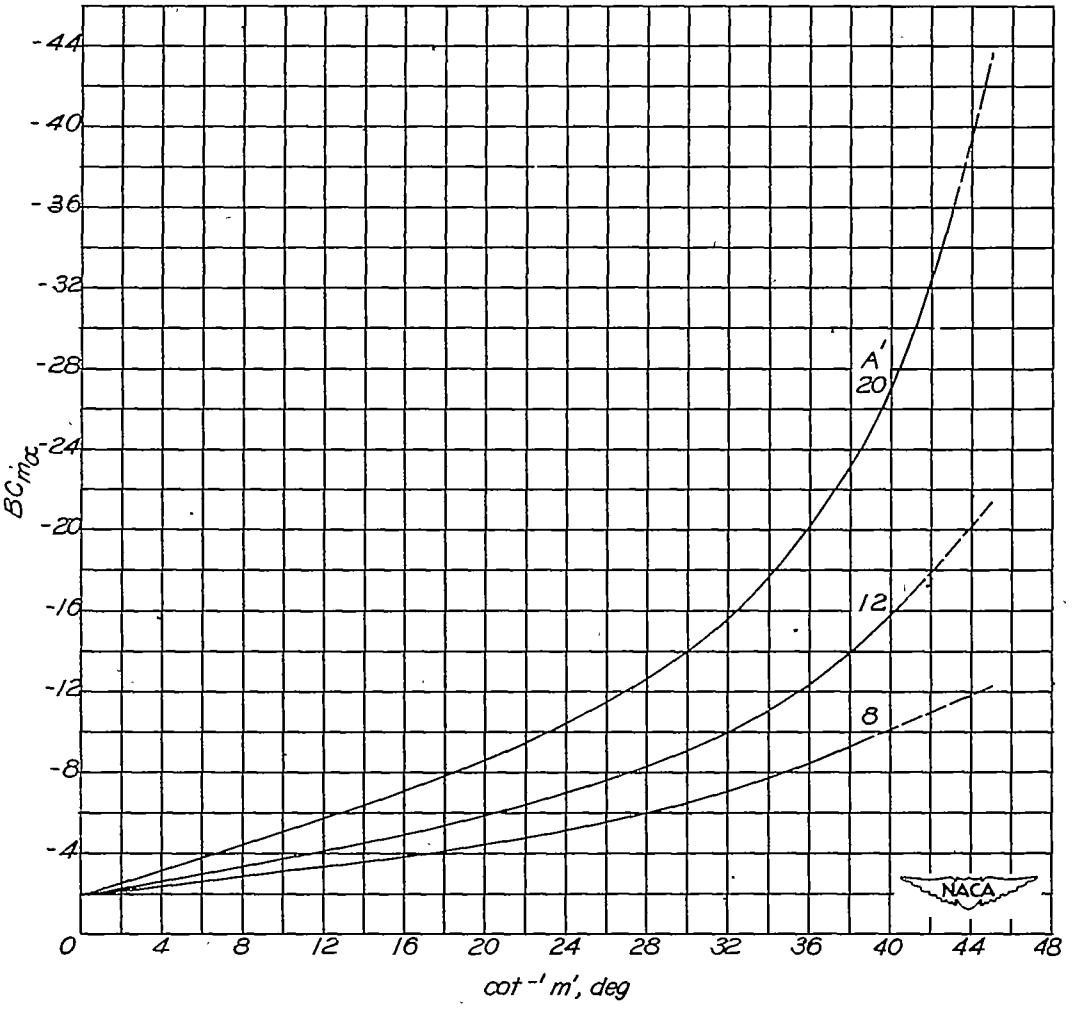

(b) $\lambda = 0.50$; $A' = 8$ to 20; $m' = \infty$ to 1.

Figure 13.- Continued.

8D

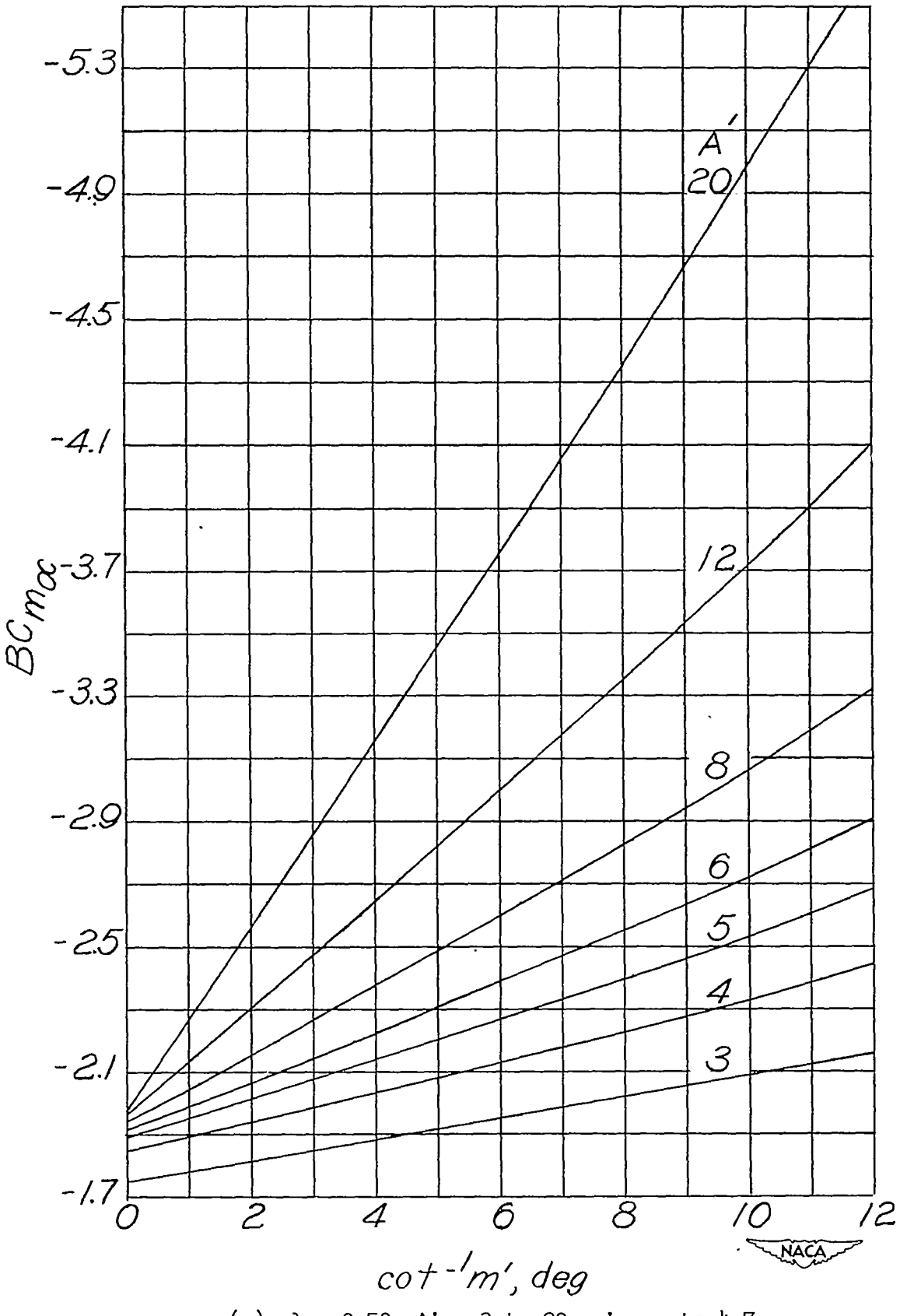

(c) $\lambda = 0.50$; $A' = 3$ to 20; $m' = \infty$ to 4.7.

Figure 13.- Concluded.

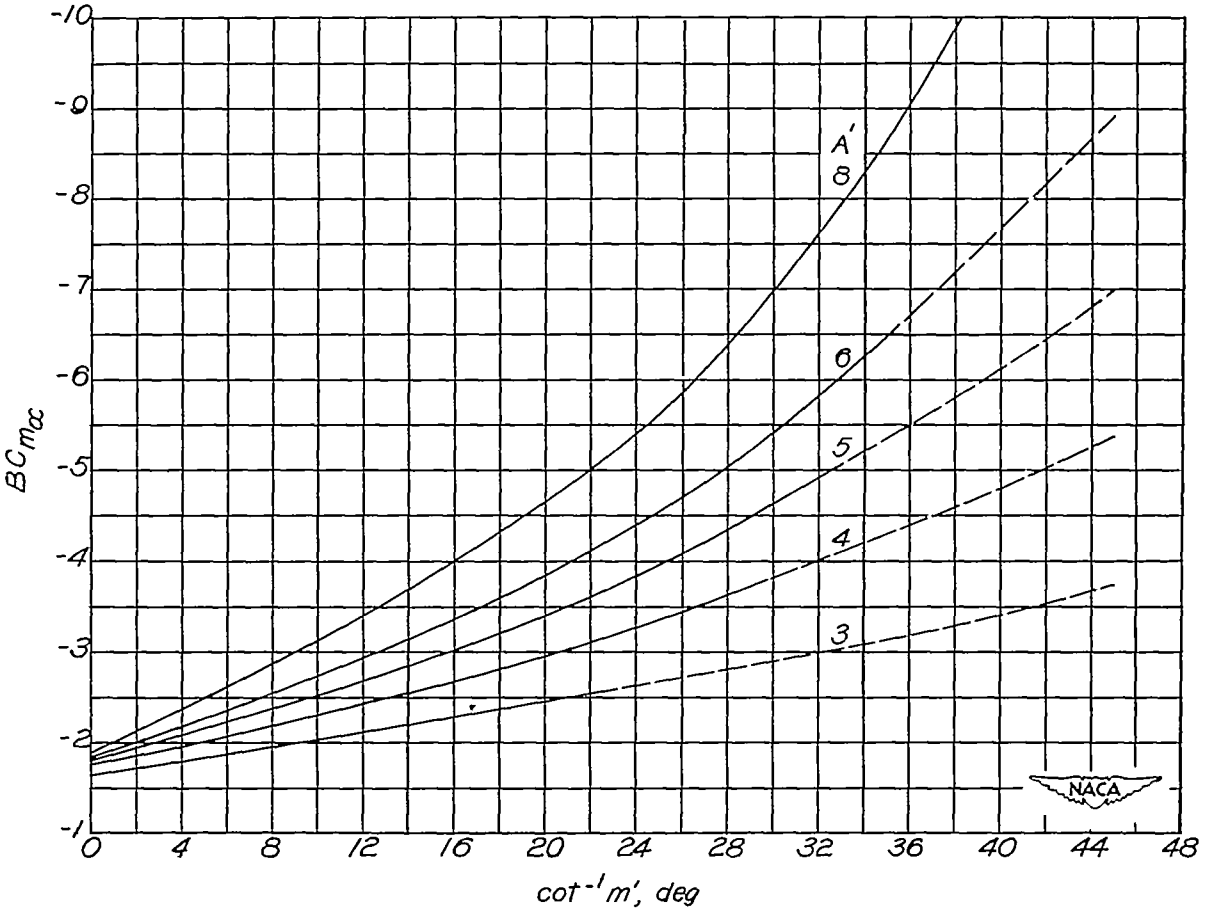

(a) $\lambda = 0.75$; $A' = 3$ to 8; $m' = \infty$ to 1.

Figure 14.- Variation of BC_{m_α} with $\cot^{-1}m'$ for various values of A'. System of body axes with origin at (0,0,0). (See text, p. 11, for significance of dashed portions of curves.)

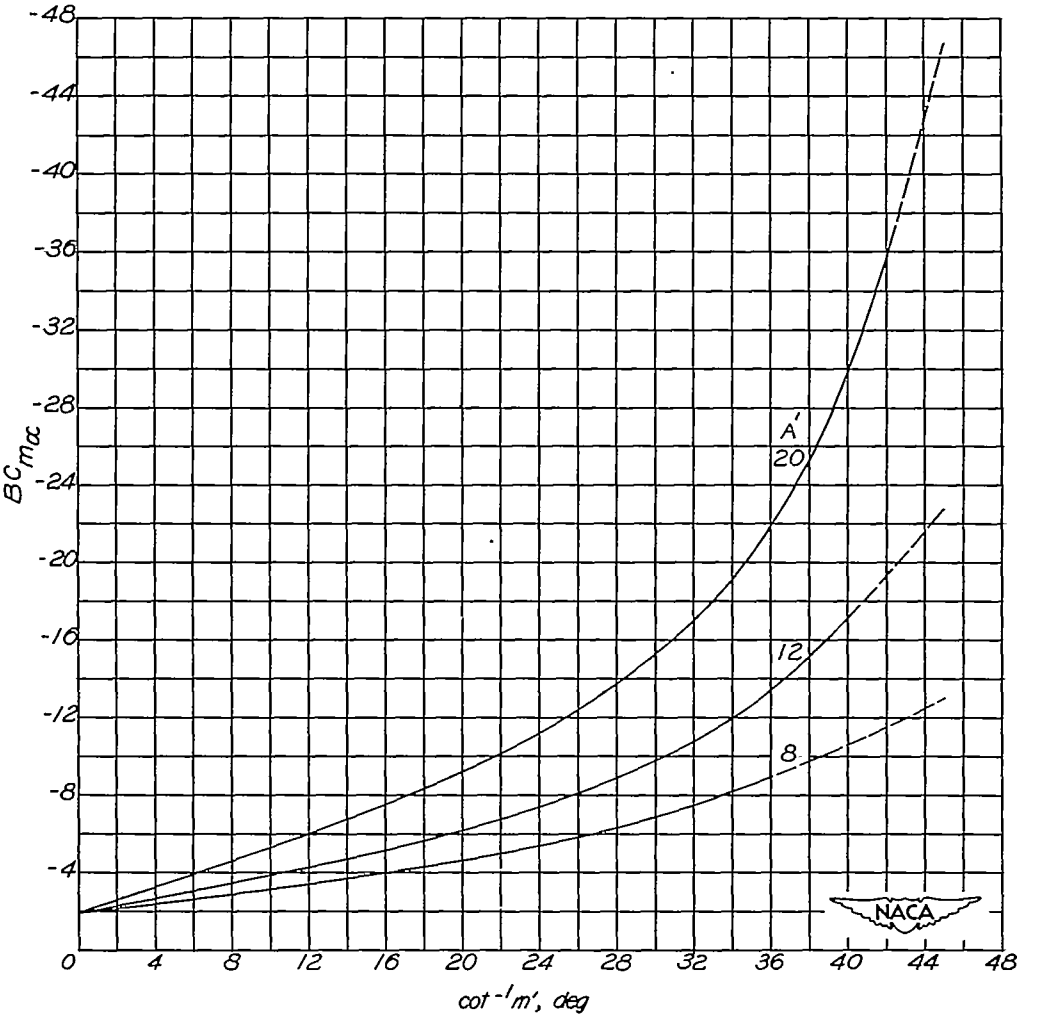

(b) $\lambda = 0.75$; A' = 8 to 20; m' = ∞ to 1.

Figure 14.- Continued.

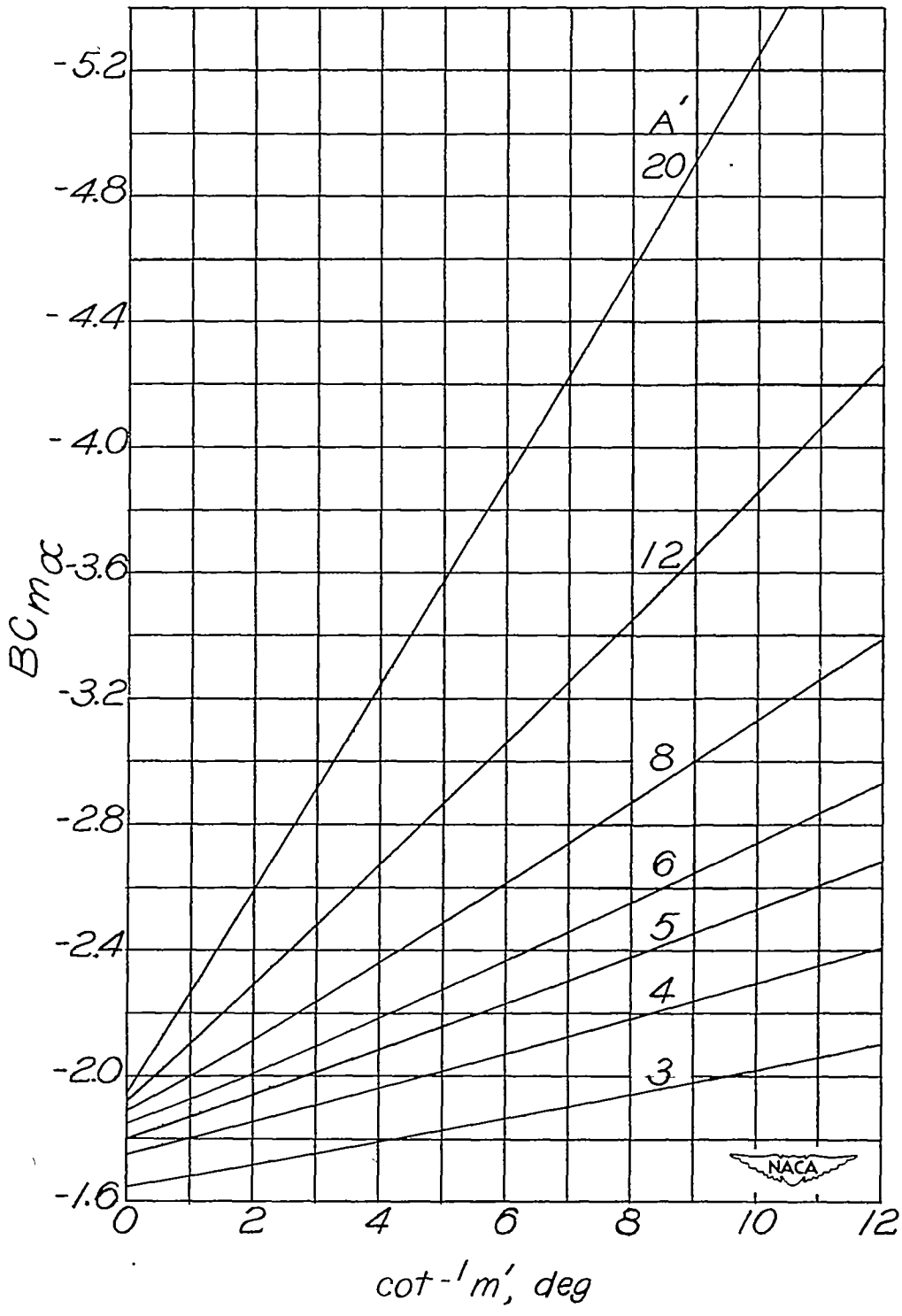

(c) $\lambda = 0.75$; A' = 3 to 20; m' = ∞ to 4.7.

Figure 14.- Concluded.

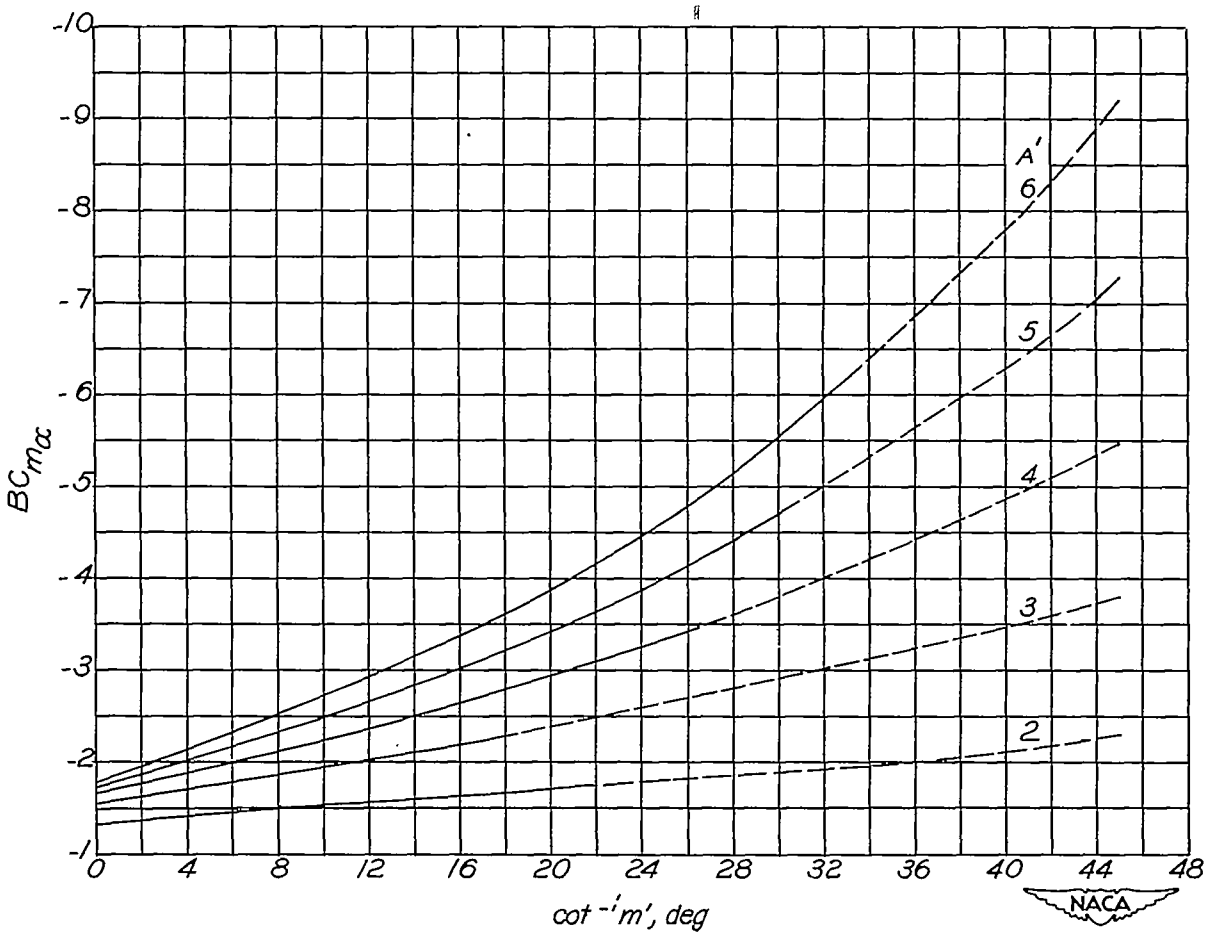

(a) $\lambda = 1.0$; $A' = 2$ to 6; $m' = \infty$ to 1.

Figure 15.- Variation of BC_{m_α} with $\cot^{-1}m'$ for various values of A'. System of body axes with origin at (0,0,0). (See text, p. 11, for significance of dashed portions of curves.)

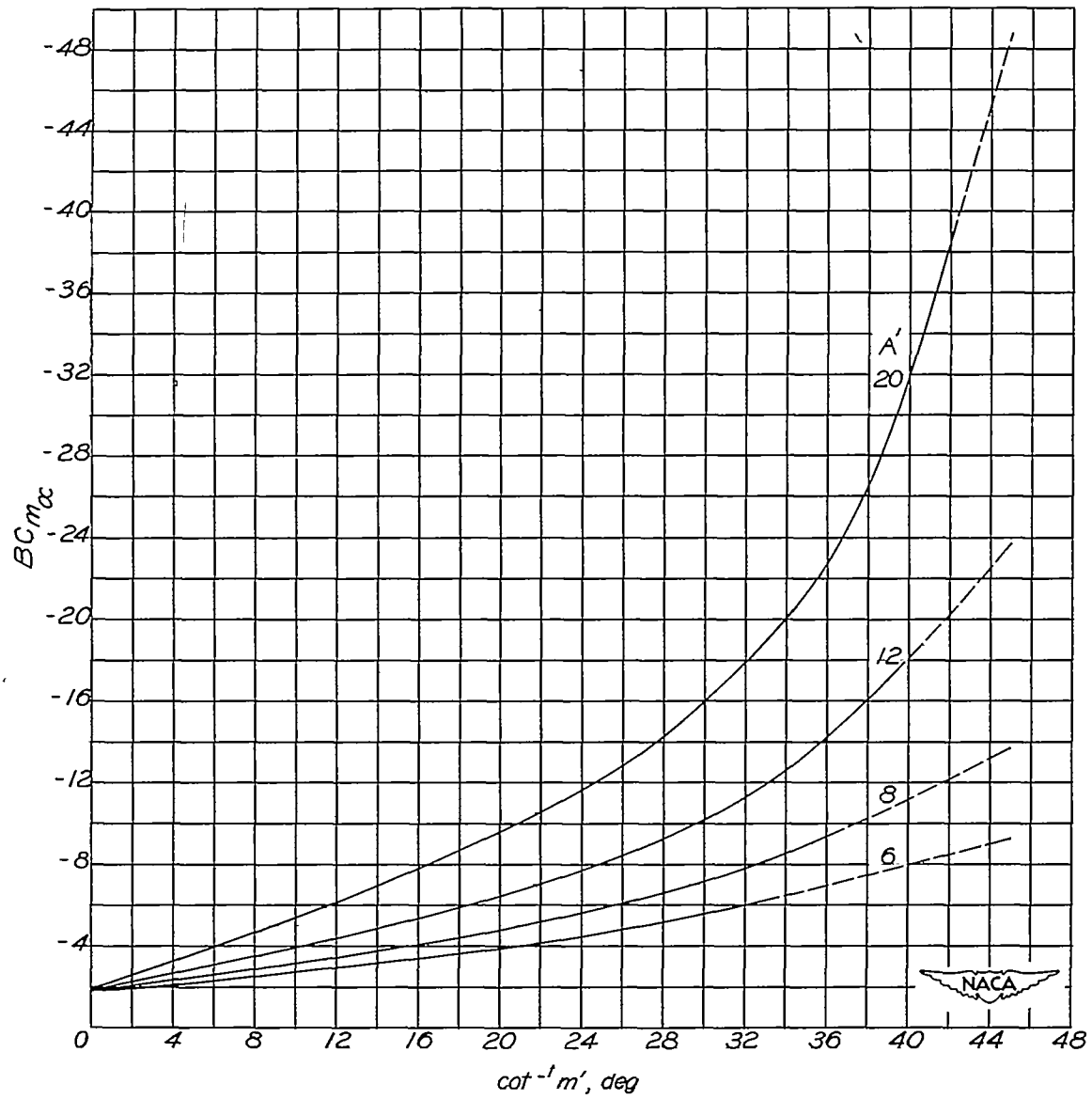

(b) $\lambda = 1.0$; $A' = 6$ to 20; $m' = \infty$ to 1.

Figure 15.- Continued.

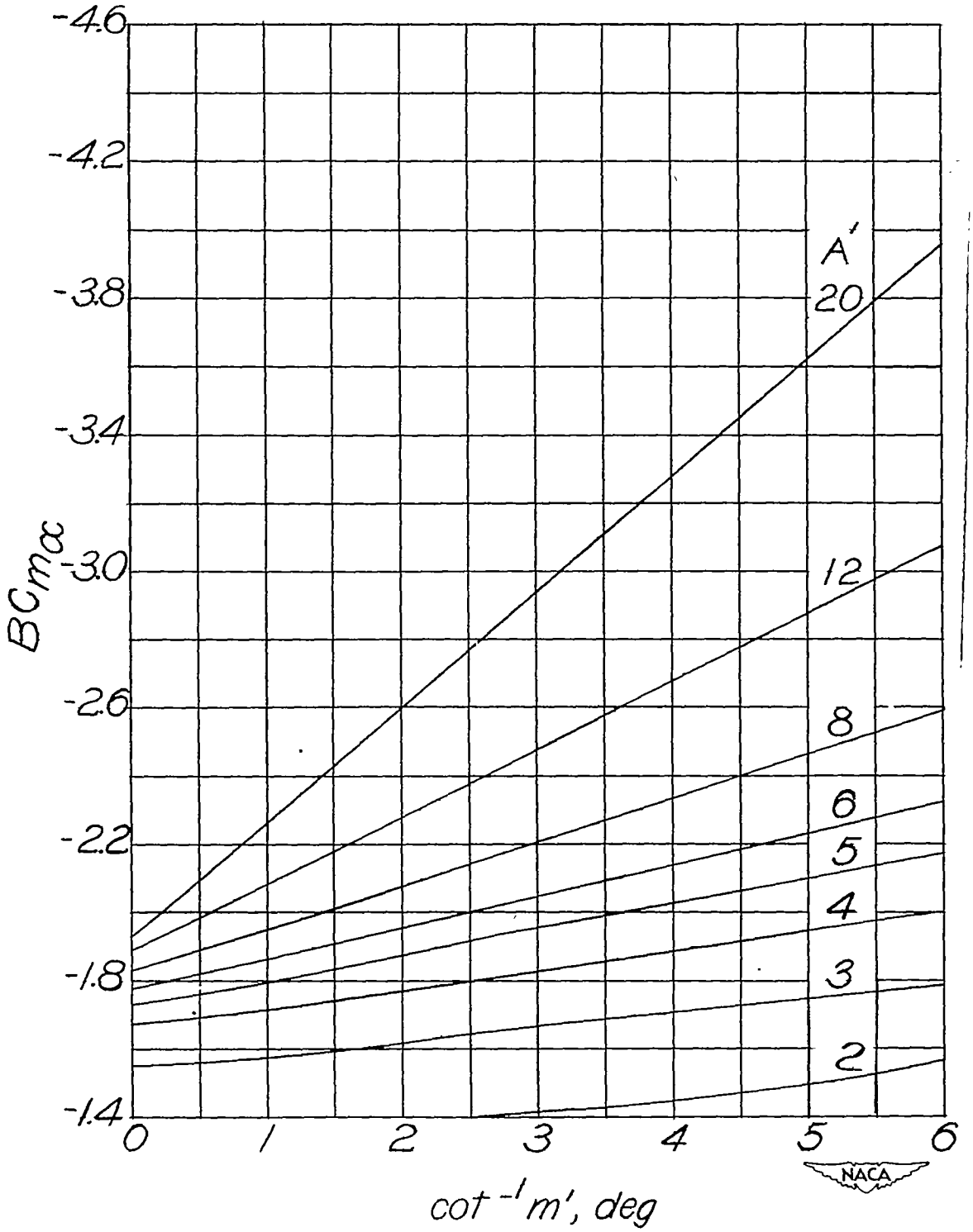

(c) $\lambda = 1.0$; $A' = 2$ to 20; $m' = \infty$ to 9.4.

Figure 15.- Concluded.

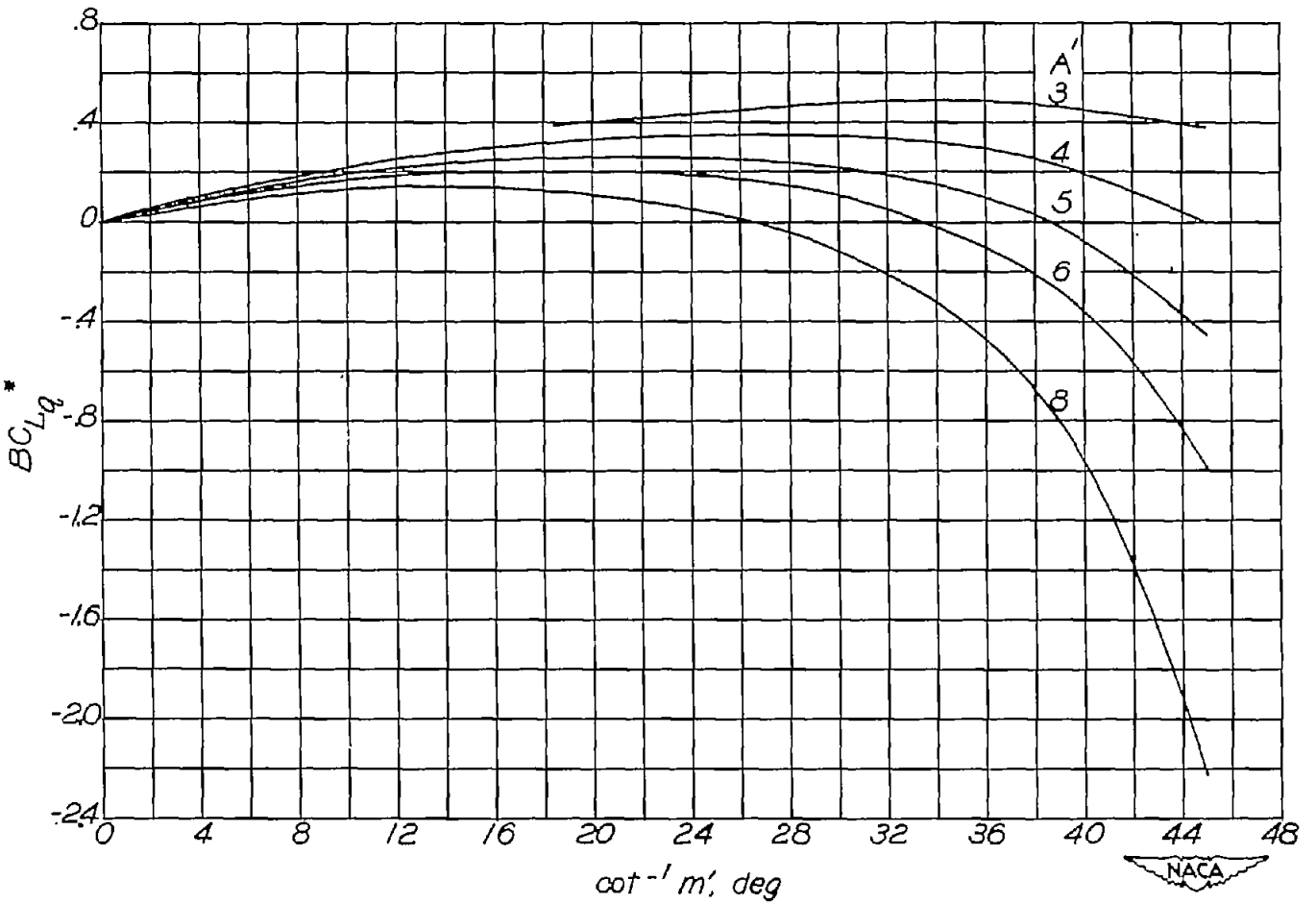

(a) $\lambda = 0$; $A' = 3$ to 8; $m' = \infty$ to 1.

Figure 16.- Variation of $BC_{L_q}^*$ with $\cot^{-1}m'$ for various values of A'. System of body axes with origin at $(\bar{x},0,0)$.

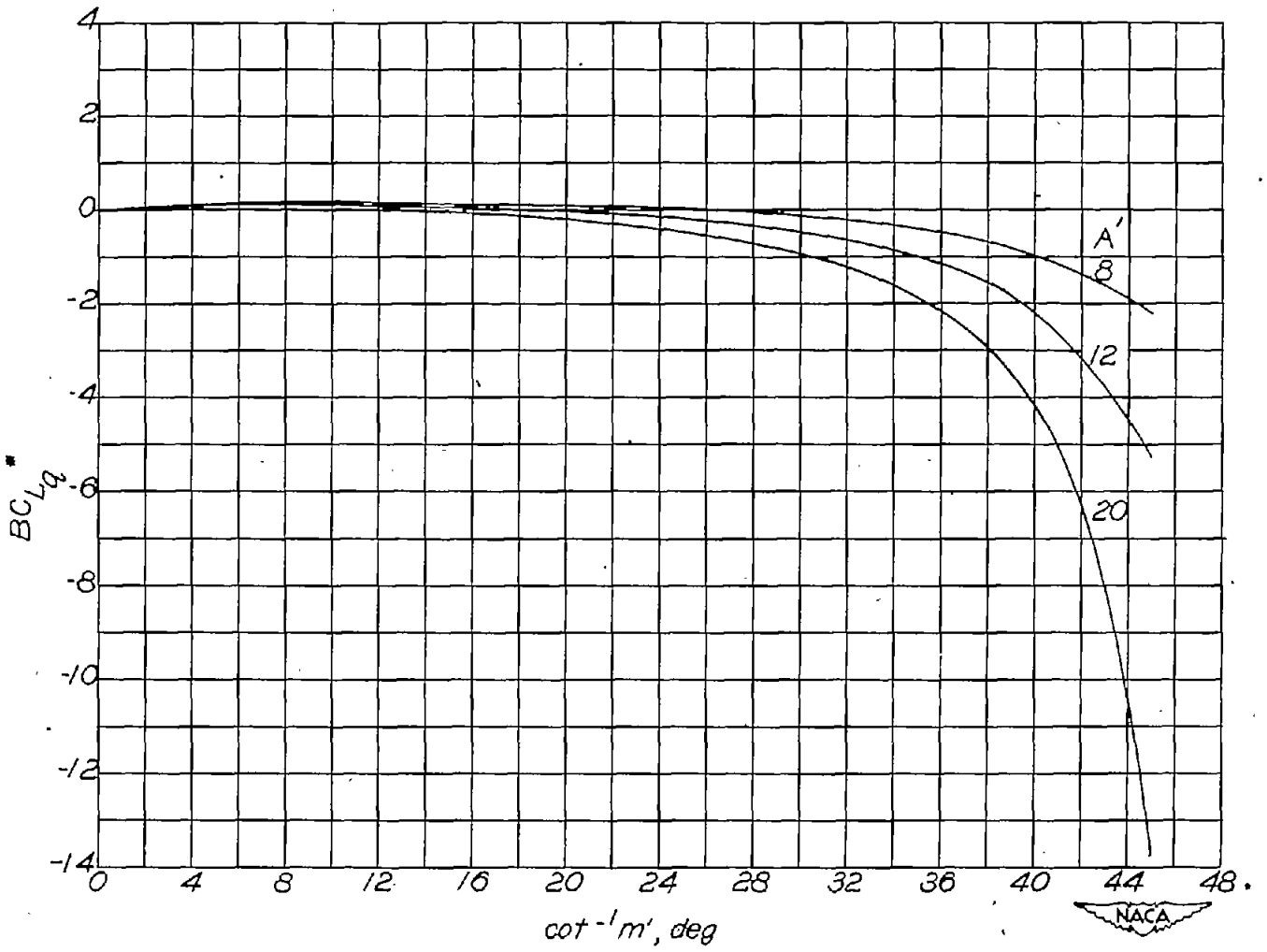

(b) $\lambda = 0$; $A' = 8$ to 20; $m' = \infty$ to 1.

Figure 16.- Continued.

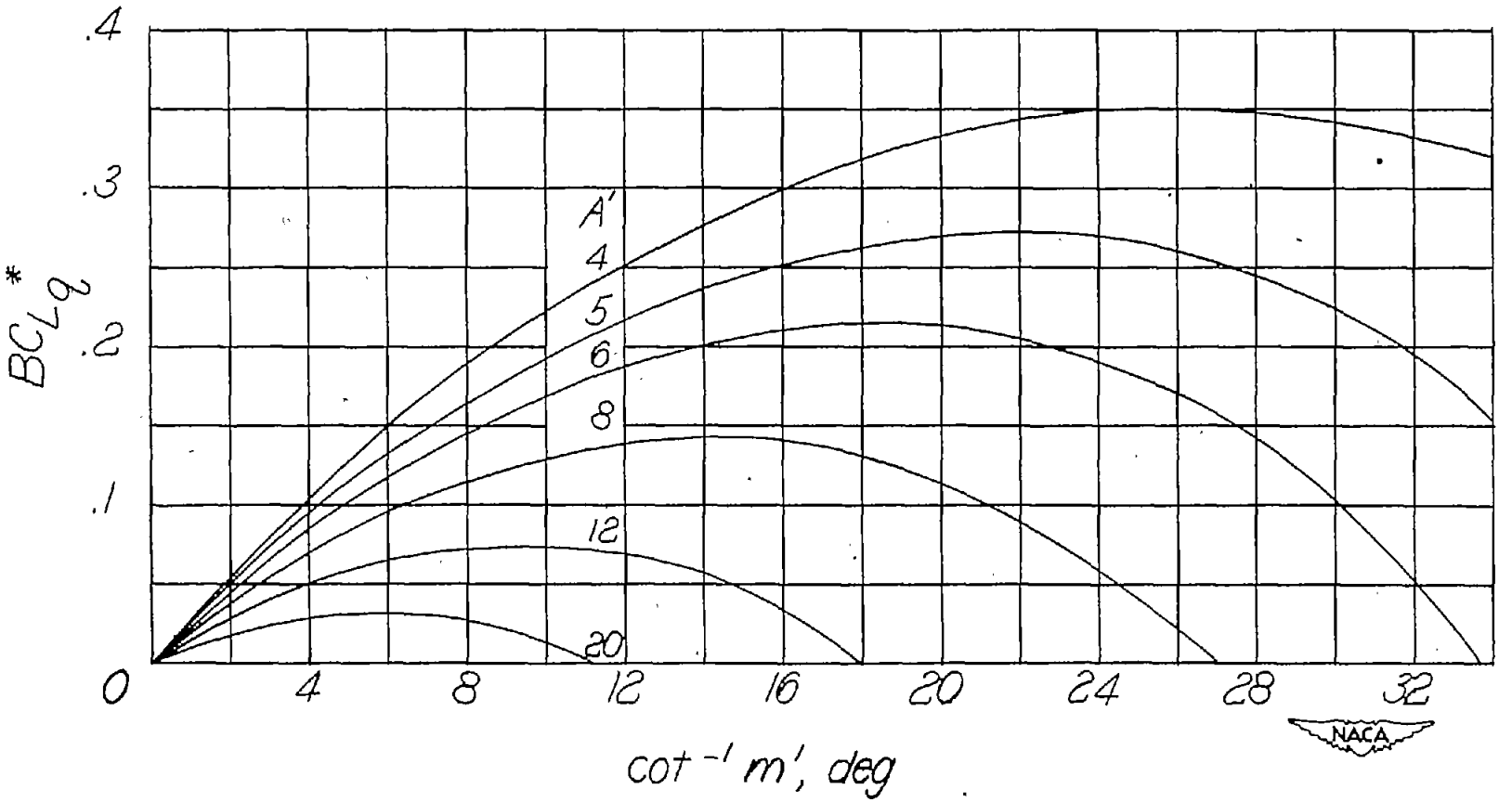

(c) $\lambda = 0$; $A' = 4$ to 20; $m' = \infty$ to 2.24.

Figure 16.- Concluded.

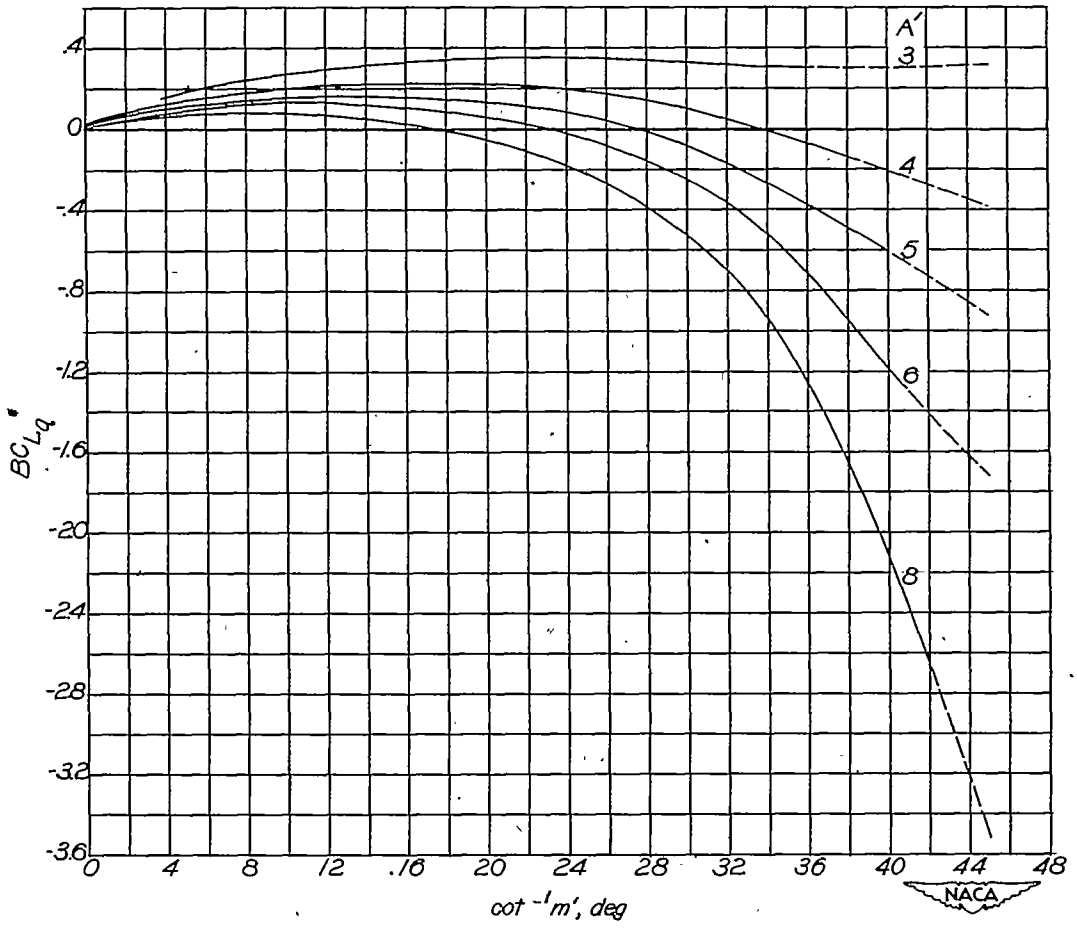

(a) $\lambda = 0.25$; $A' = 3$ to 8; $m' = \infty$ to 1.

Figure 17.- Variation of $BC_{L_q}{}^*$ with $\cot^{-1}m'$ for various values of A'. System of body axes with origin at $(\bar{x},0,0)$. (See text, p. 11, for significance of dashed portions of curves.)

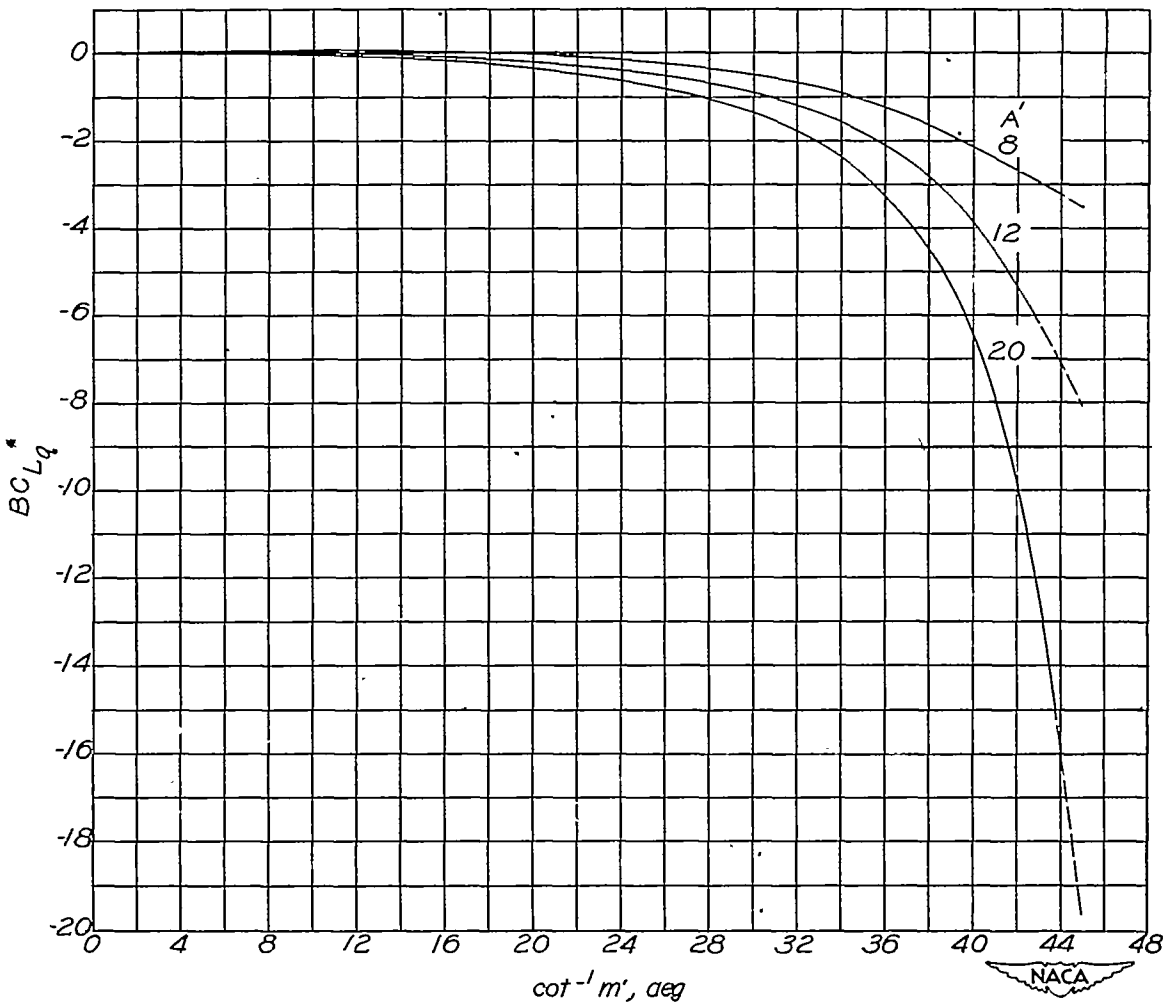

(b) $\lambda = 0.25$; $A' = 8$ to 20; $m' = \infty$ to 1.

Figure 17.- Continued.

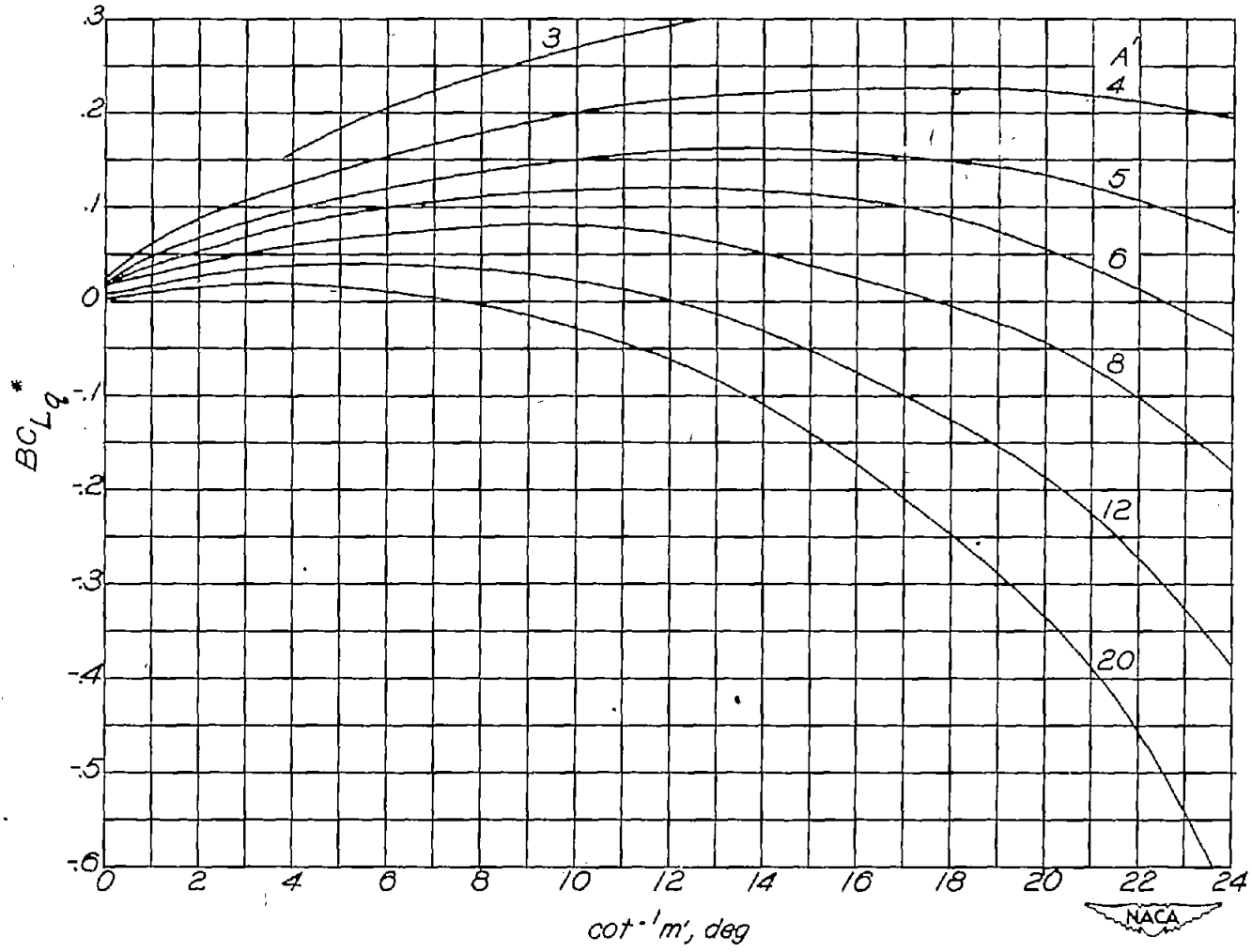

(c) $\lambda = 0.25$; $A' = 3$ to 20; $m' = \infty$ to 2.05.

Figure 17.- Concluded.

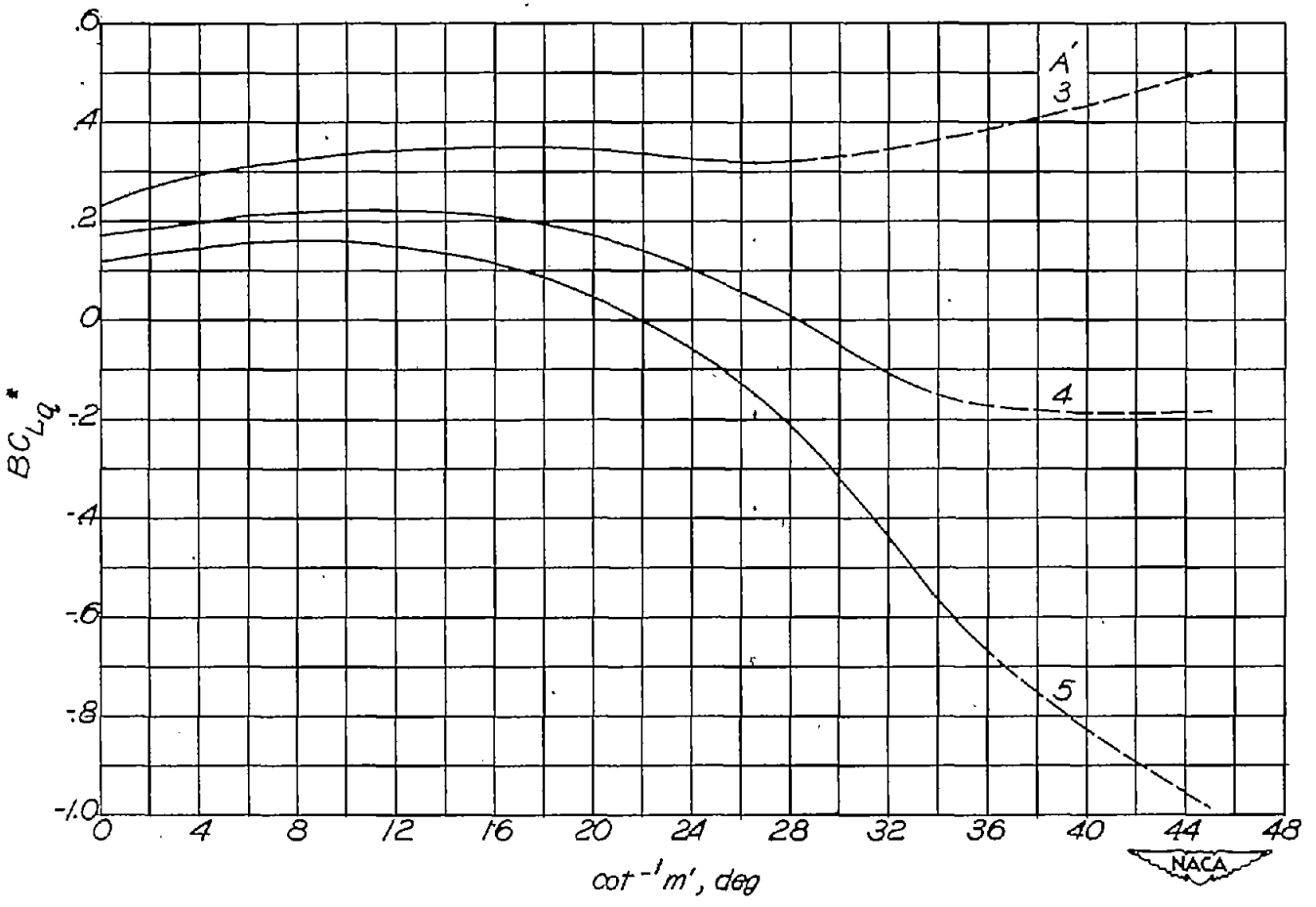

(a) $\lambda = 0.50$; $A' = 3$ to 5; $m' = \infty$ to 1.

Figure 18.- Variation of $BC_{L_q}^*$ with $\cot^{-1} m'$ for various values of A'.

System of body axes with origin at $(\bar{x},0,0)$. (See text, p. 11, for significance of dashed portions of curves.)

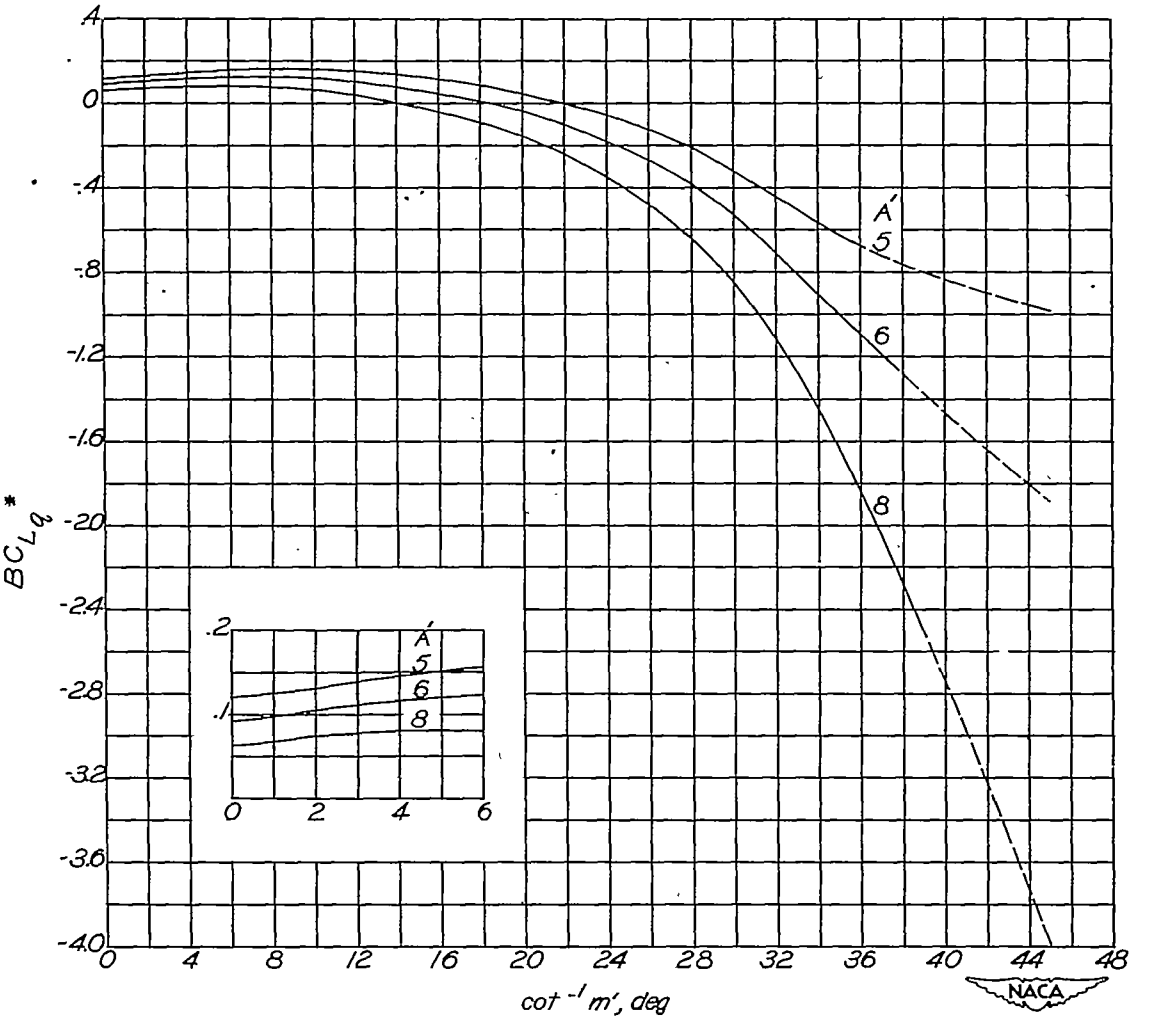

(b) $\lambda = 0.50$; $A' = 5$ to 8; $m' = \infty$ to 1.

Figure 18.- Continued.

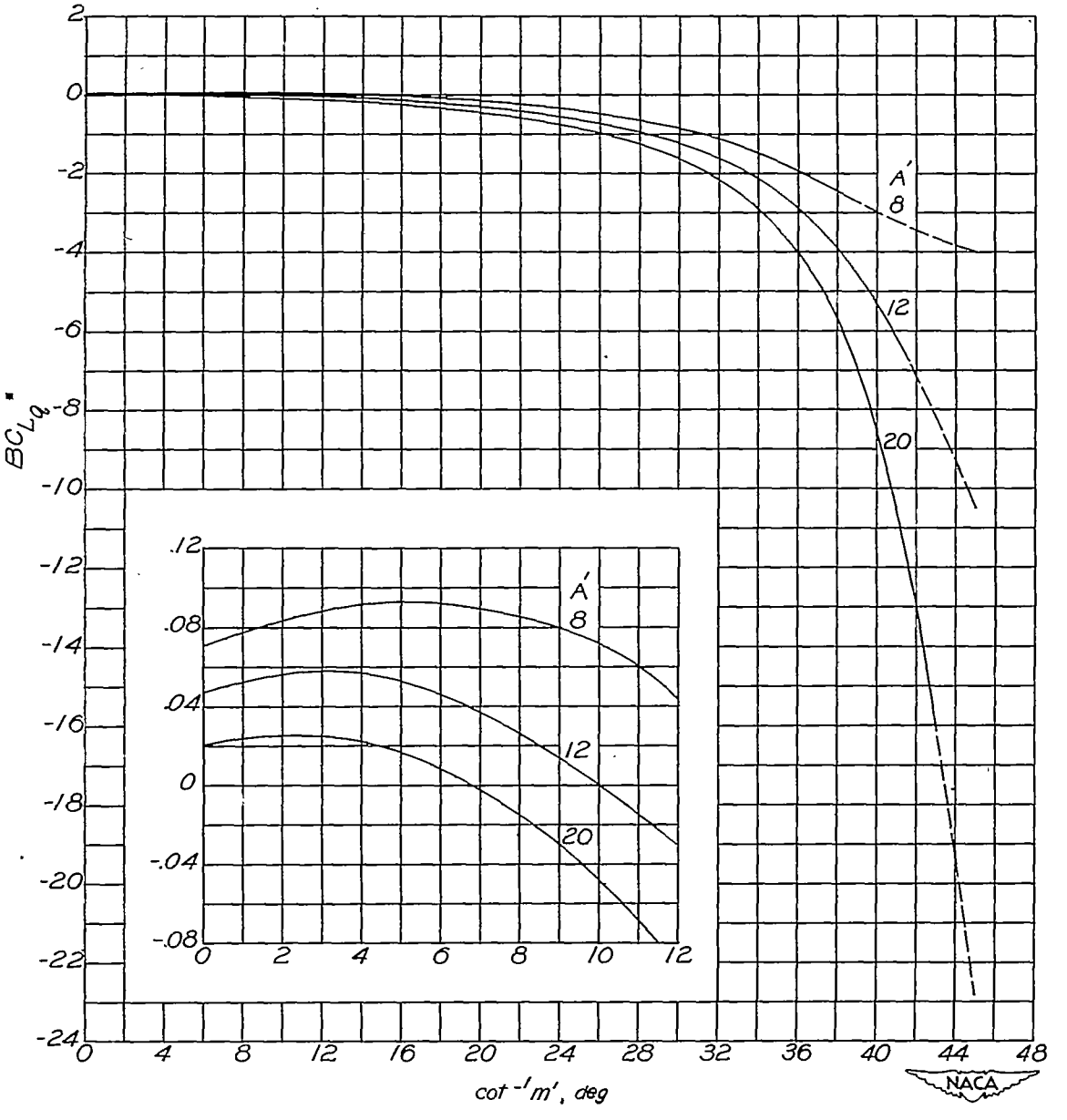

(c) $\lambda = 0.50$; A' = 8 to 20; m' = ∞ to 1.

Figure 18.- Concluded.

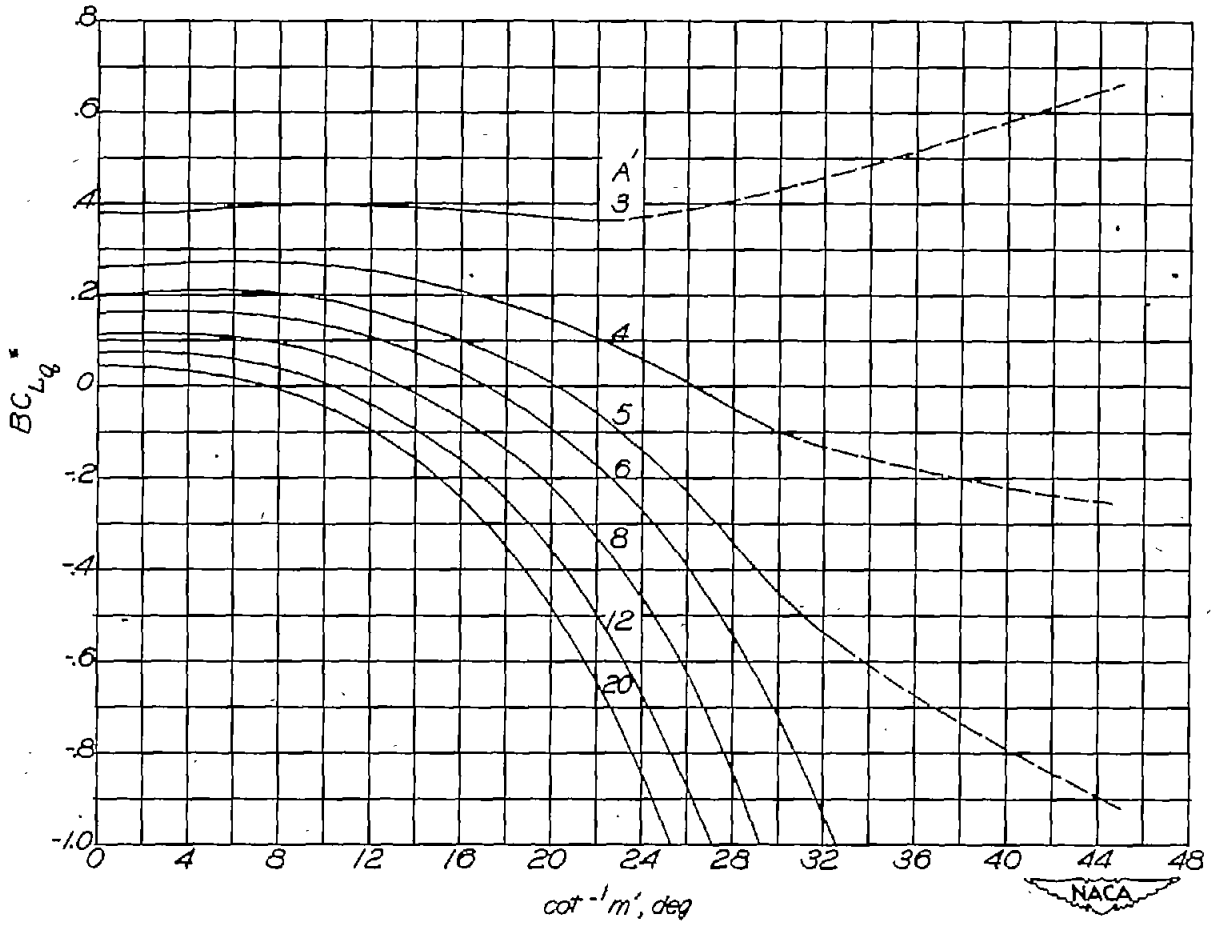

(a) $\lambda = 0.75$; $A' = 3$ to 20; $m' = \infty$ to 1.

Figure 19.- Variation of $BC_{L_q}{}^*$ with $\cot^{-1}m'$ for various values of A'. System of body axes with origin at $(\bar{x},0,0)$. (See text, p. 11, for significance of dashed portions of curves.)

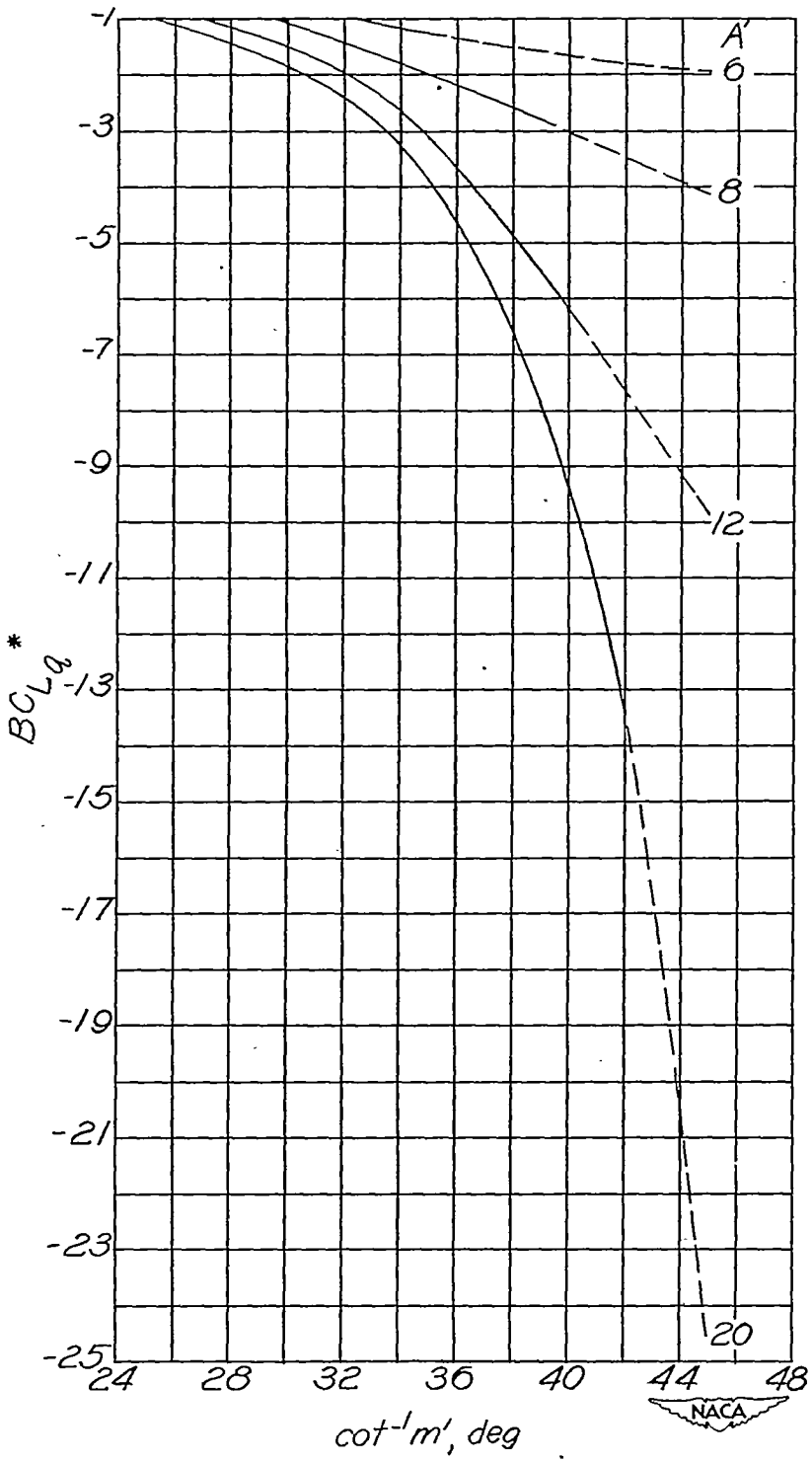

(b) $\lambda = 0.75$; $A' = 6$ to 20; $m' = 2.13$ to 1.

Figure 19.- Concluded.

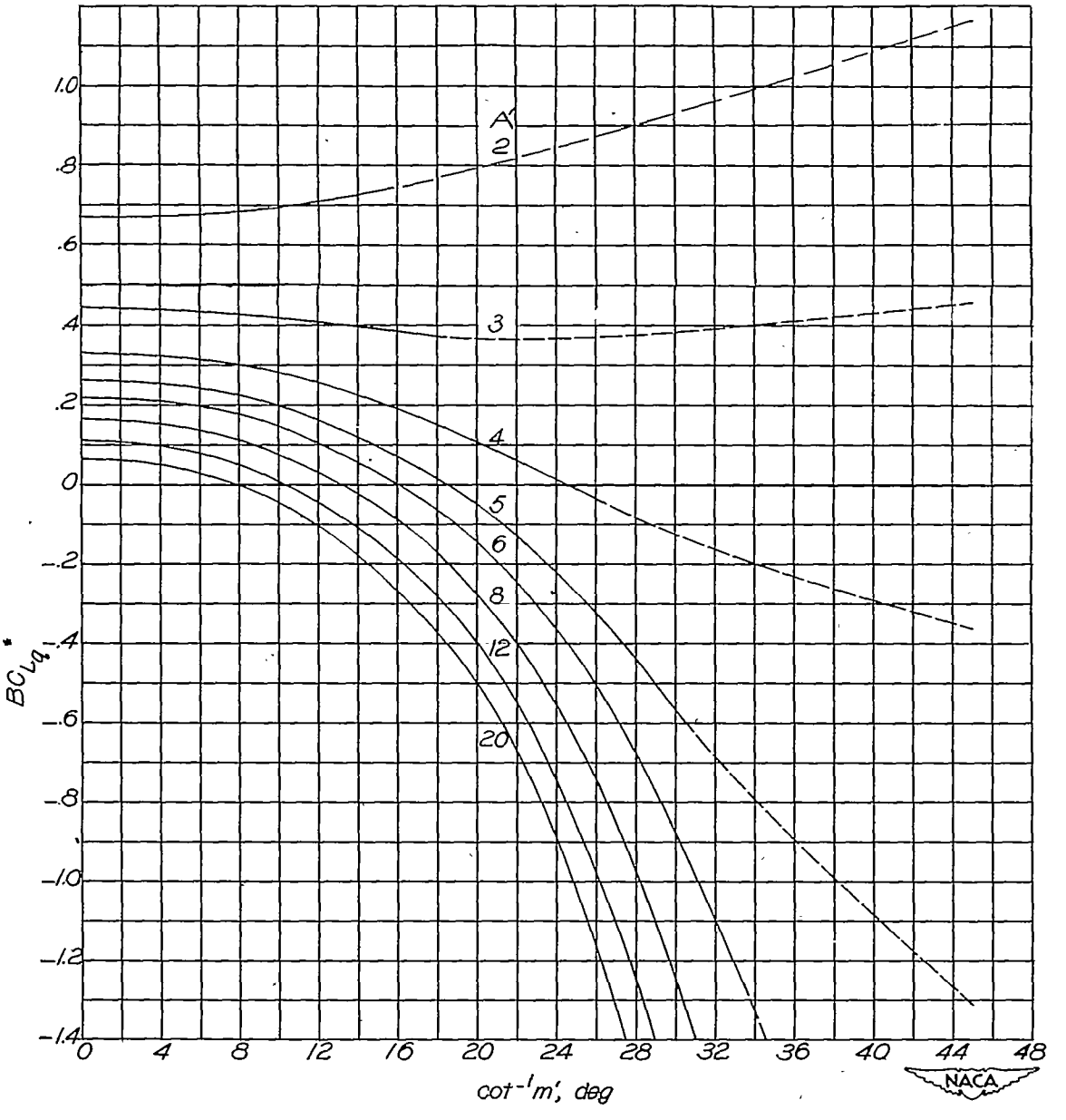

(a) $\lambda = 1.0$; $A' = 2$ to 20; $m' = \infty$ to 1.

Figure 20.- Variation of $BC_{L_q}^*$ with $\cot^{-1}m'$ for various values of A'. System of body axes with origin at $(\bar{x},0,0)$. (See text, p. 11, for significance of dashed portions of curves.)

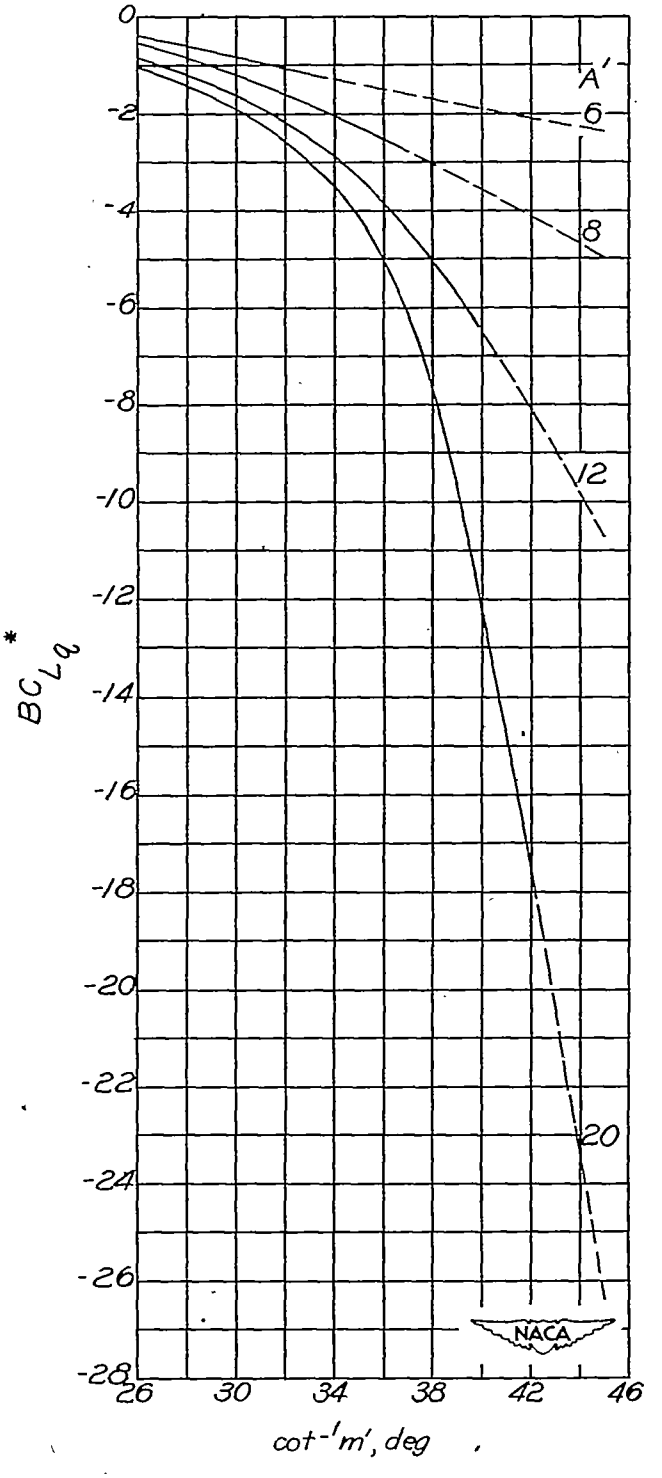

(b) $\lambda = 1.0$; $A' = 6$ to 20; $m' = 2.05$ to 1.

Figure 20.- Concluded.

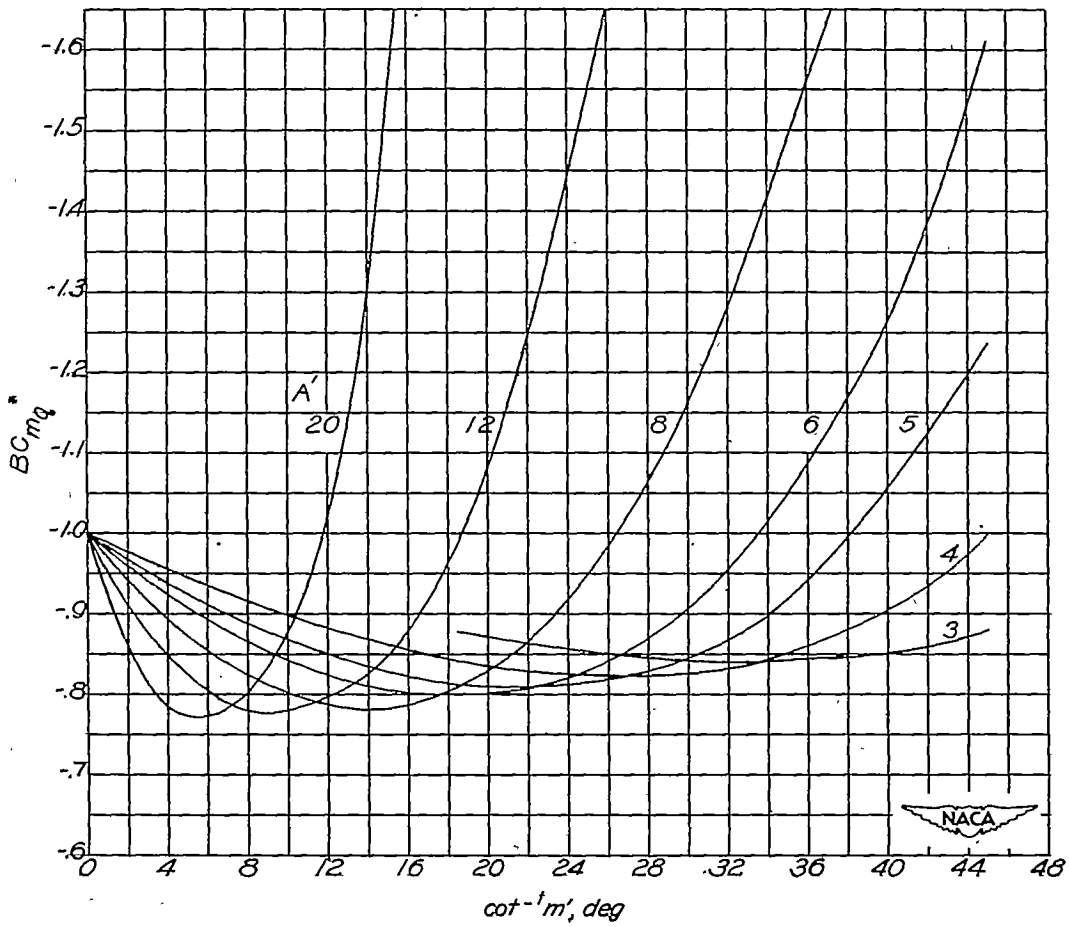

(a) $\lambda = 0$; $A' = 3$ to 20; $m' = \infty$ to 1.

Figure 21.- Variation of $BC_{m_q}^*$ with $\cot^{-1}m'$ for various values of A'. System of body axes with origin at $(\bar{x},0,0)$.

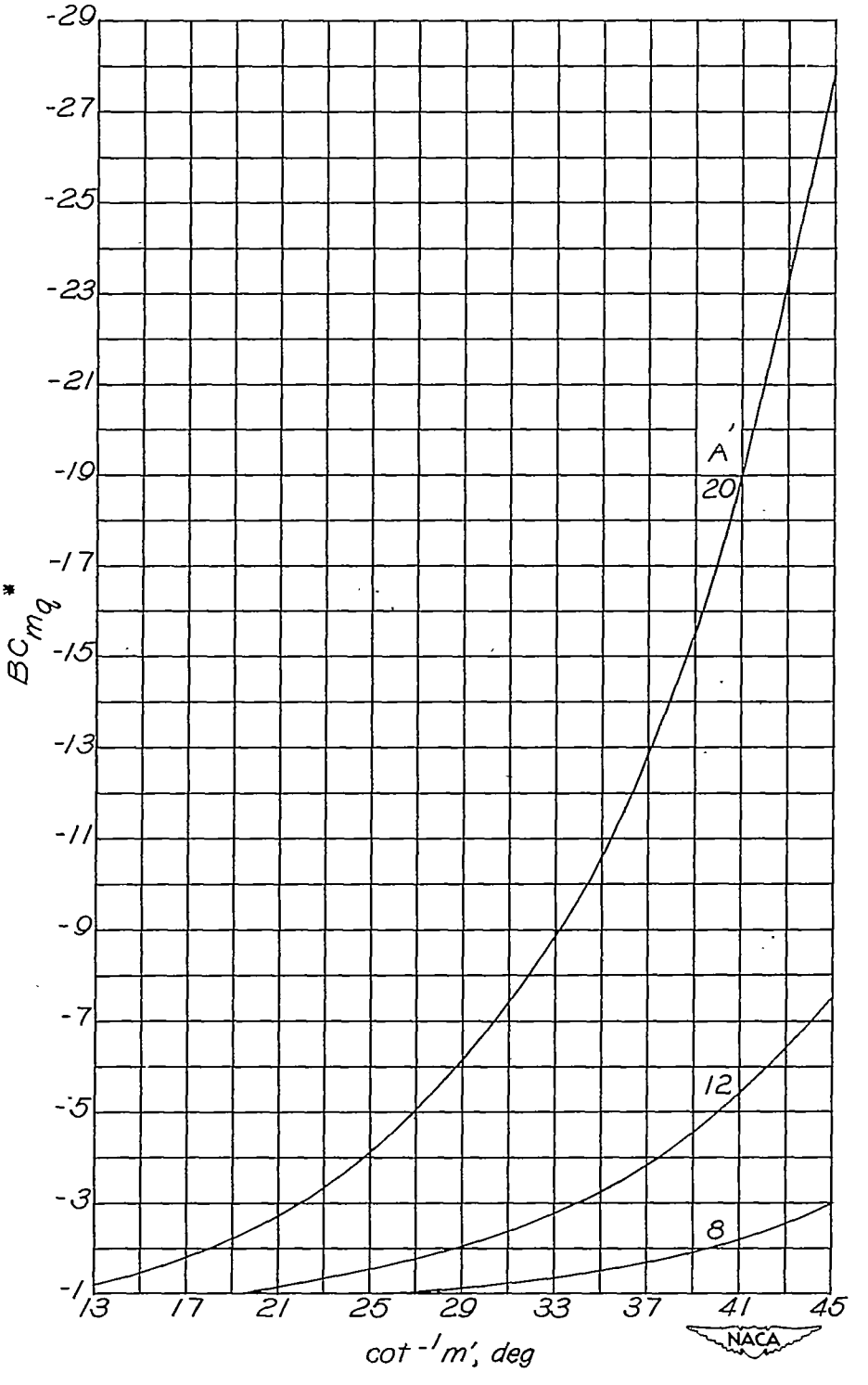

(b) $\lambda = 0$; $A' = 8$ to 20; $m' = 4.33$ to 1.

Figure 21.- Concluded.

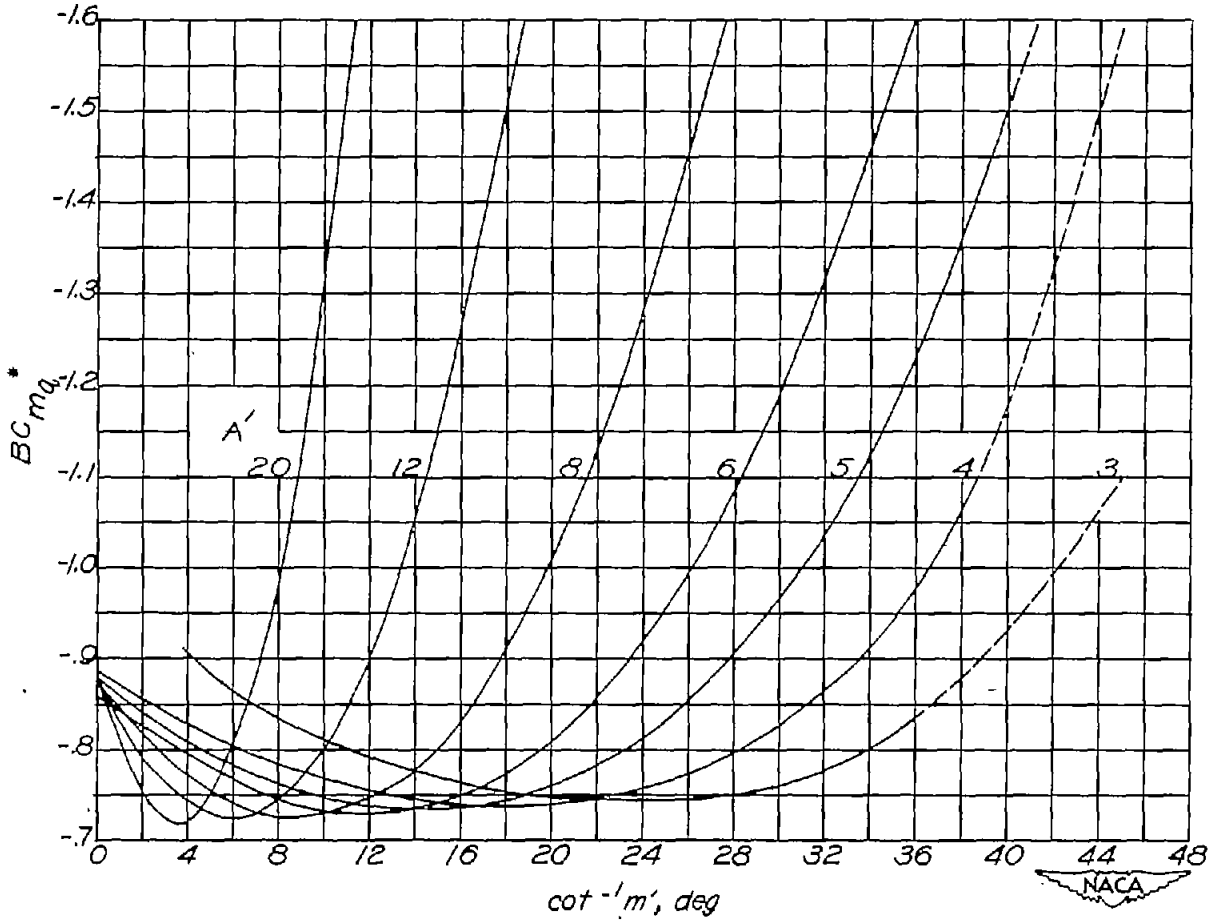

(a) $\lambda = 0.25$; $A' = 3$ to 20; $m' = \infty$ to 1.

Figure 22.- Variation of $BC_{m_q}^*$ with $\cot^{-1} m'$ for various values of A'. System of body axes with origin at $(\bar{x},0,0)$. (See text, p. 11, for significance of dashed portions of curves.)

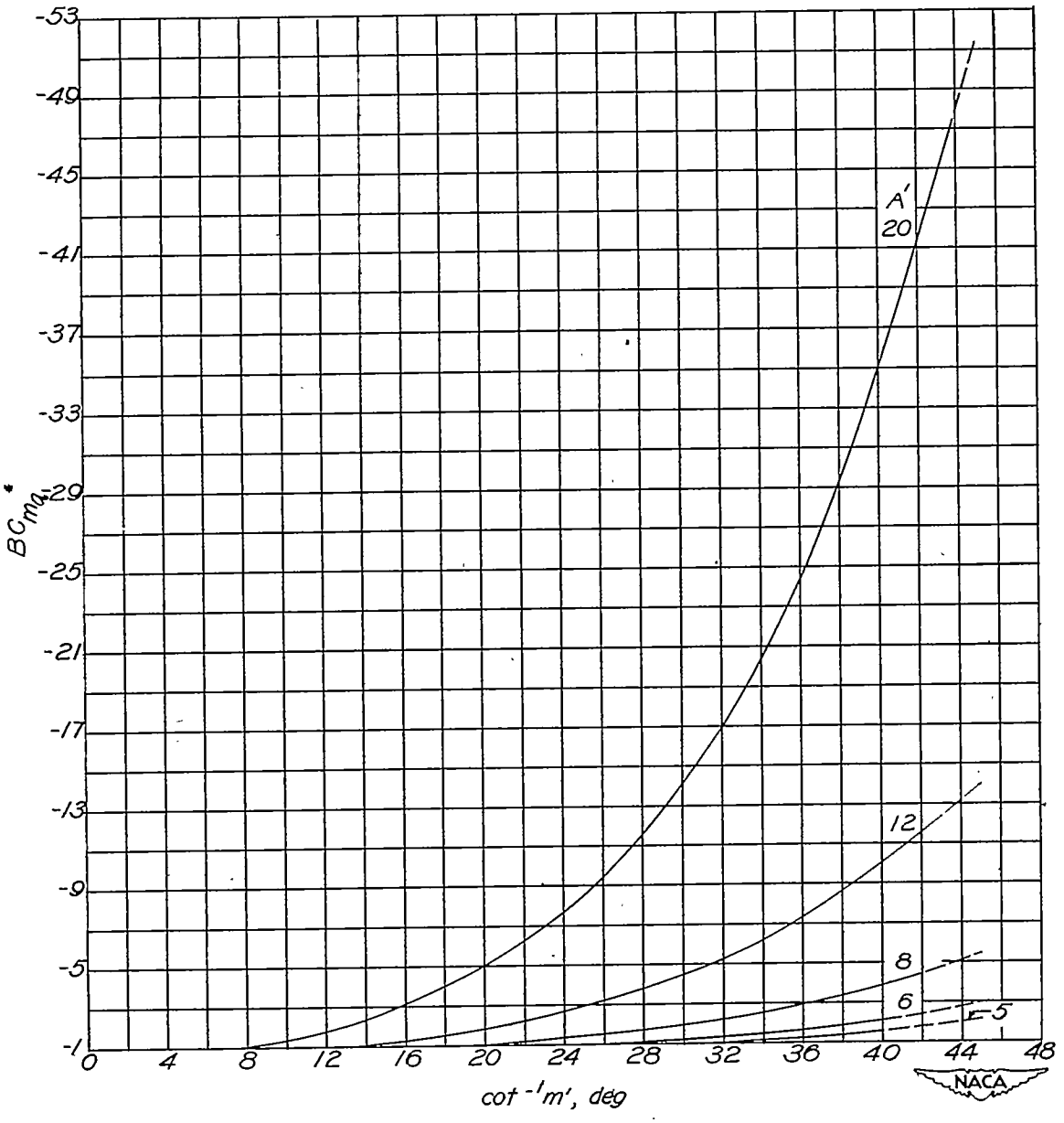

(b) $\lambda = 0.25$; A' = 5 to 20; m' = 7.12 to 1.

Figure 22.- Concluded.

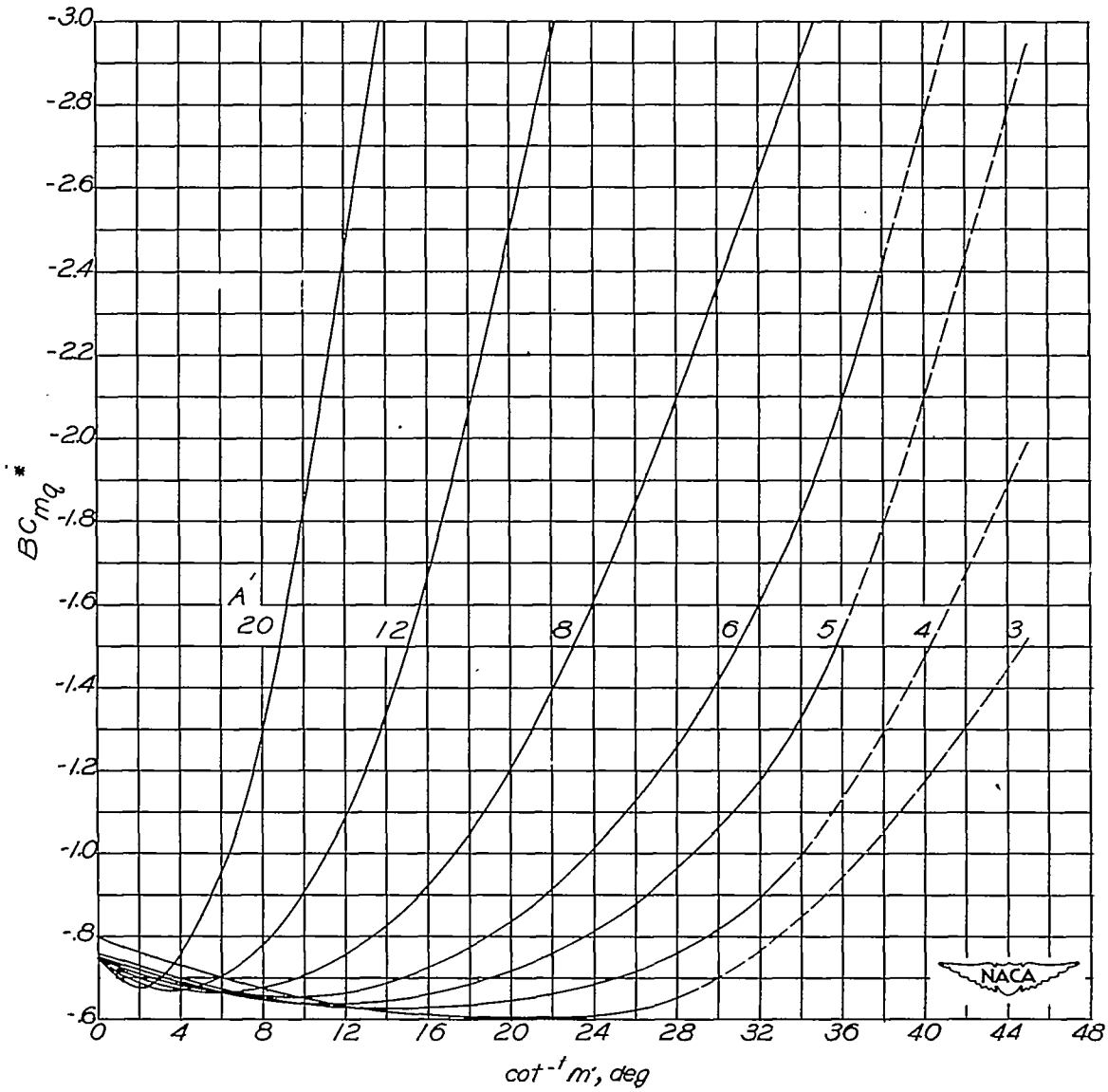

(a) $\lambda = 0.50$; $A' = 3$ to 20; $m' = \infty$ to 1.

Figure 23.- Variation of $BC_{m_q}^*$ with $\cot^{-1}m'$ for various values of A'. System of body axes with origin at $(\bar{x},0,0)$. (See text, p. 11, for significance of dashed portions of curves.)

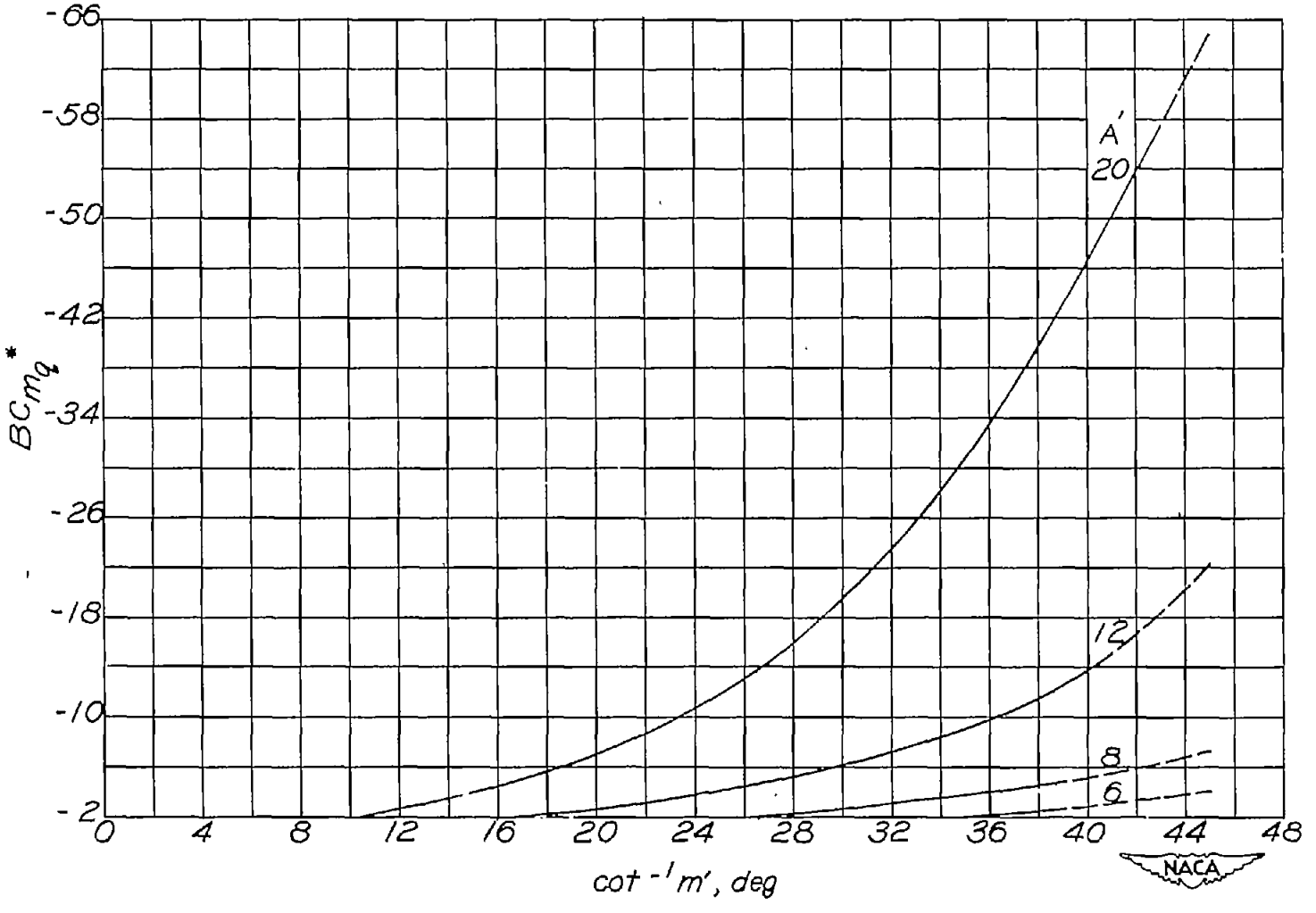

(b) $\lambda = 0.50$; $A' = 6$ to 20; $m' = 5.45$ to 1.

Figure 23.- Continued.

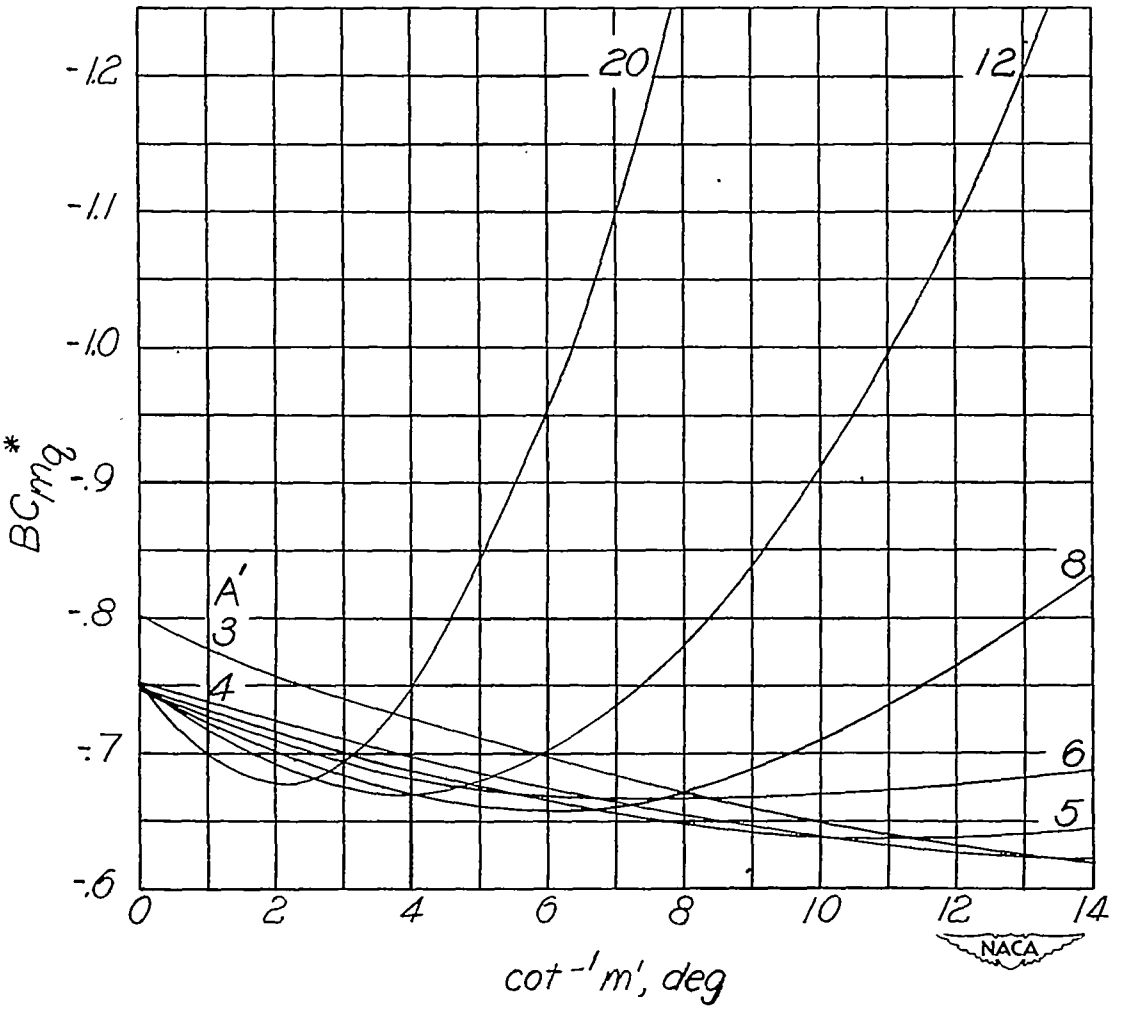

(c) $\lambda = 0.50$; $A' = 3$ to 20; $m' = \infty$ to 4.

Figure 23.- Concluded.

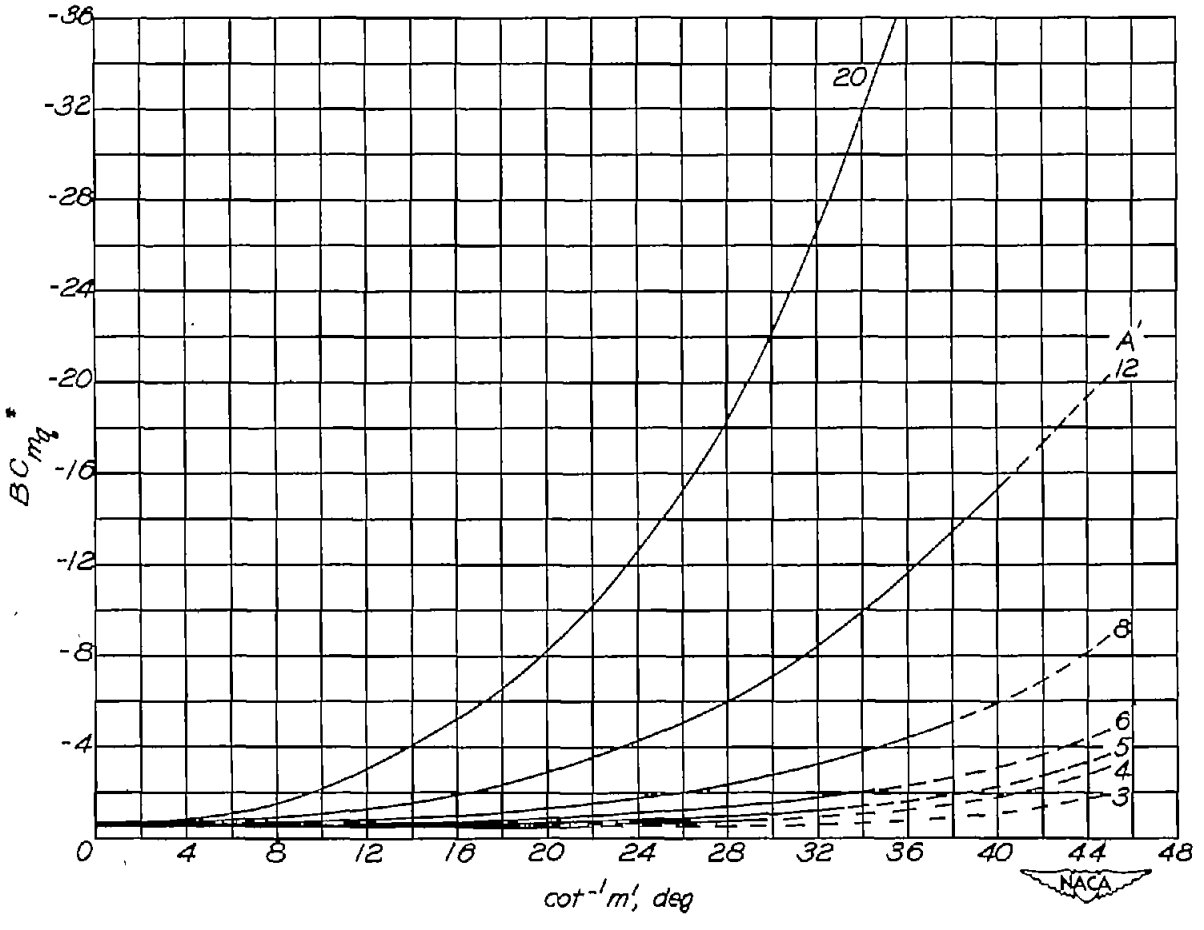

(a) $\lambda = 0.75$; $A' = 3$ to 20; $m' = \infty$ to 1.

Figure 24.- Variation of $BC_{m_q}^*$ with $\cot^{-1} m'$ for various values of A'. System of body axes with origin at $(\bar{x},0,0)$. (See text, p. 11, for significance of dashed portions of curves.)

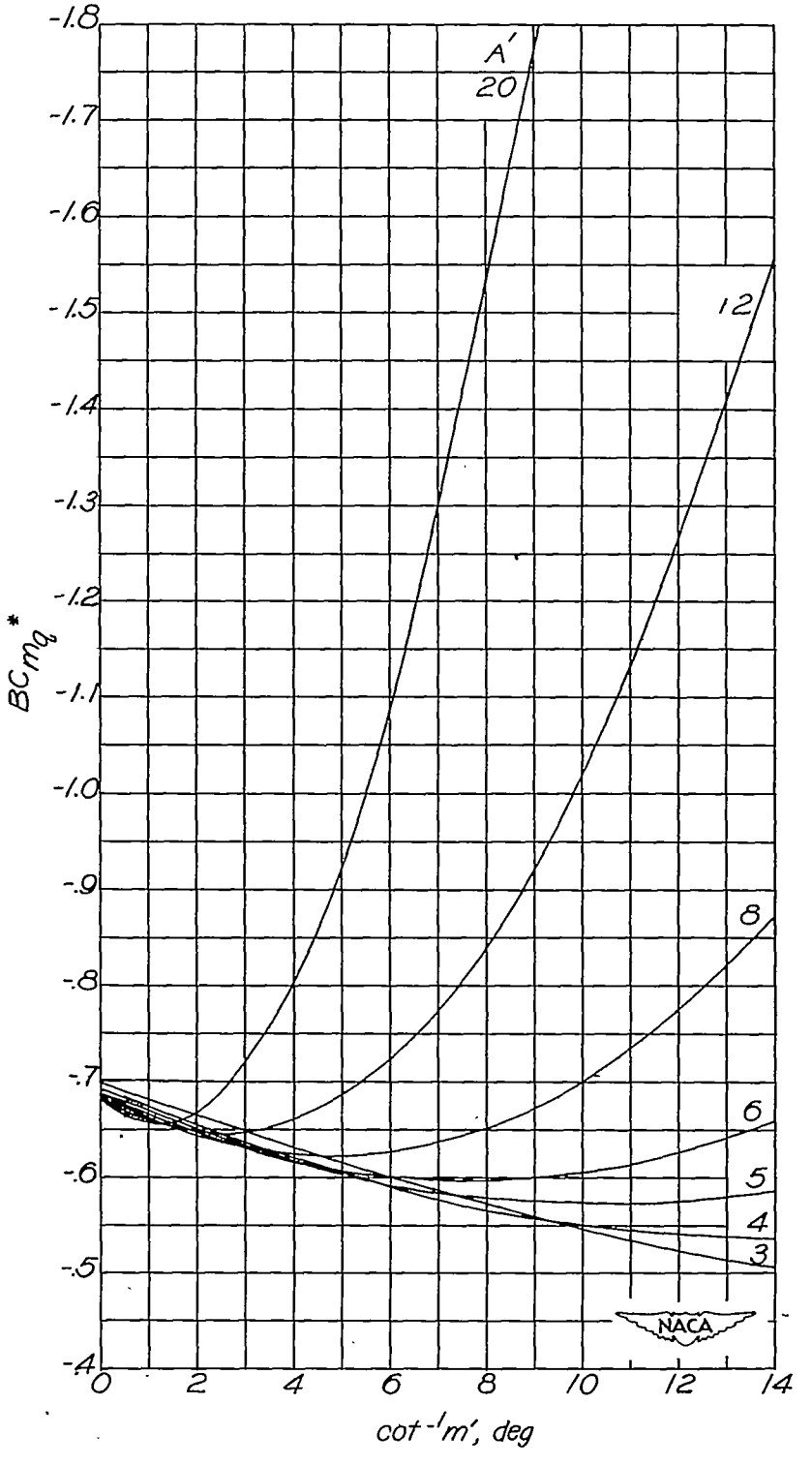

(b) $\lambda = 0.75$; $A' = 3$ to 20; $m' = \infty$ to 4.

Figure 24.- Continued.

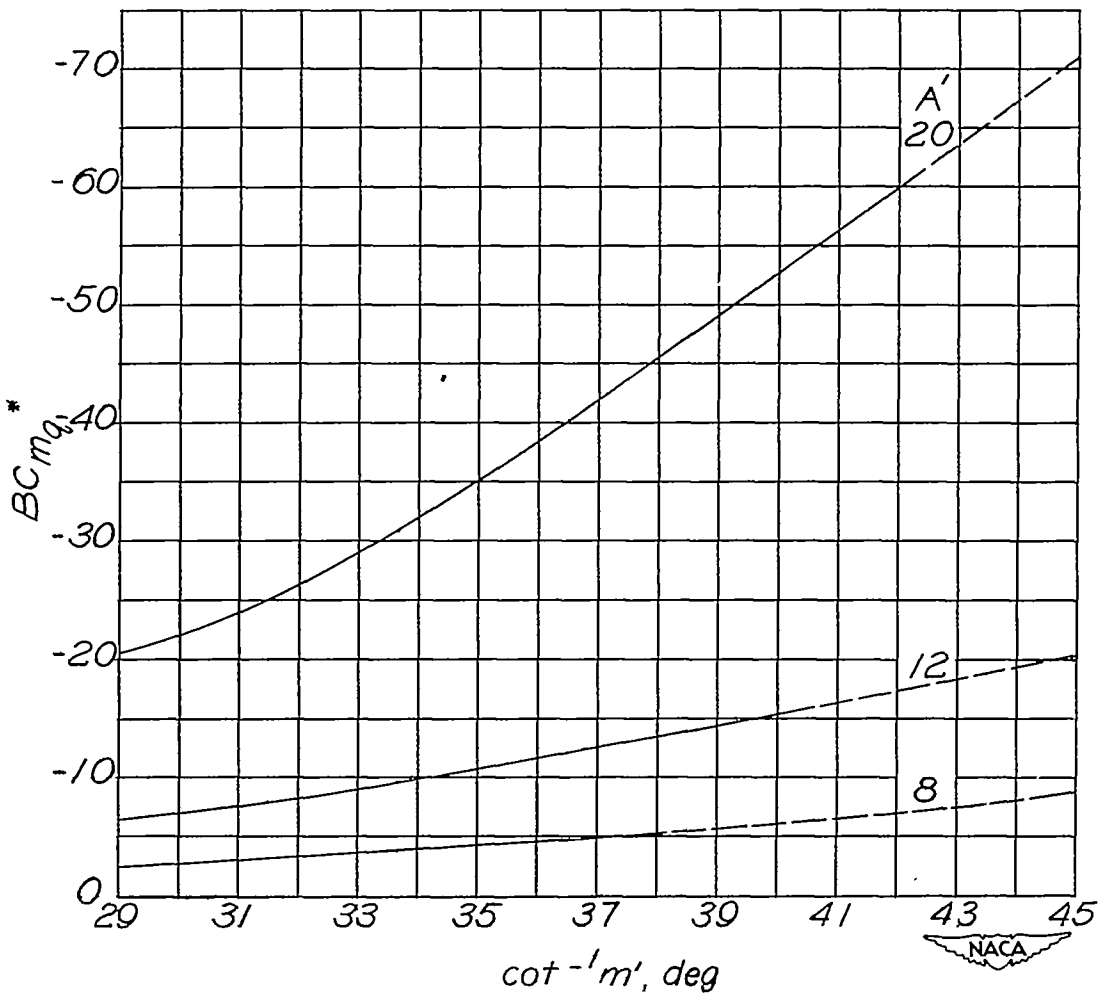

(c) $\lambda = 0.75$; $A' = 8$ to 20; $m' = 1.8$ to 1.

Figure 24.- Concluded.

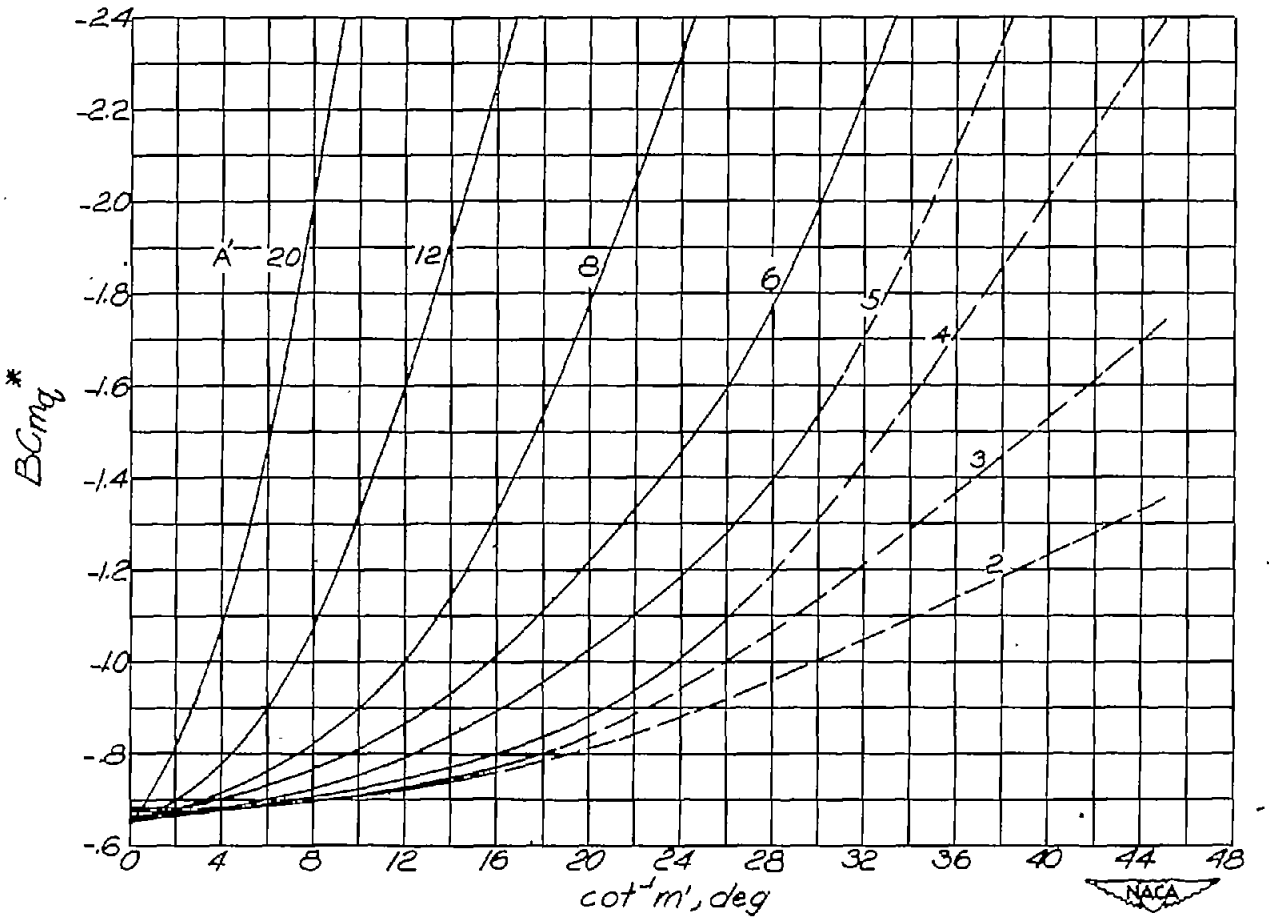

(a) $\lambda = 1.0$; $A' = 2$ to 20; $m' = \infty$ to 1.

Figure 25.- Variation of $BC_{m_q}^*$ with $\cot^{-1}m'$ for various values of A'. System of body axes with origin at $(\bar{x},0,0)$. (See text, p. 11, for significance of dashed portions of curves.)

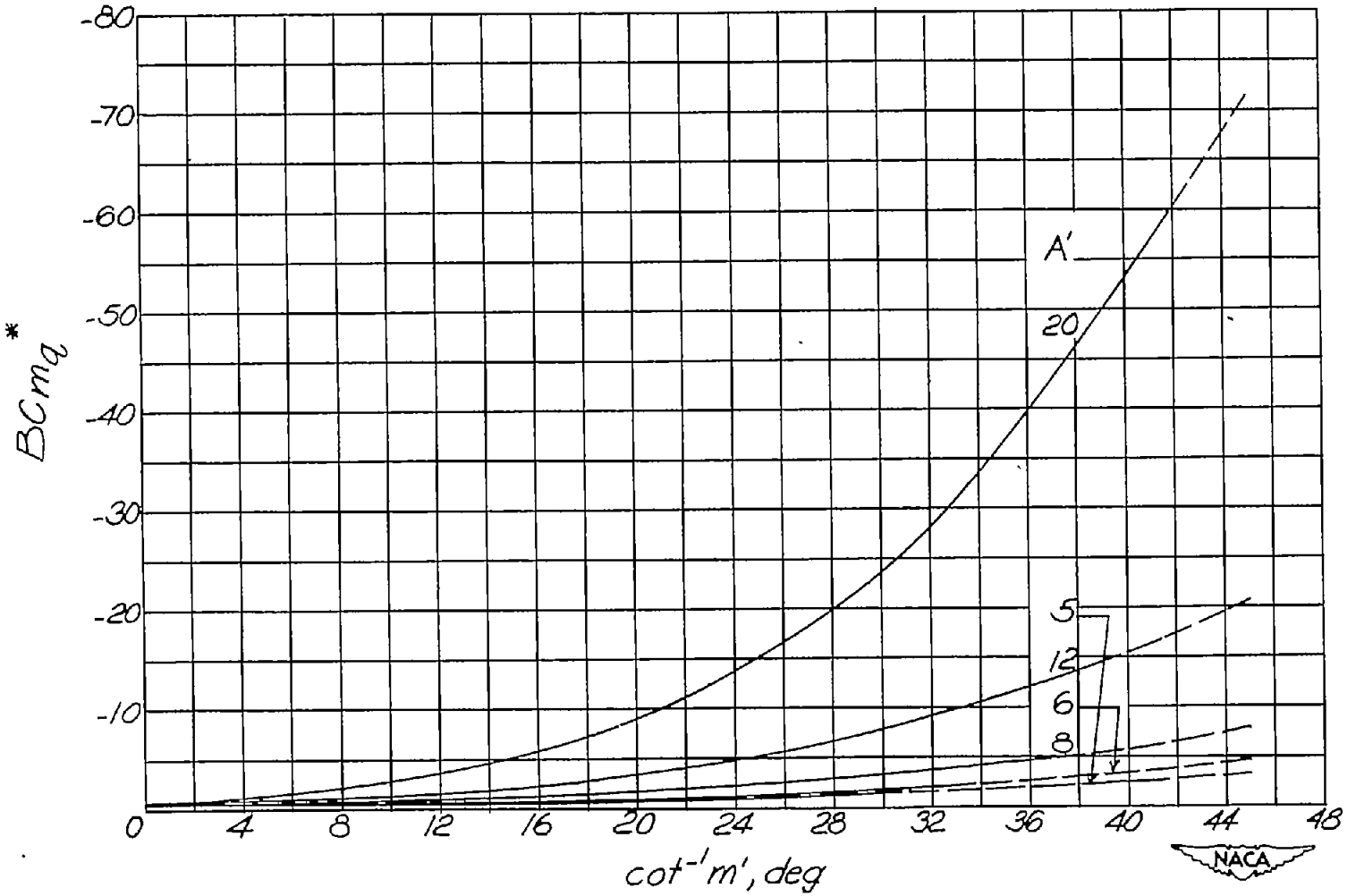

(b) $\lambda = 1.0$; $A' = 5$ to 20; $m' = \infty$ to 1.

Figure 25.- Concluded.

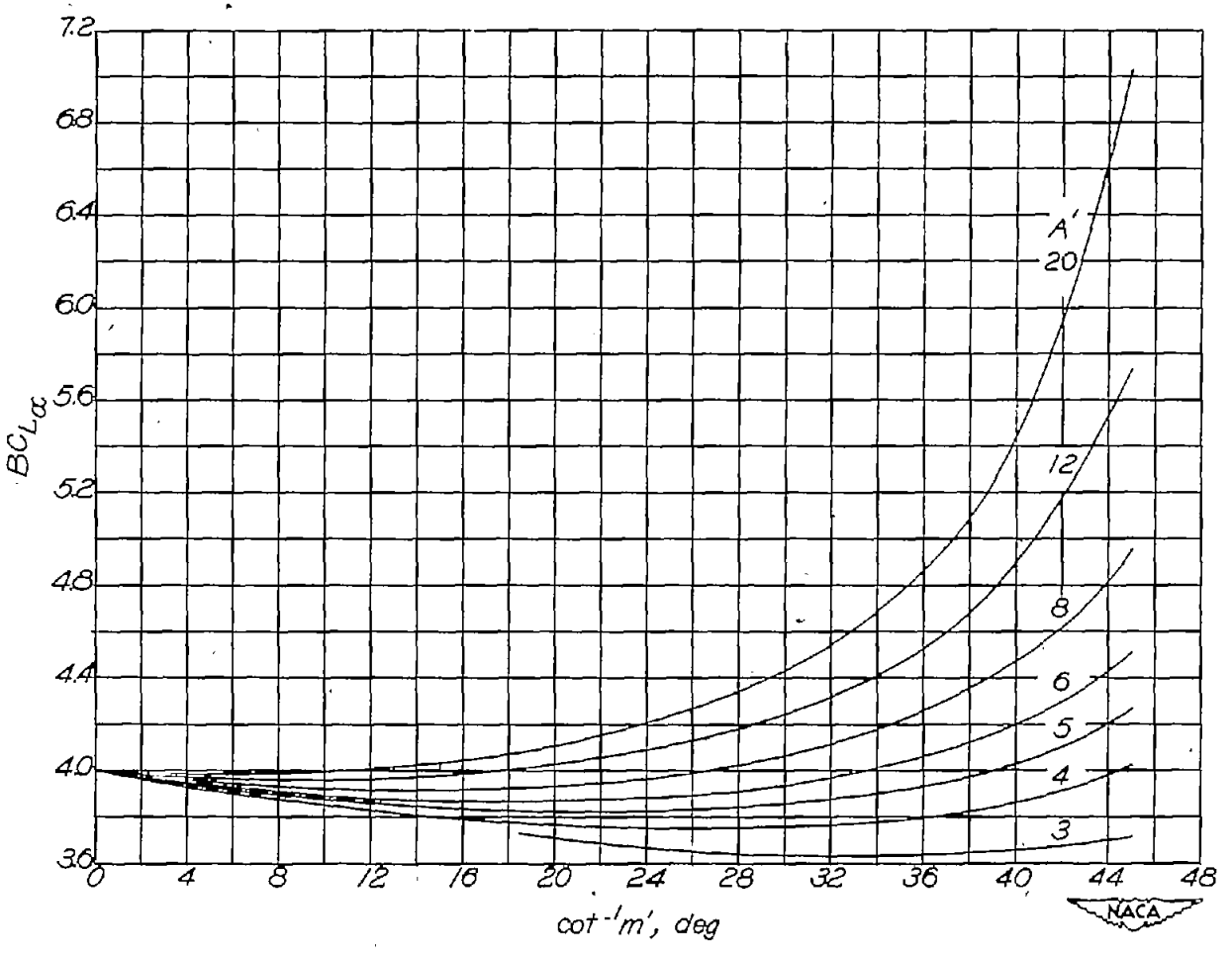

(a) $\lambda = 0$; $A' = 3$ to 20; $m' = \infty$ to 1.

Figure 26.- Variation of BC_{L_α} with $\cot^{-1}m'$ for various values of A'. System of body axes.

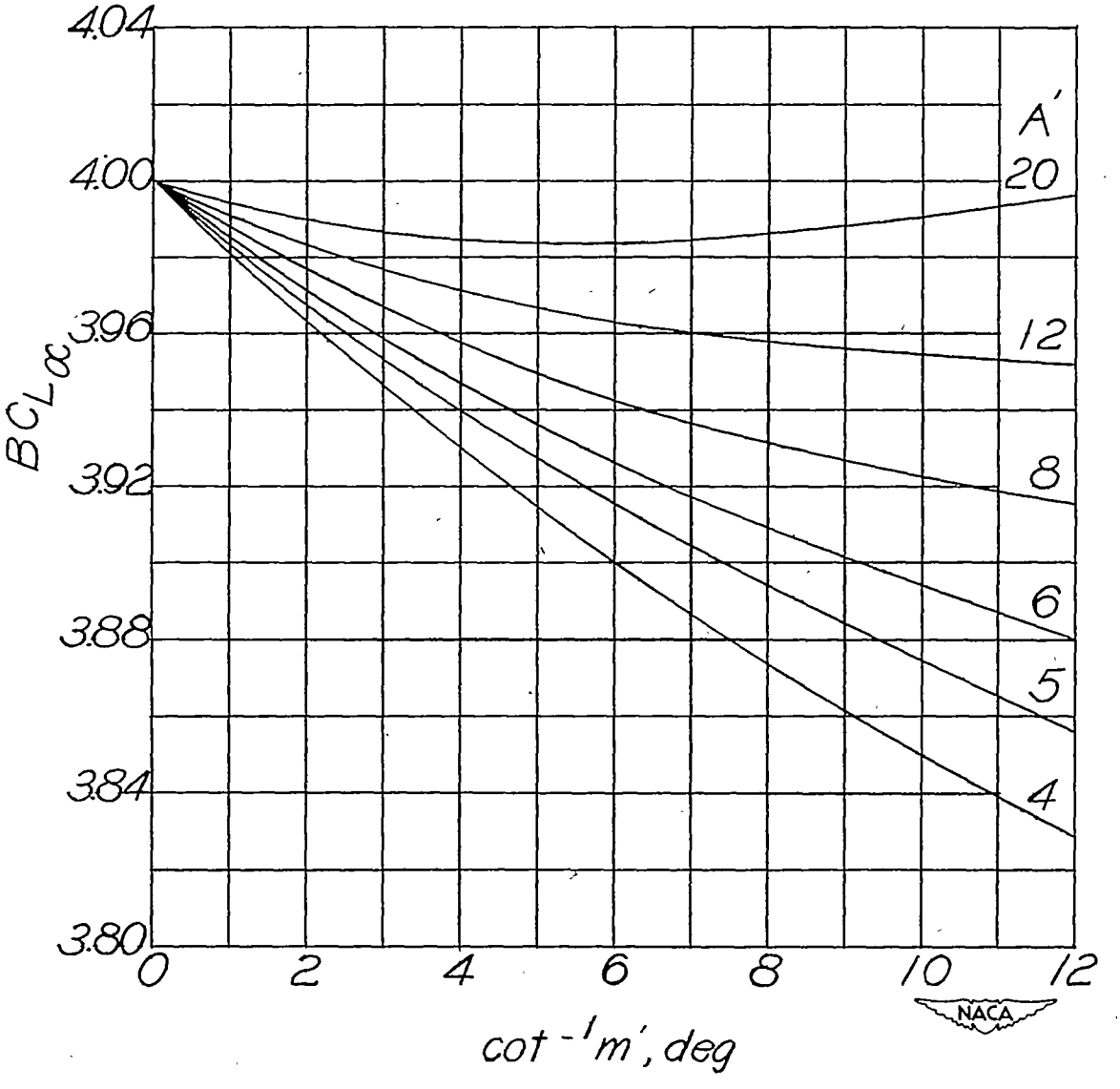

(b) $\lambda = 0$; $A' = 4$ to 20; $m' = \infty$ to 4.7.

Figure 26.- Concluded.

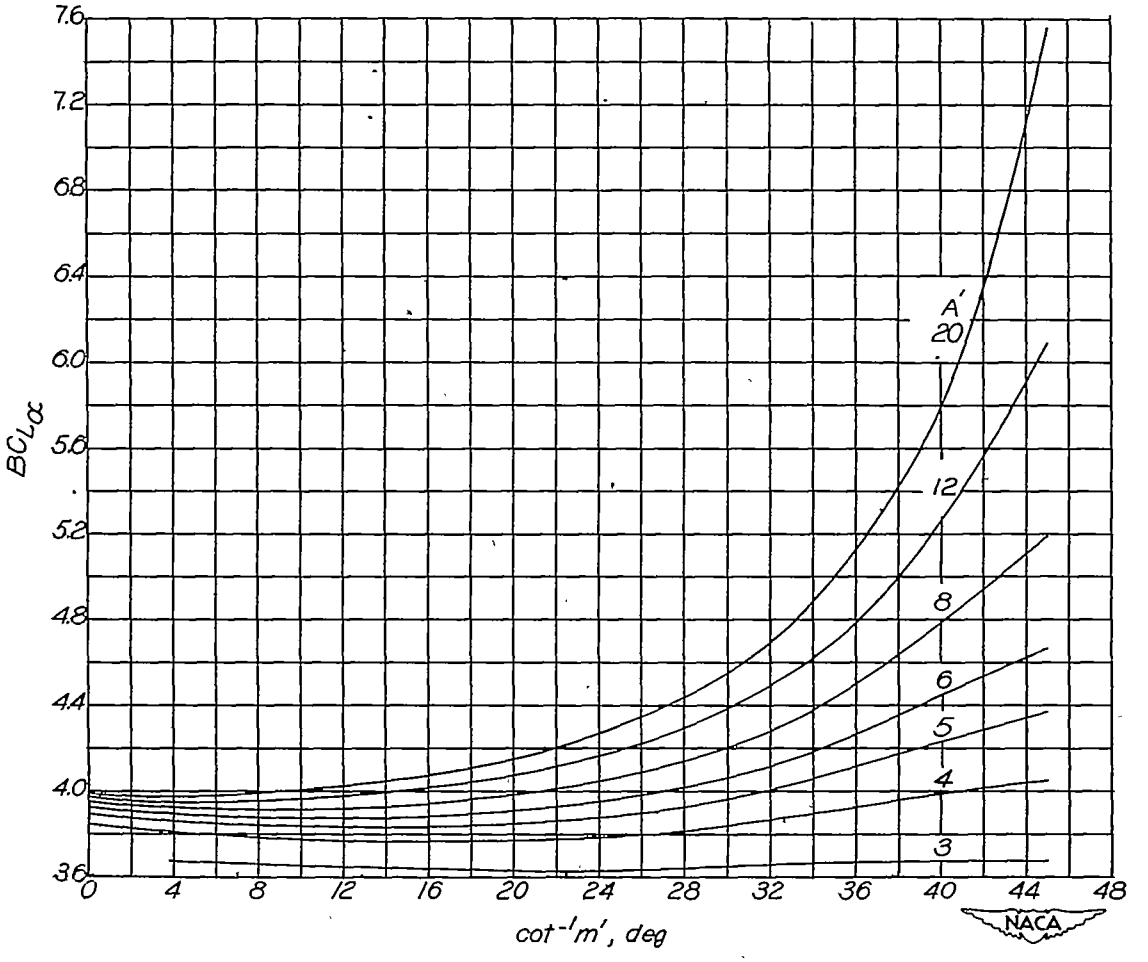

(a) $\lambda = 0.25$; $A' = 3$ to 20; $m' = \infty$ to 1.

Figure 27.- Variation of BC_{L_α} with $\cot^{-1}m'$ for various values of A'. System of body axes.

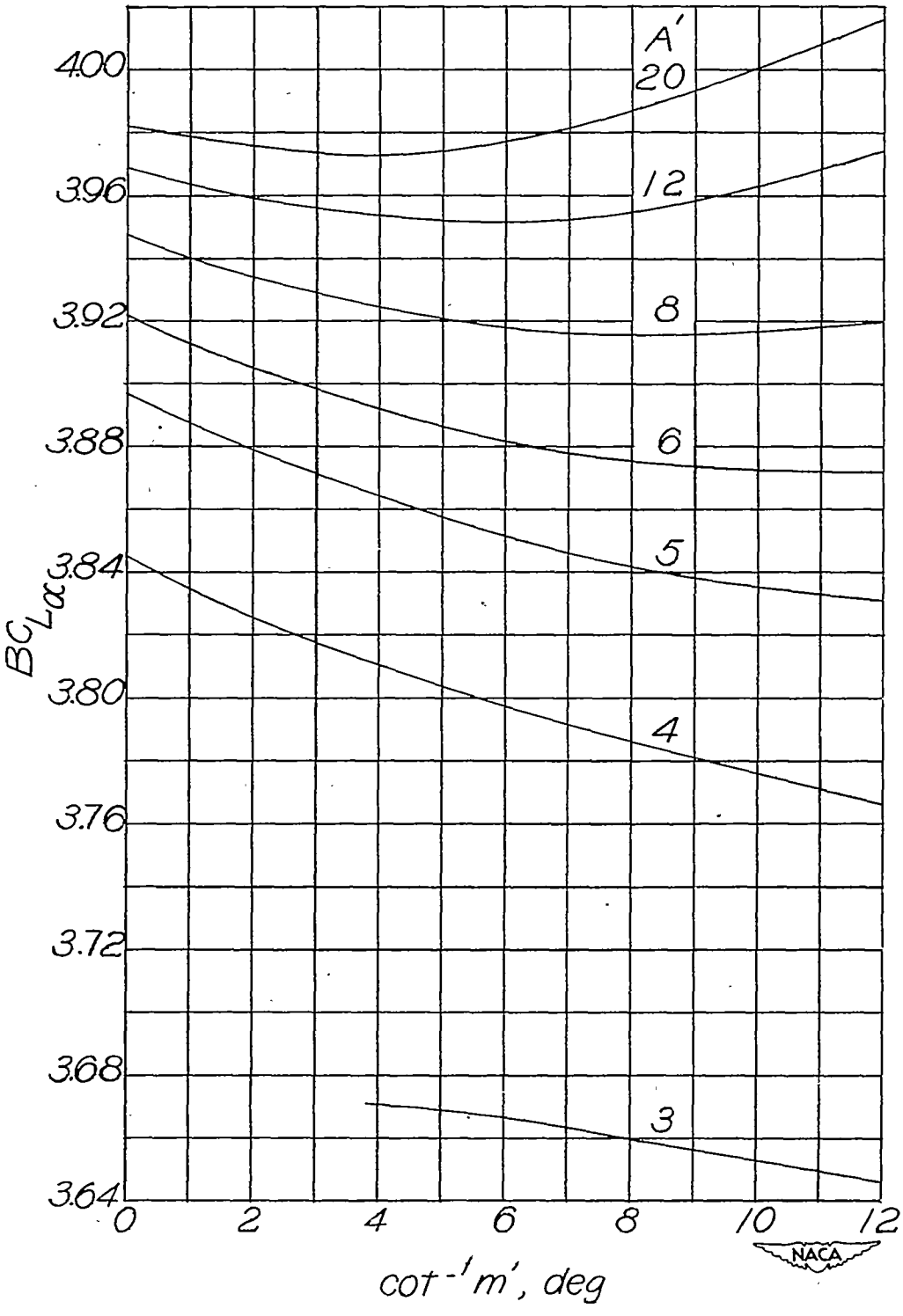

(b) $\lambda = 0.25$; $A' = 3$ to 20; $m' = \infty$ to 4.7.

Figure 27.- Concluded.

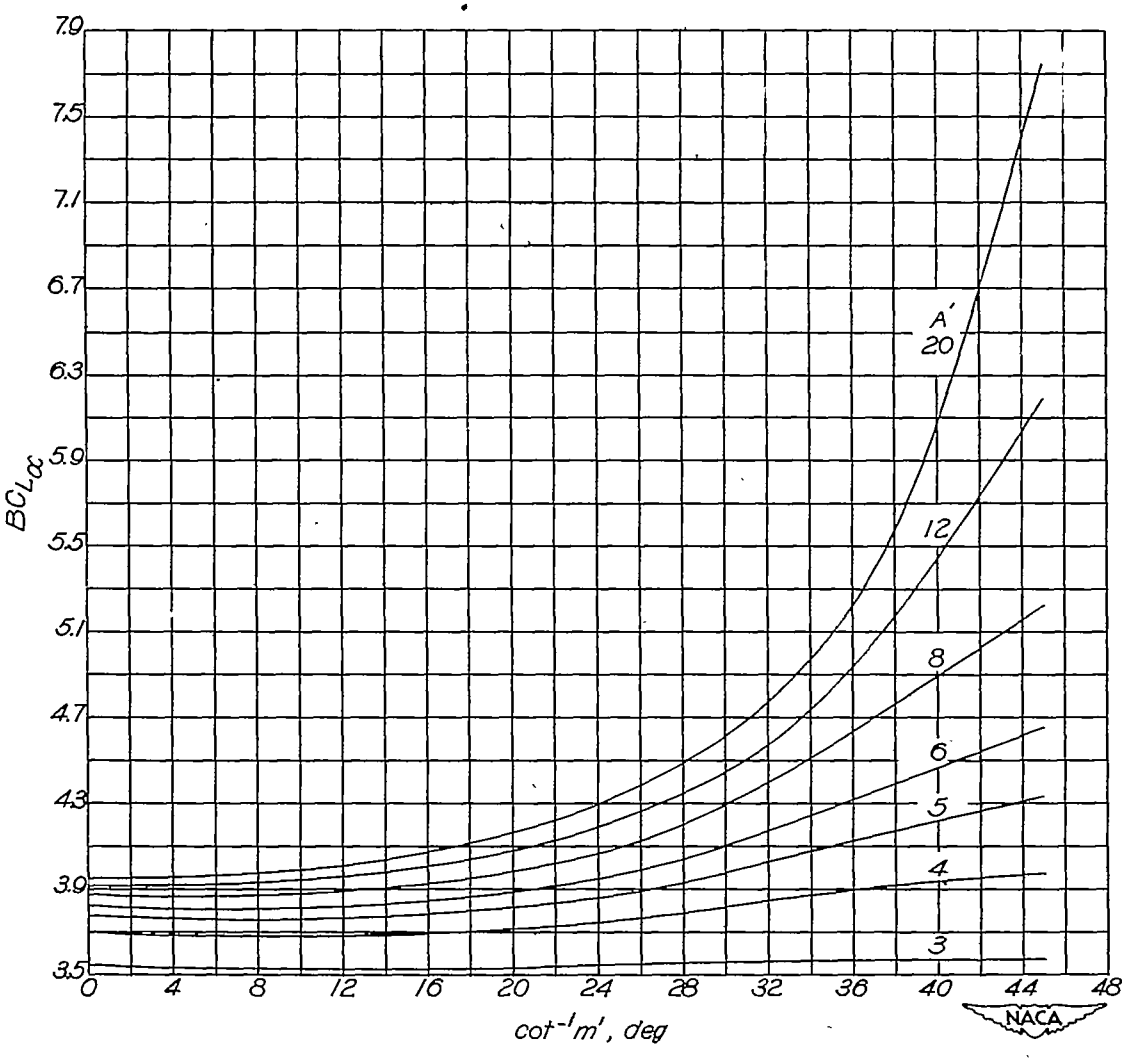

Figure 28.- Variation of BC_{L_α} with $\cot^{-1}m'$ for various values of A'. System of body axes; $\lambda = 0.50$.

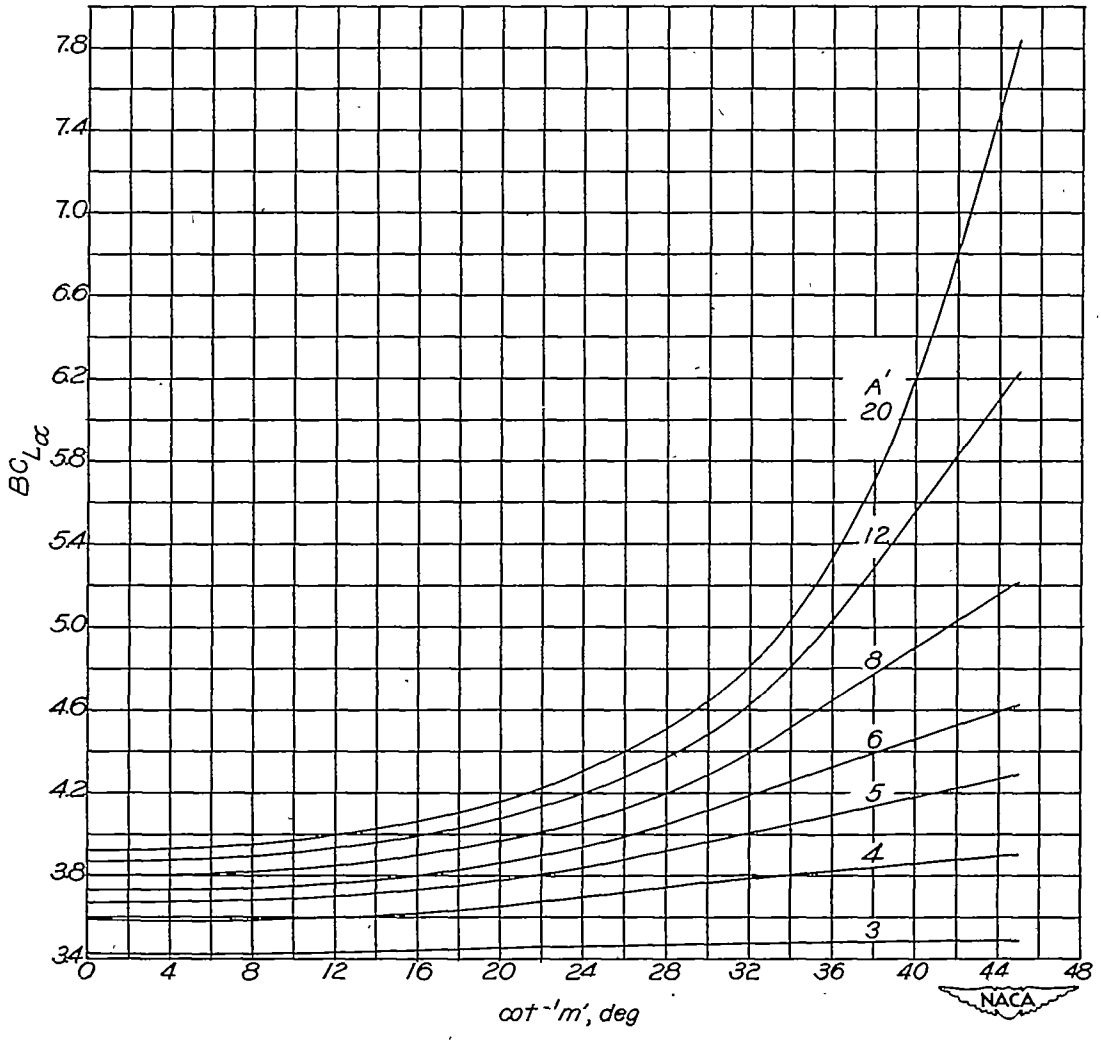

Figure 29.- Variation of BC_{L_α} with $\cot^{-1}m'$ for various values of A'. System of body axes; $\lambda = 0.75$.

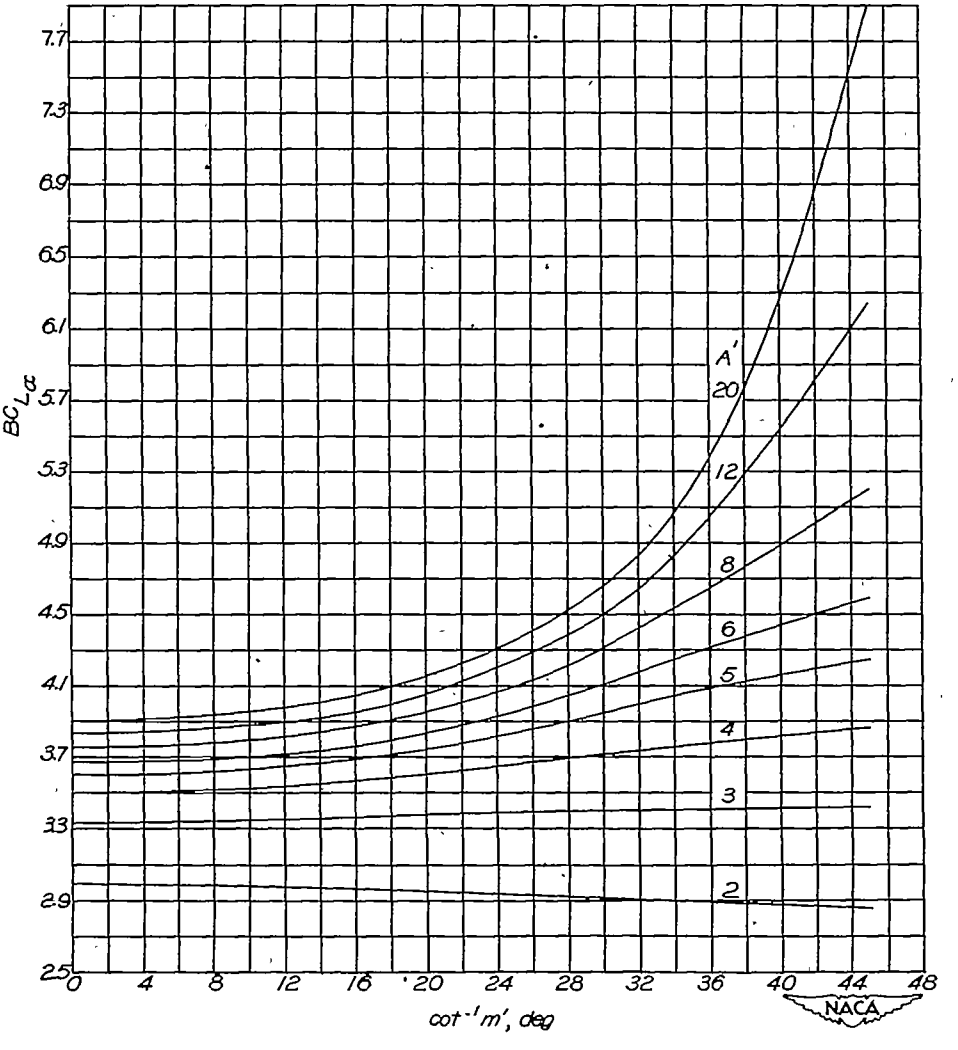

Figure 30.- Variation of BC_{L_α} with $\cot^{-1}m'$ for various values of A'. System of body axes; $\lambda = 1.0$.

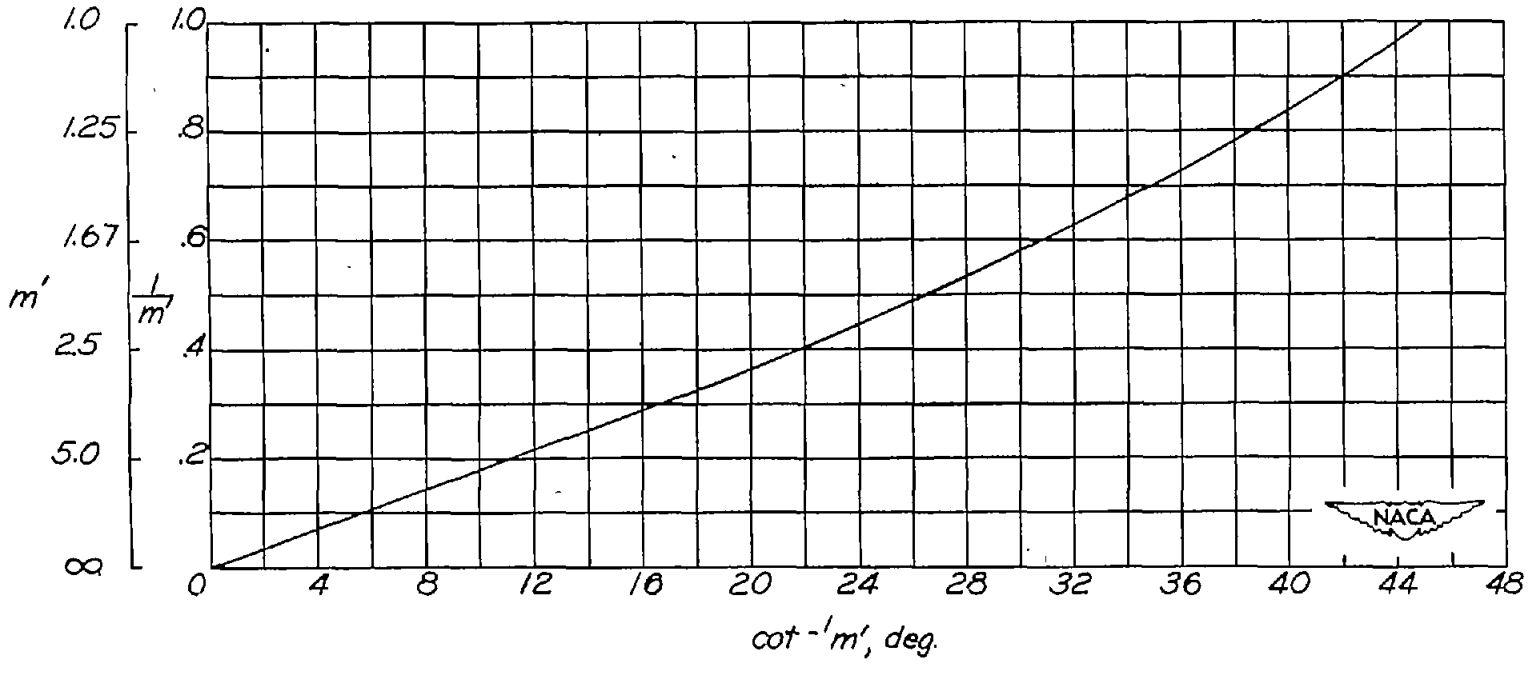

Figure 31.- Relation of the parameters $\cot^{-1}m'$ and m'.

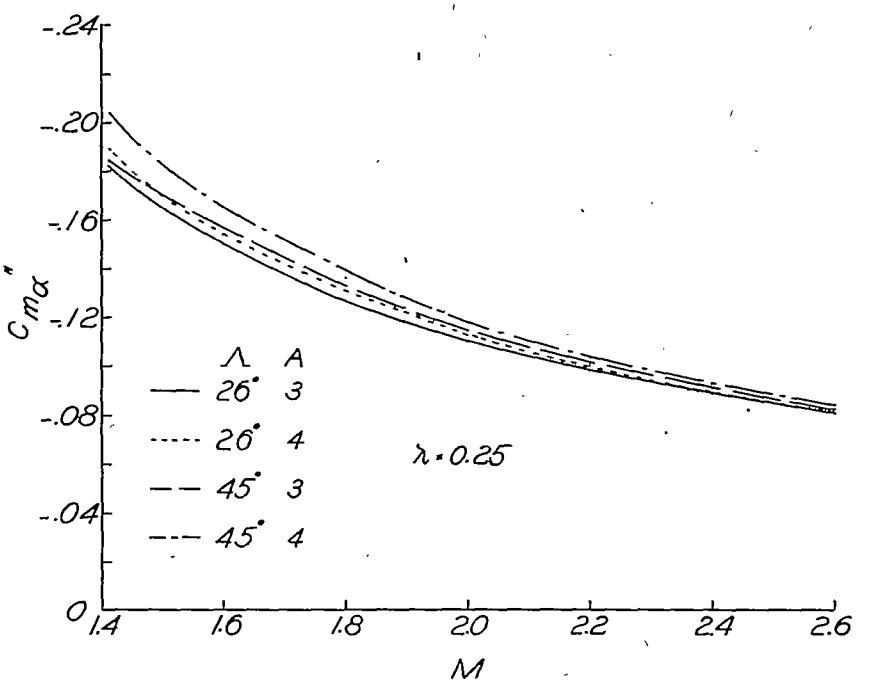

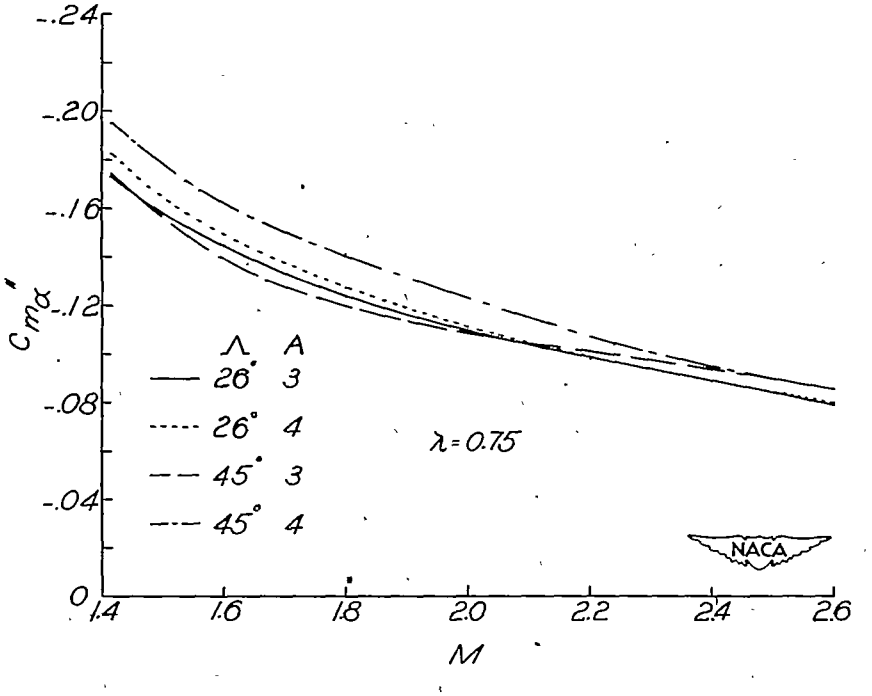

(a) Variation with Mach number.

Figure 32.- Some illustrative variations of the stability derivative C_{m_α}'' with Mach number, aspect ratio, sweepback, and taper ratio. System of stability axes; static margin, $0.05\bar{c}$.

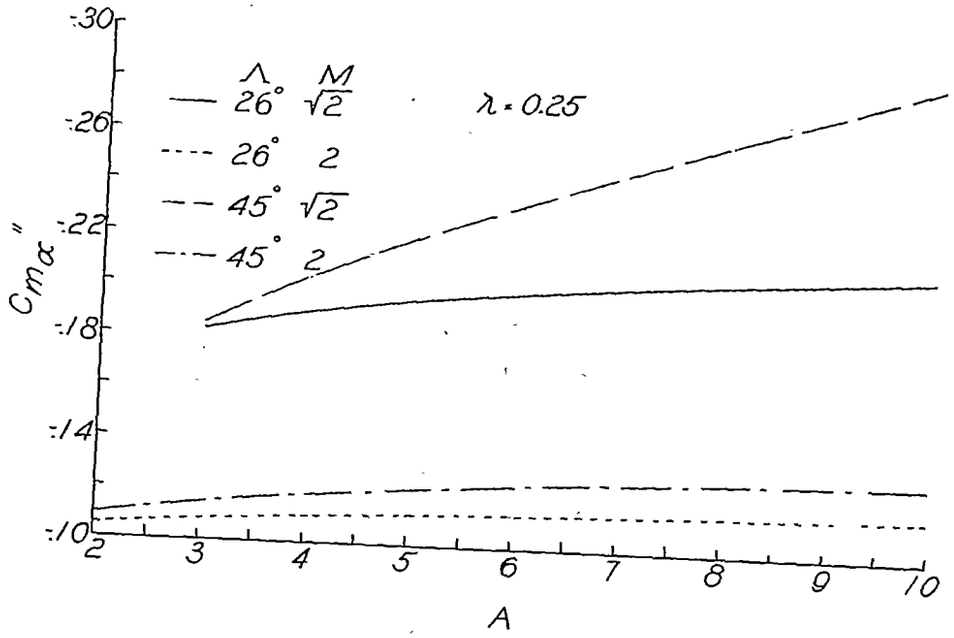

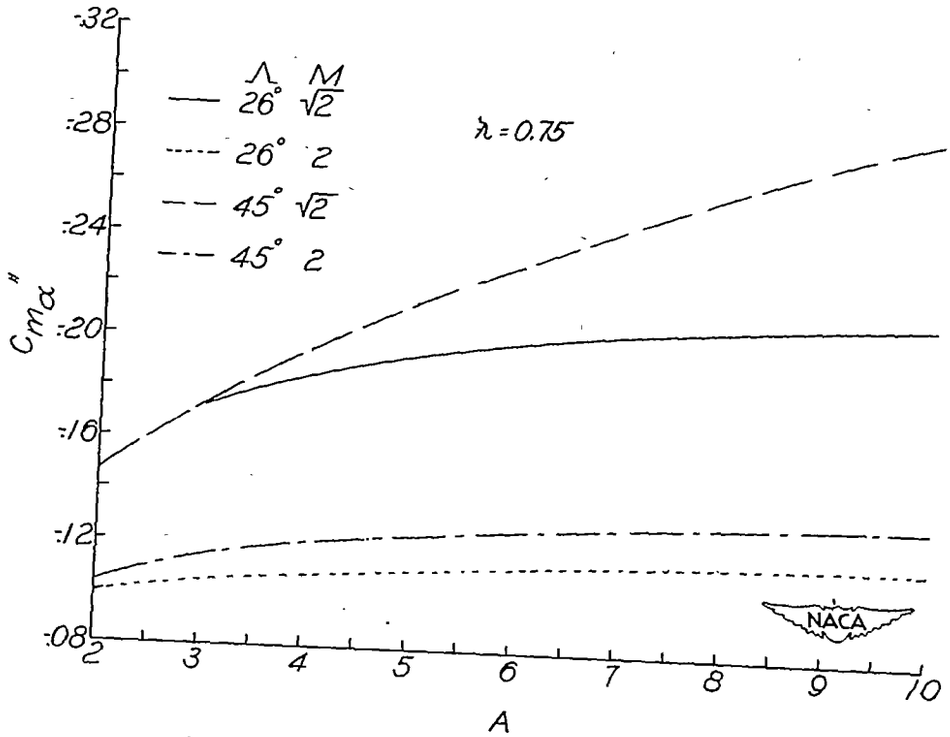

(b) Variation with aspect ratio.

Figure 32.- Continued.

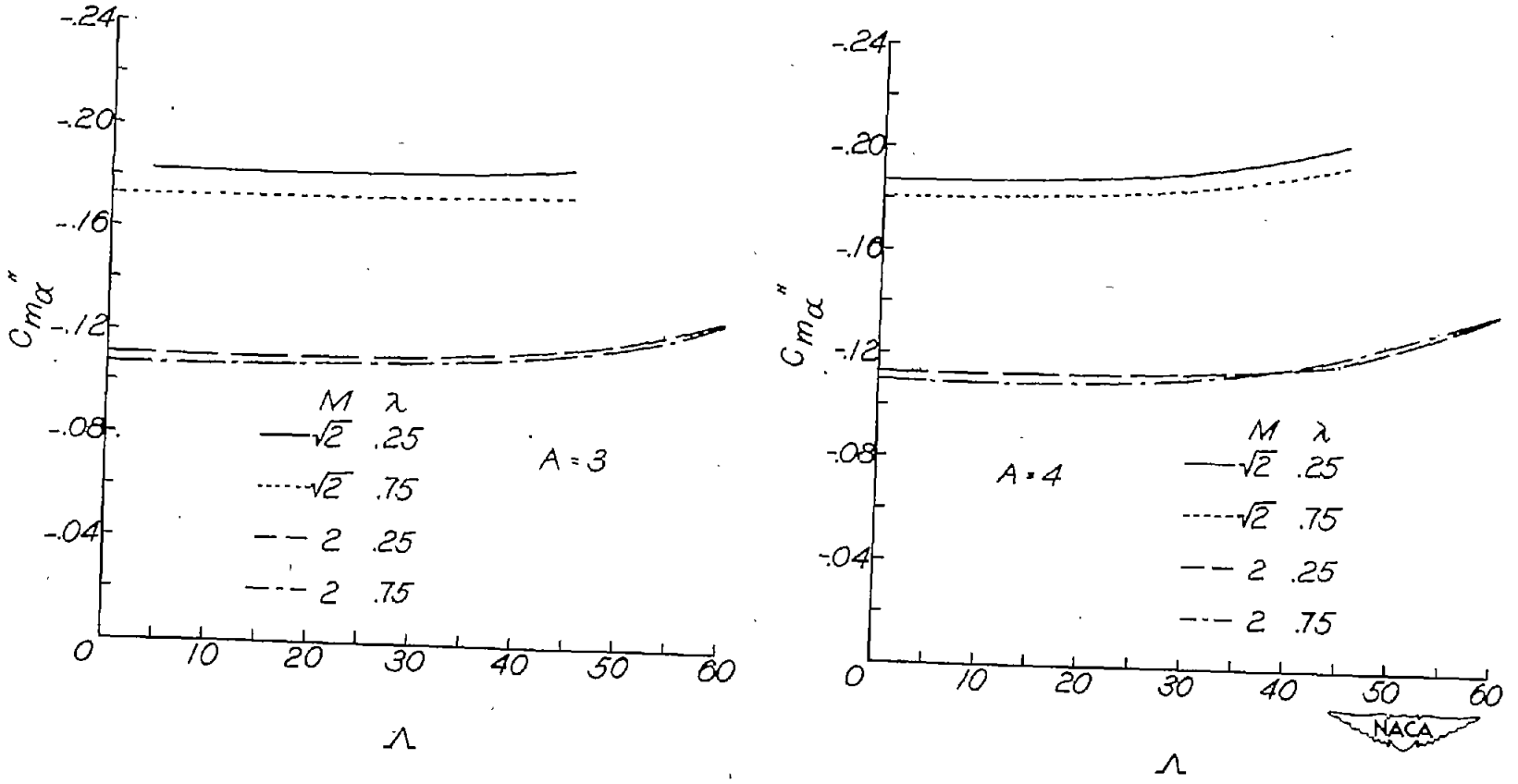

(c) Variation with sweepback.

Figure 32.- Continued.

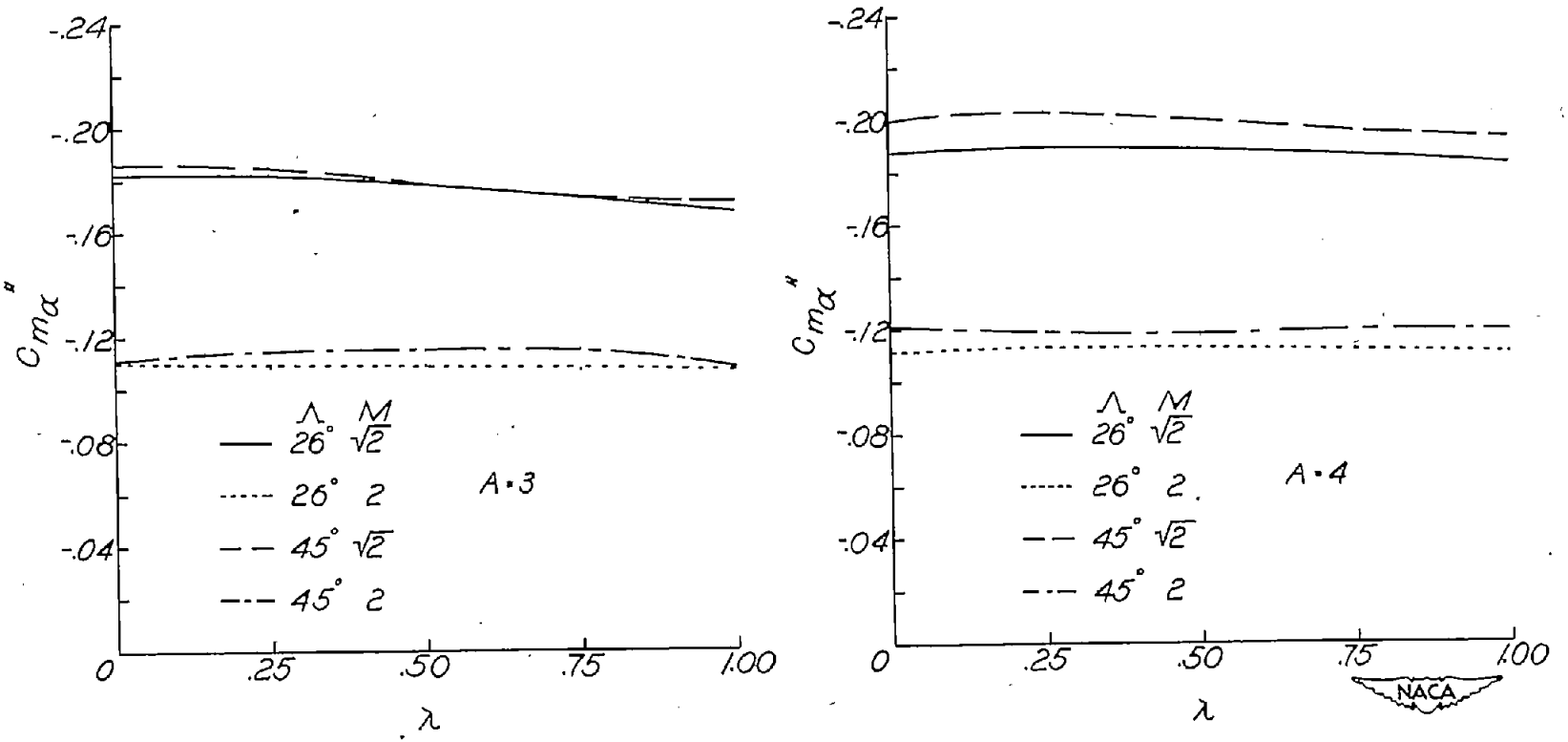

(d) Variation with taper ratio.

Figure 32.- Concluded.

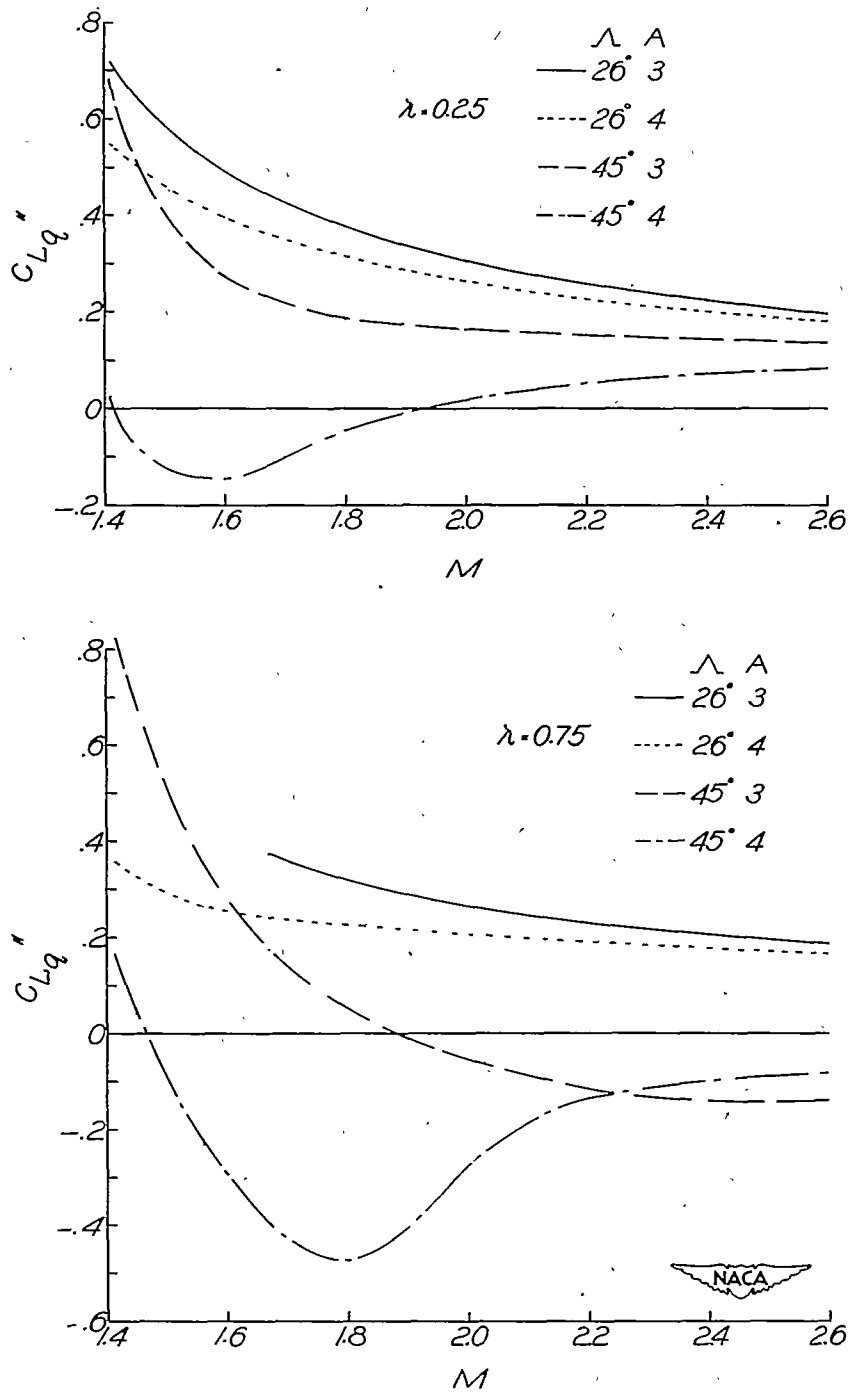

(a) Variation with Mach number.

Figure 33.- Some illustrative variations of the stability derivative C_{L_q}'' with Mach number, aspect ratio, sweepback, and taper ratio. System of stability axes; static margin, $0.05\bar{c}$.

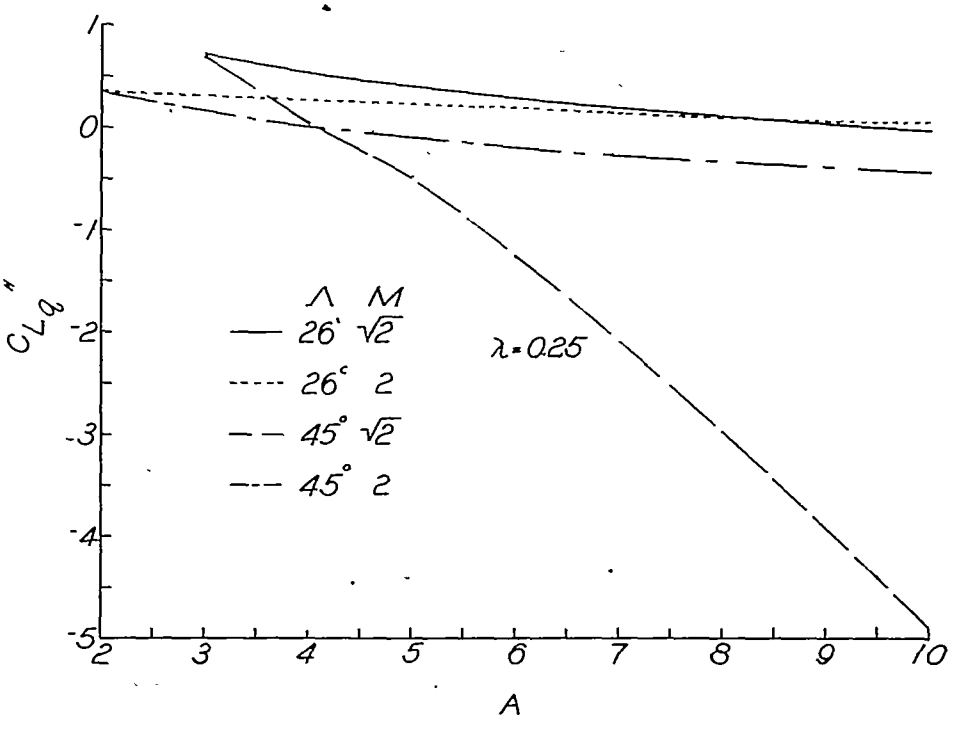

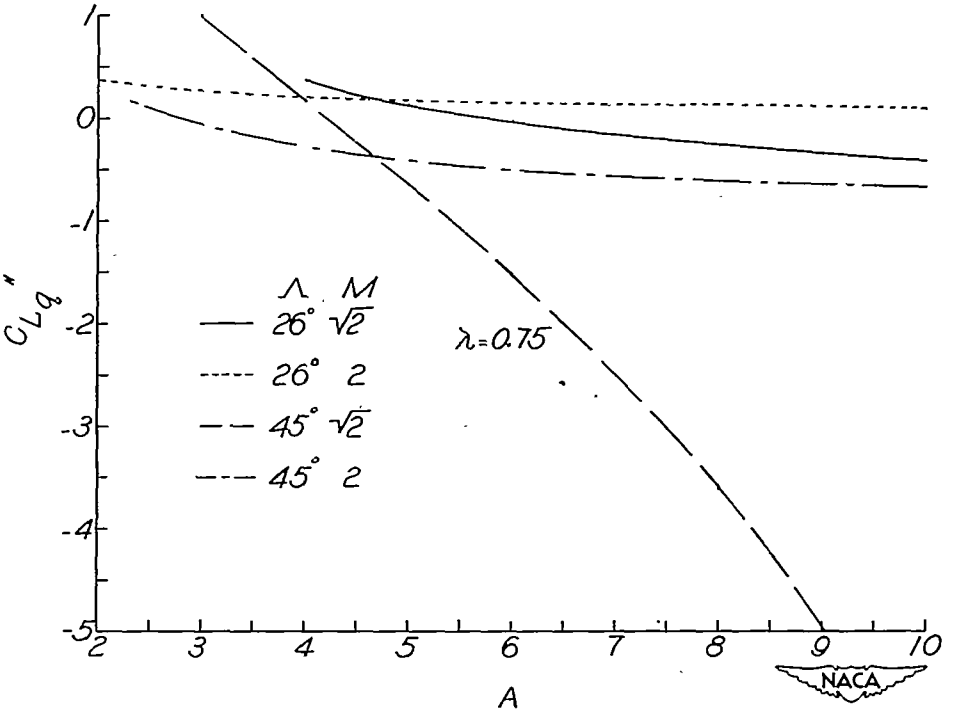

(b) Variation with aspect ratio.

Figure 33.- Continued.

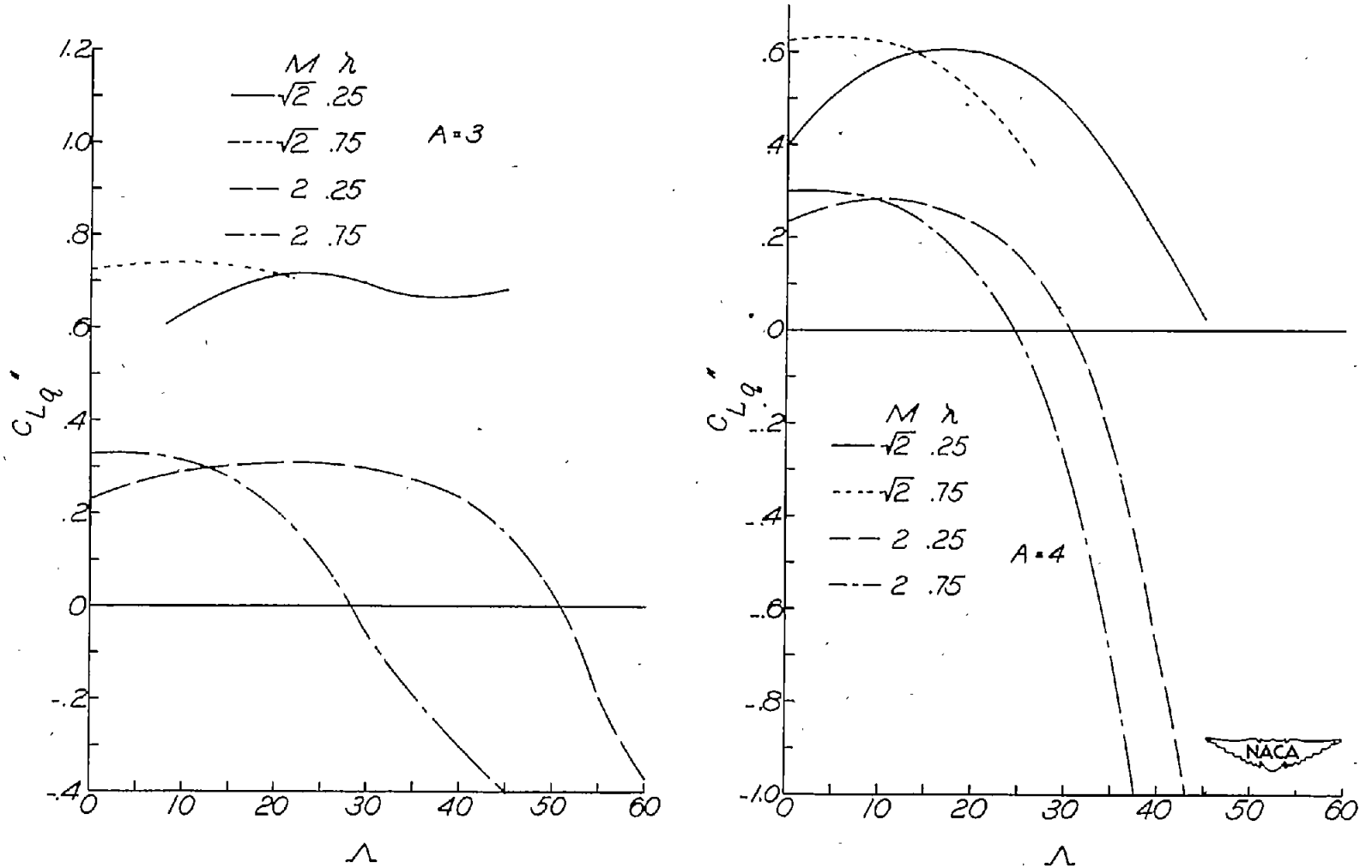

(c) Variation with sweepback.

Figure 33.- Continued.

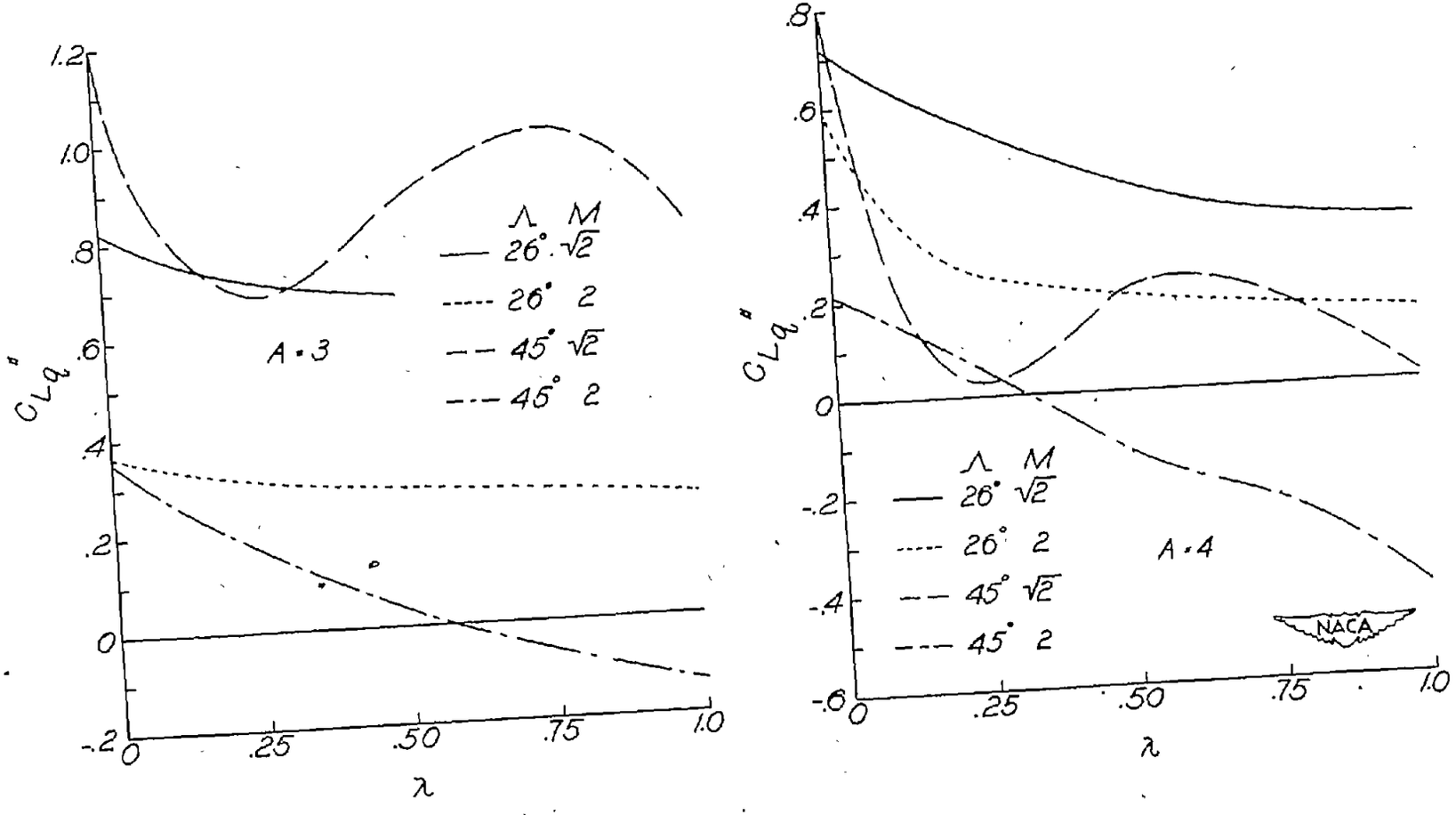

(d) Variation with taper ratio.

Figure 33.- Concluded.

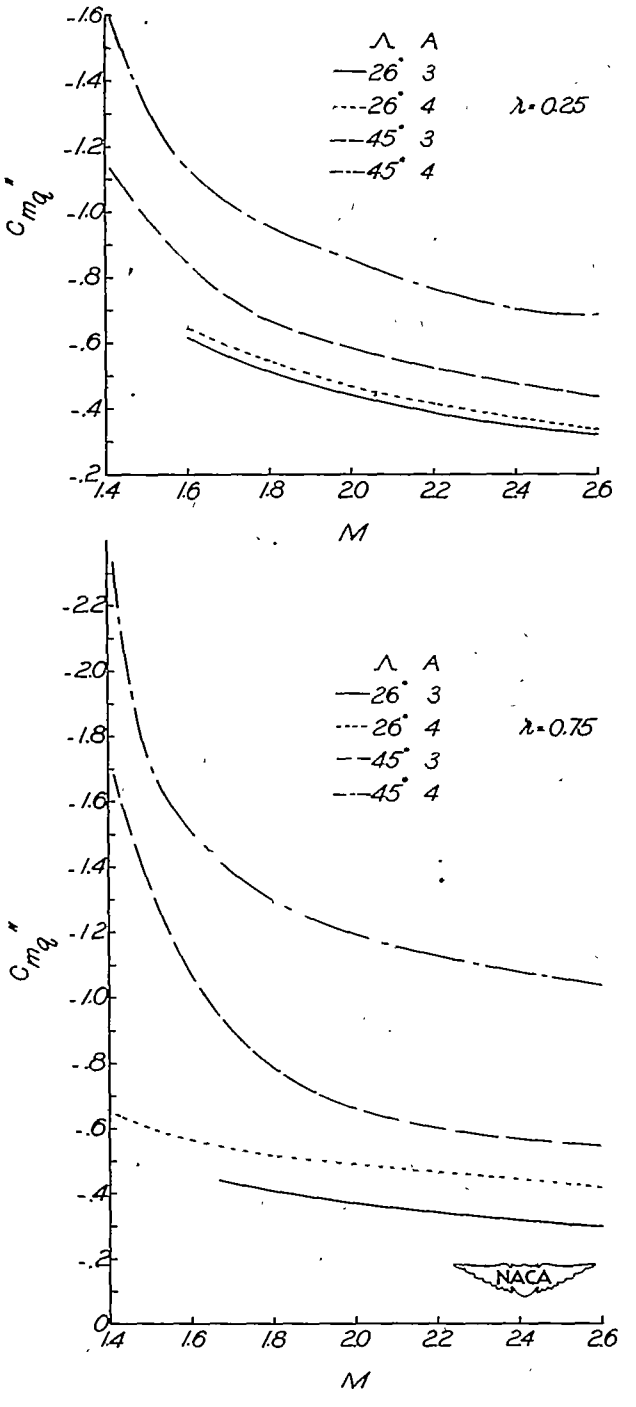

(a) Variation with Mach number.

Figure 34.- Some illustrative variations of the stability derivative C_{m_q}'' with Mach number, aspect ratio, sweepback, and taper ratio. System of stability axes; static margin, $0.05\bar{c}$.

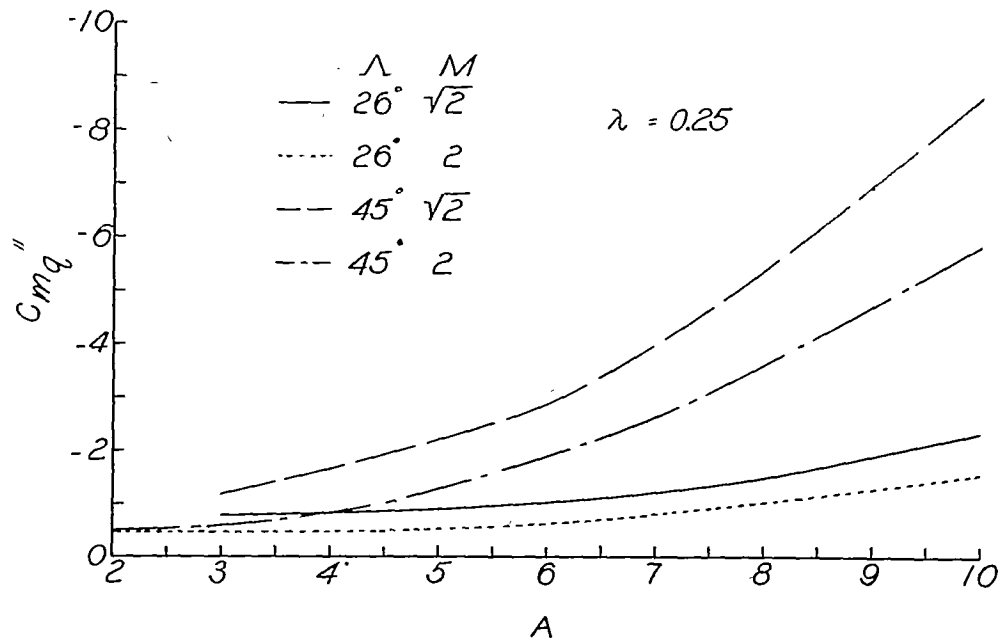

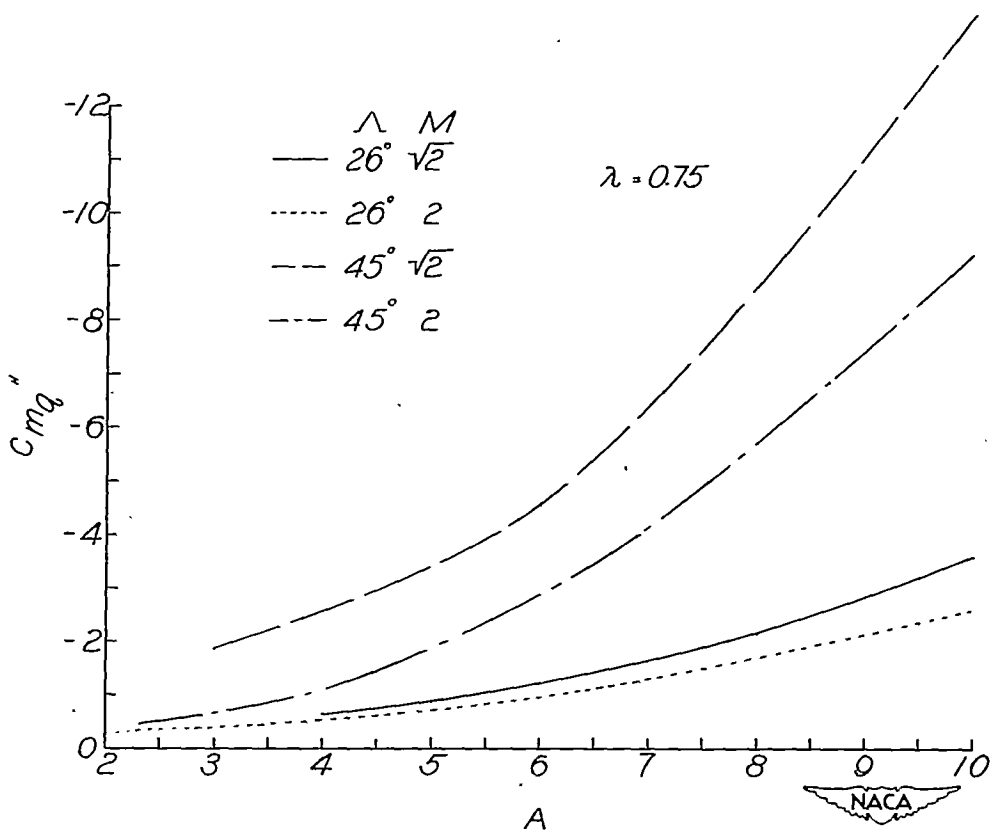

(b) Variation with aspect ratio.

Figure 34.- Continued.

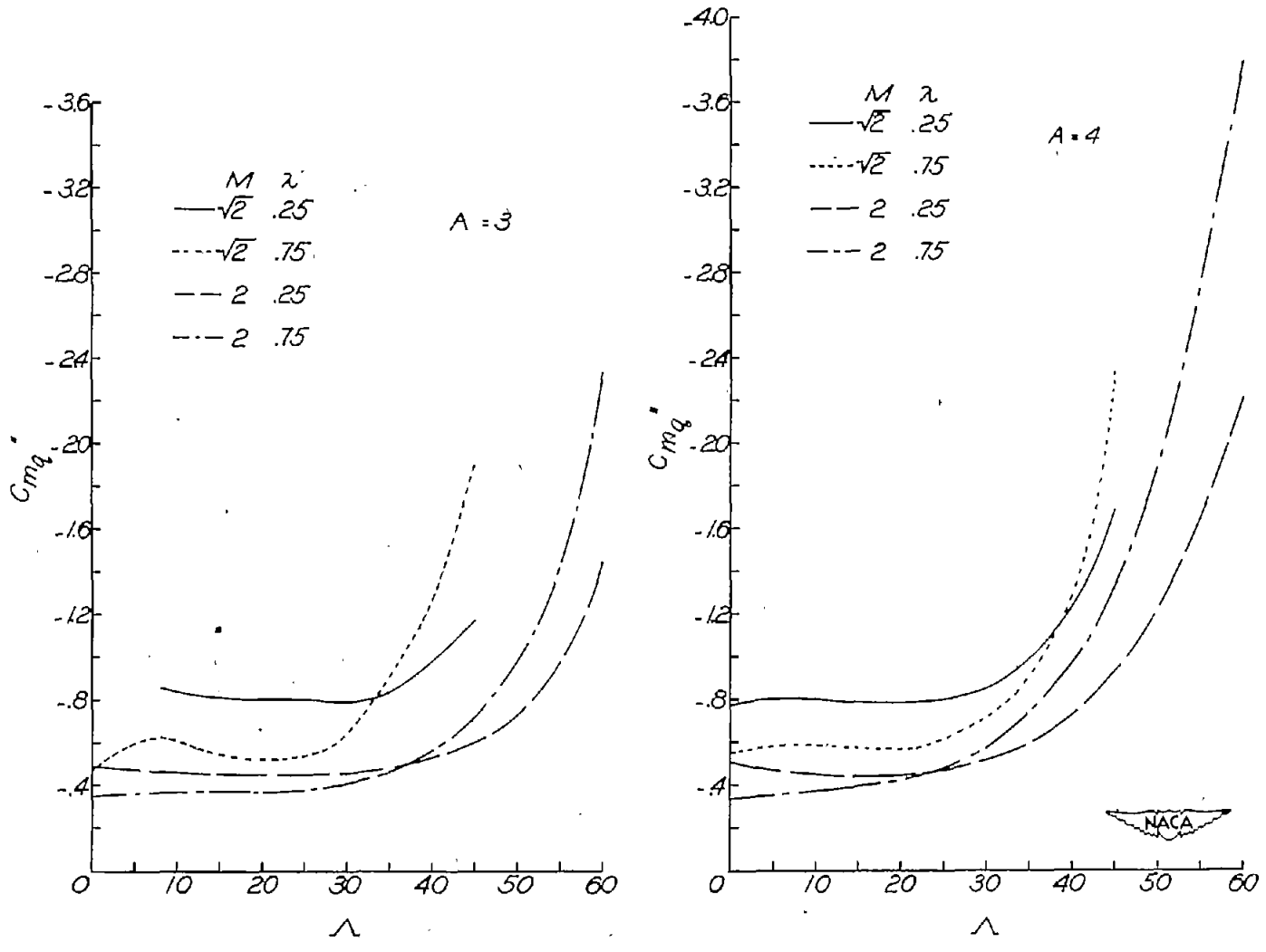

(c) Variation with sweepback.

Figure 34.- Continued.

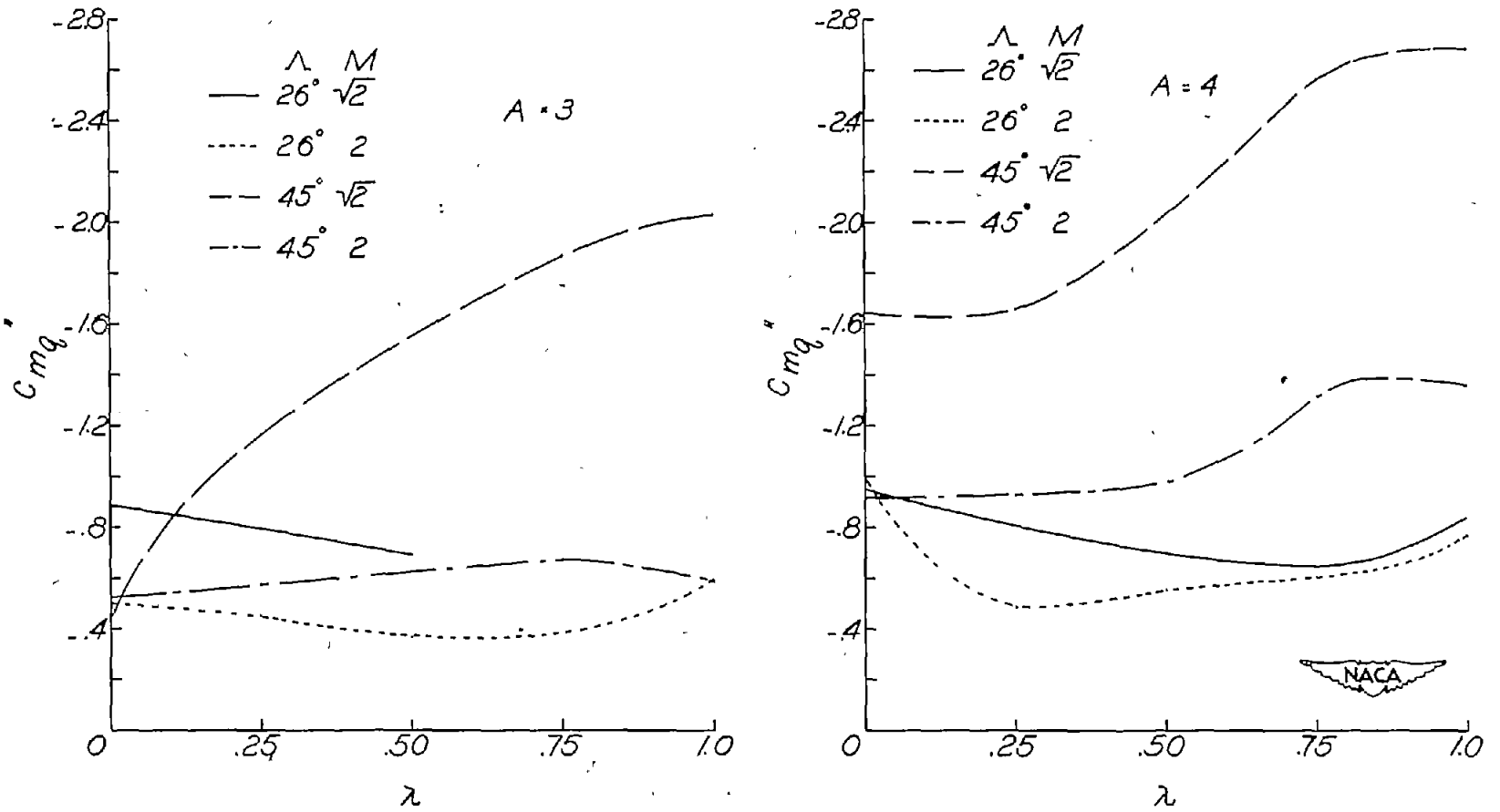

(d) Variation with taper ratio.

Figure 34.- Concluded.

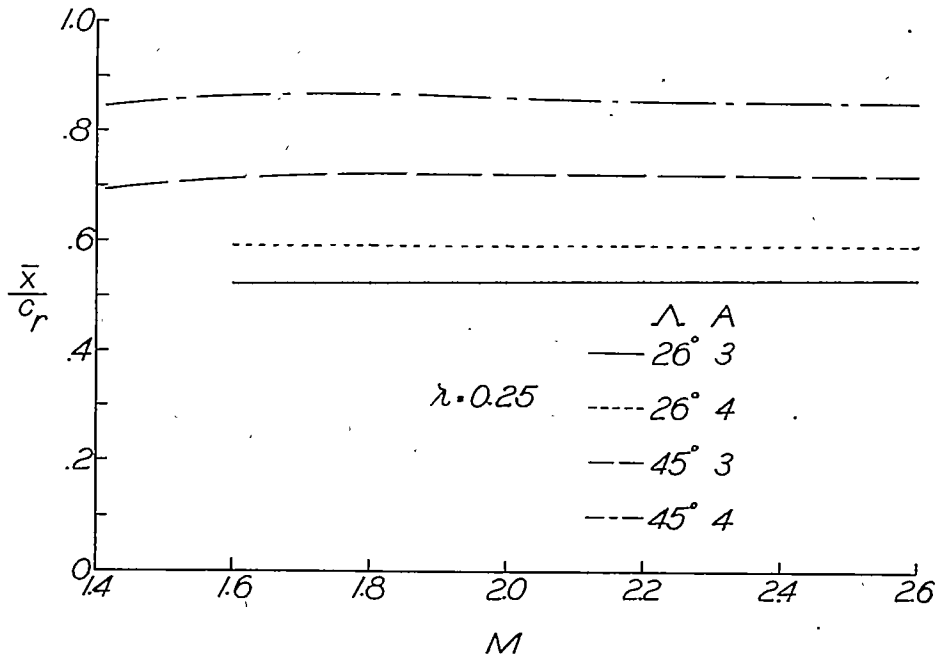

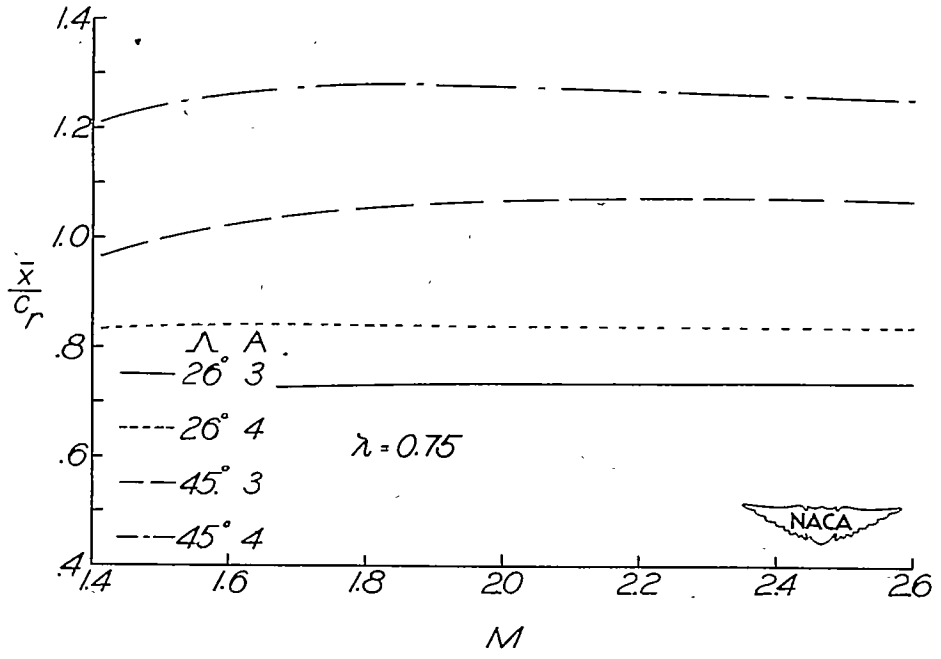

(a) Variation with Mach number.

Figure 35.- Some illustrative variations of the center of pressure due to angle of attack with Mach number, aspect ratio, sweepback, and taper ratio. System of body axes.

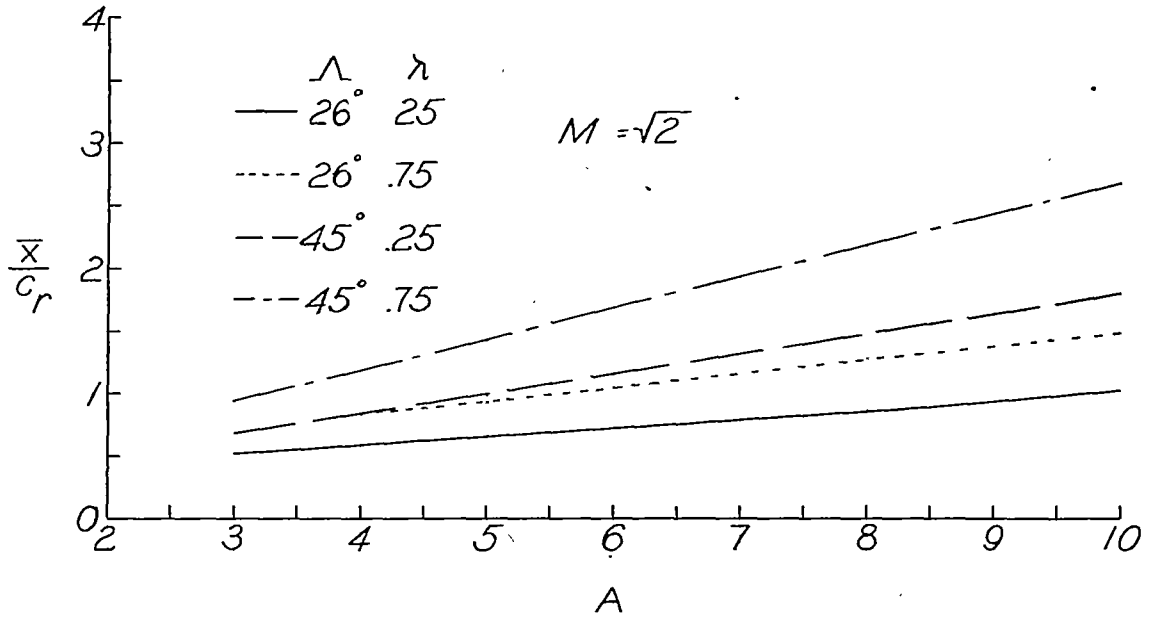

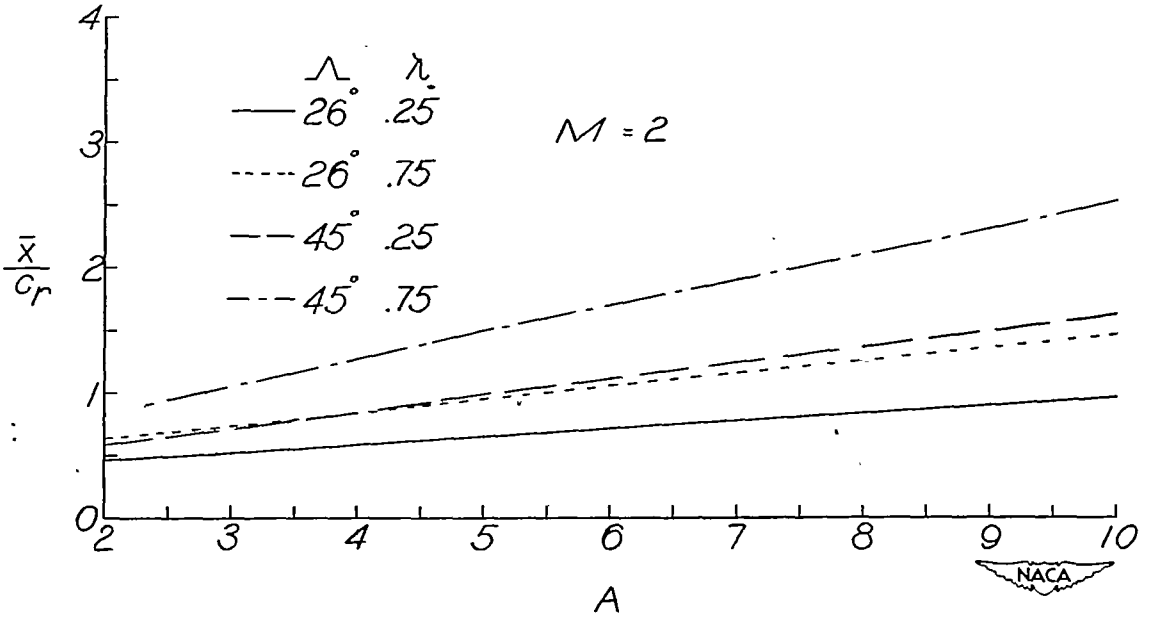

(b) Variation with aspect ratio.

Figure 35.- Continued.

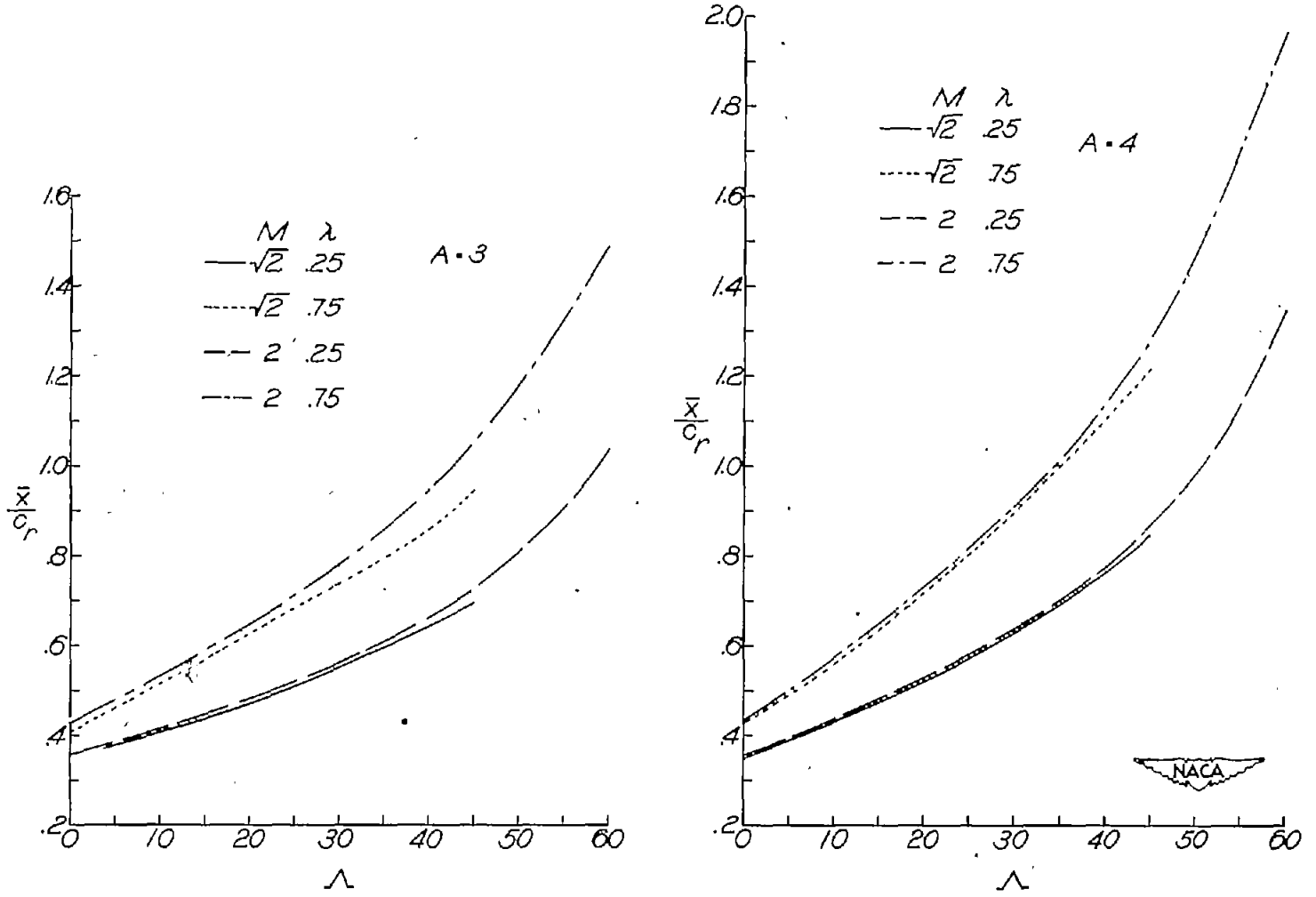

(c) Variation with sweepback.

Figure 35.- Continued.

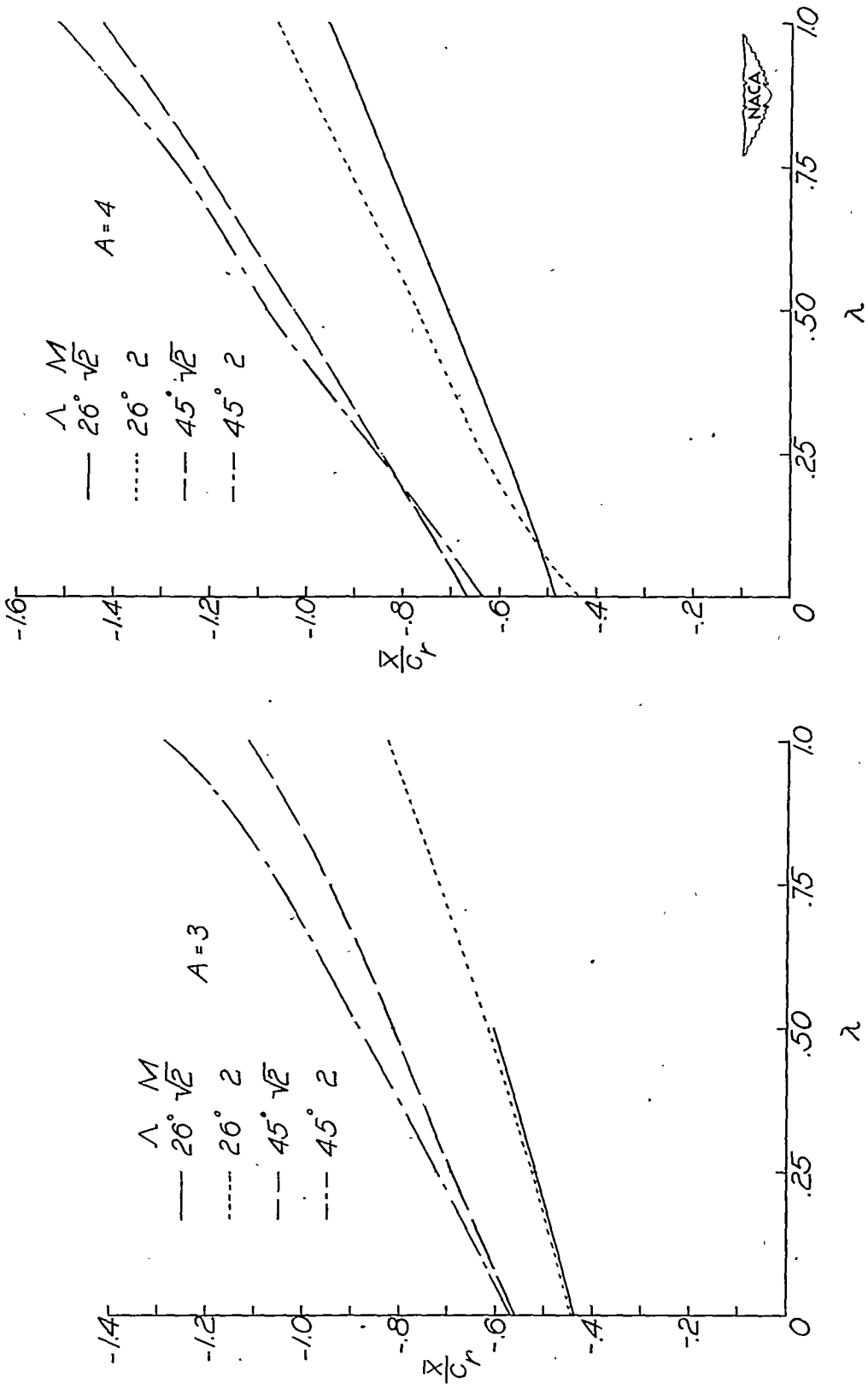

(d) Variation with taper ratio.

Figure 35.- Concluded.

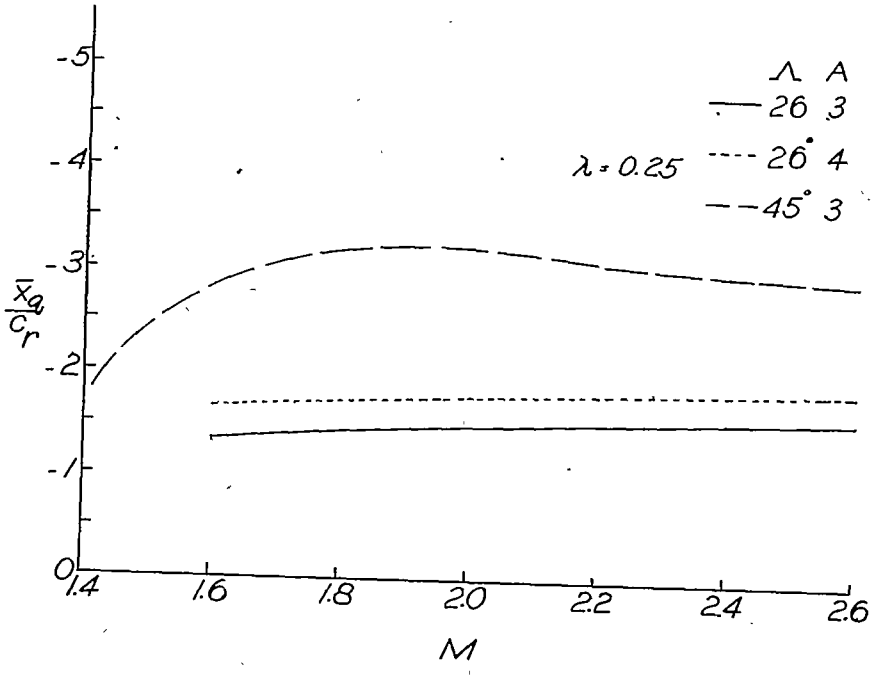

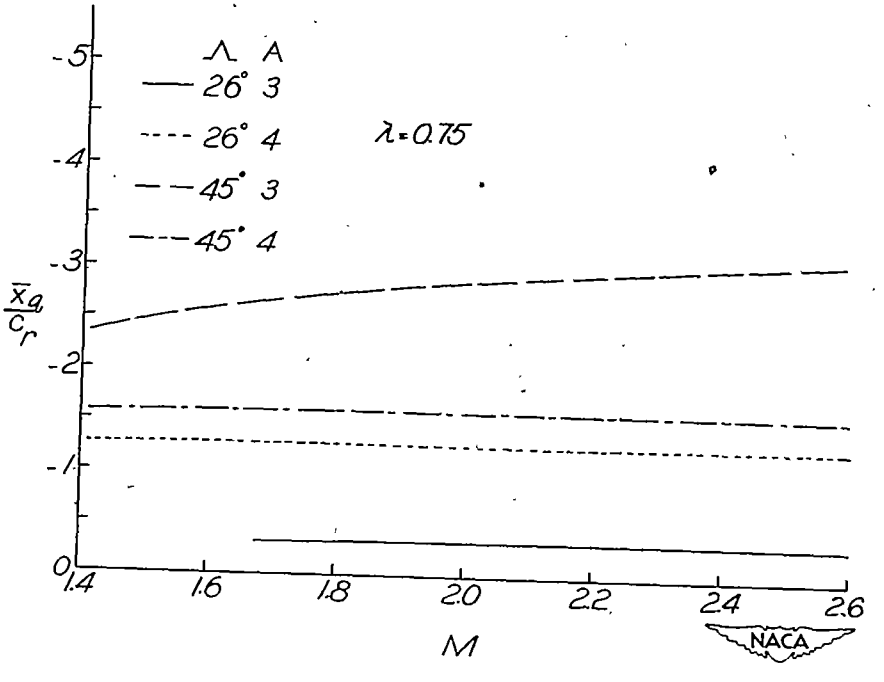

(a) Variation with Mach number.

Figure 36.- Some illustrative variations of the center of pressure due to steady pitching velocity with Mach number, aspect ratio, sweepback, and taper ratio. System of body axes; static margin, $0.05\bar{c}$.

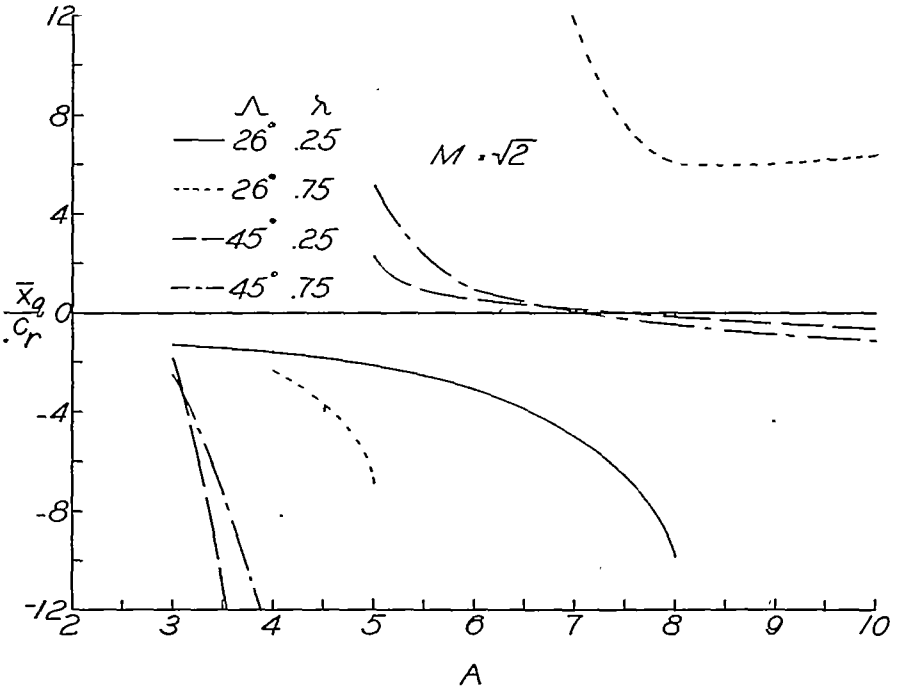

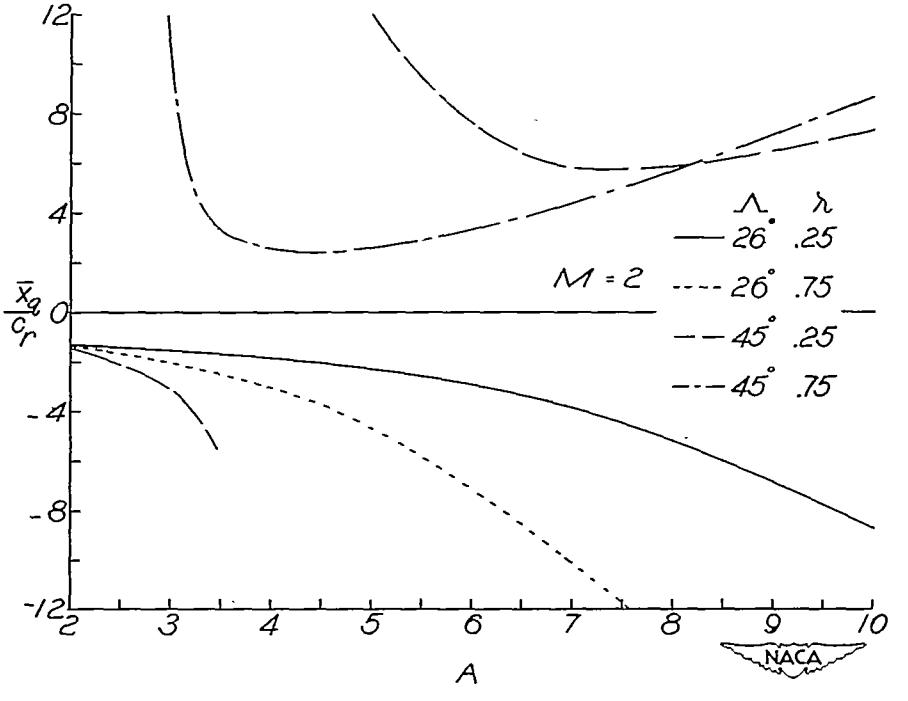

(b) Variation with aspect ratio.

Figure 36.- Continued.

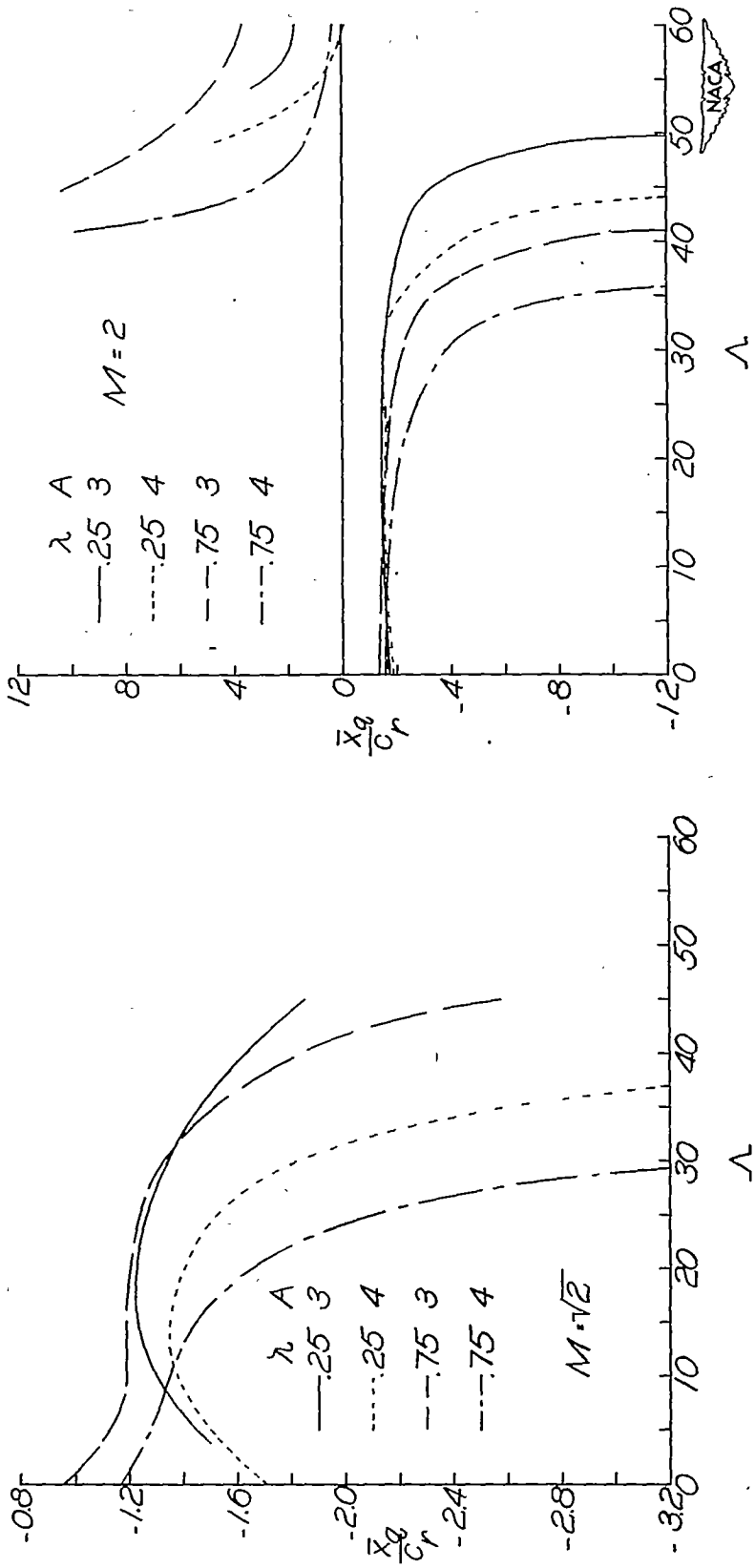

(c) Variation with sweepback.

Figure 36.- Continued.

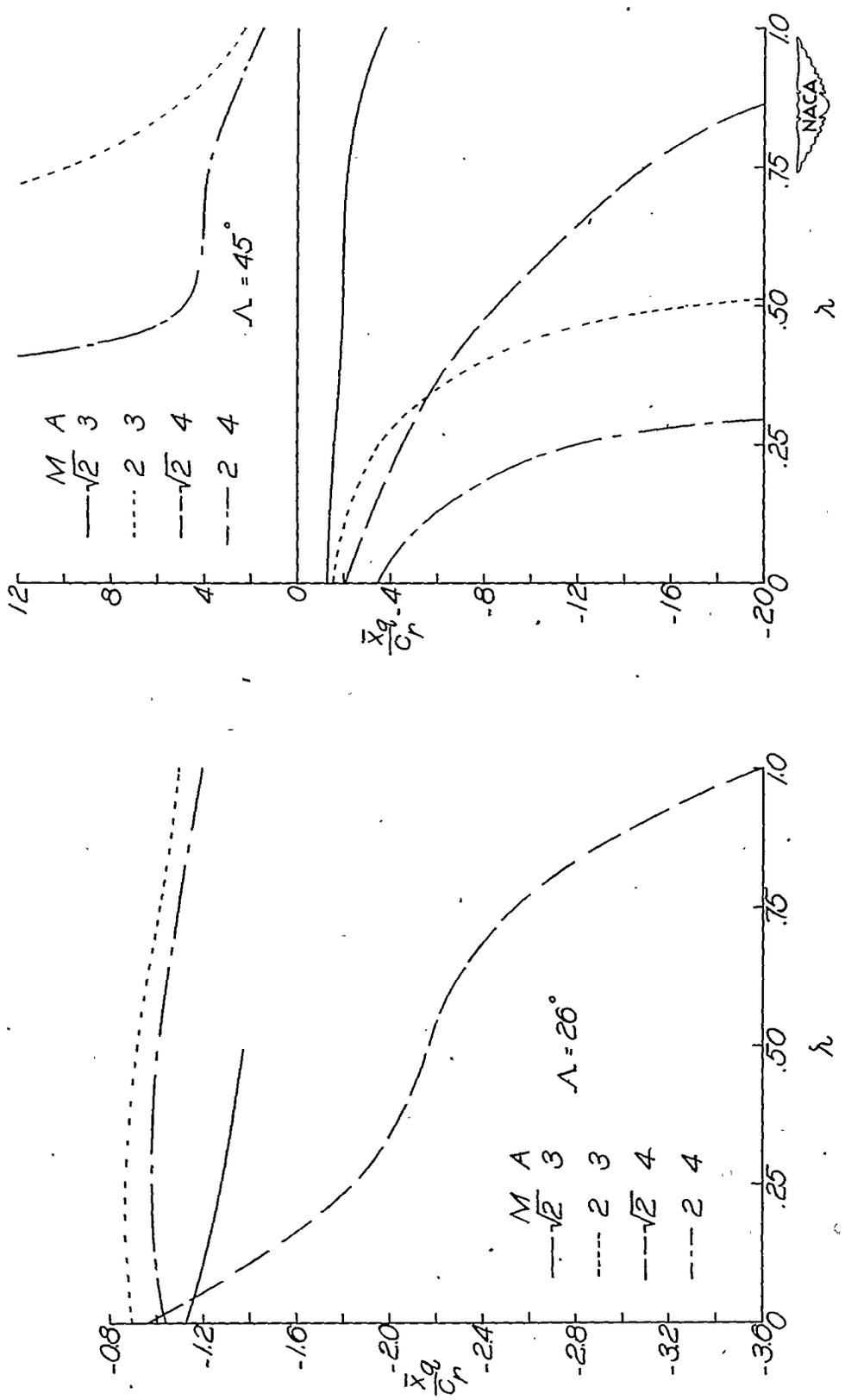

(d) Variation with taper ratio.

Figure 36.- Concluded.

NACA-Langley - 6-25-52 - 1000